

# Topological insulators and superconductors - Notes of TKMI 2013/2014 guest lectures

Panagiotis Kotetes\*

*Institut für Theoretische Festkörperphysik, Karlsruhe Institute of Technology, 76128 Karlsruhe, Germany*

## Contents

|  |    |
|--|----|
| <b>I. Introduction</b>   | 2  |
| <b>II. Symmetries and topological classification</b>   | 4  |
| <b>III. Quantum anomalous Hall effect in a Jackiw and Rebbi-like model</b>                                   | 5  |
| A. 1d model - zero-energy bound states with fixed chirality  | 6  |
| B. 2d model - chiral edge modes - QAHE   | 8  |
| C. Non relativistic kinetic term - disorder - symmetry class transition - topological protection             | 9  |
| <b>IV. Quantum anomalous Hall effect in a <math>\mathcal{T}</math>-violating topological insulator model</b> | 10 |
| A. 1d model  | 10 |
| B. 2d model  | 12 |
| C. Quantized Hall conductivity of the 2d bulk system - topological invariant                                 | 13 |
| 1. Bulk eigen-states   | 13 |
| 2. Coupling to an external constant electric field - Adiabatic eigen-states                                  | 14 |
| 3. Time-dependent perturbation theory based on adiabatic eigen-states  | 14 |
| 4. Adiabatic current   | 15 |
| 5. Hall conductivity formula   | 16 |
| 6. Quantized Hall conductivity in a $\mathcal{T}$ -violating topological insulator                           | 17 |
| 7. The first encounter of space compactification in physics: Kaluza - Klein theory                           | 19 |
| D. Topological invariant for the 1d bulk system from dimensional reduction                                   | 20 |
| <b>V. <math>\mathcal{T}</math>-invariant topological insulators</b>  | 22 |
| 1. 2d $\mathcal{T}$ -invariant topological insulators  | 22 |
| 2. Interlude: 2d topological semi-metals - graphene  | 23 |
| 3. 3d topological insulators - topologically protected Dirac surface modes                                   | 25 |
| <b>VI. Topological superconductors</b>   | 27 |
| A. Majorana fermions and topological quantum computing   | 27 |
| B. Unconventional superconductivity  | 29 |
| C. Majorana fermions in chiral p-wave superconductors  | 30 |
| D. Kitaev's lattice model for a 1d p-wave superconductor - unpaired Majorana fermions                        | 31 |
| E. Majorana fermions in engineered 1d p-wave superconductors   | 34 |
| <b>References</b>  | 36 |

---

\*Electronic address: [panagiotis.kotetes@kit.edu](mailto:panagiotis.kotetes@kit.edu)

## I. INTRODUCTION

Recently, the theoretical and experimental efforts in the field of Condensed Matter Physics have focused on the investigation of insulating materials which exhibit topologically non-trivial properties [1–5, 7–14, 17–22, 43]. Topological materials had been already predicted in the past [23, 24] but were only recently realized in the laboratory with the discovery of two-dimensional (2d) topological insulators [25] which respect time-reversal symmetry ( $\mathcal{T}$ ). The latter 2d systems are insulating in the bulk and exhibit helical edge modes confined in the vicinity of the boundary separating them from the vacuum. These edge modes are called helical because depending on the direction of their motion, they are characterized by a specific spin polarization or more generally chirality. As we will discuss later, chirality constitutes a quantum number which labels these edge eigen-states. On each edge, there exists a single pair of these modes with opposite spin projection or chirality (see Fig. 1). The latter is reflected in the following energy dispersion  $E_\sigma(k) = \sigma k$ , with  $\sigma = \pm 1$  (blue, red in Fig. 1) denoting the two different values of chirality. The most important feature of these edge modes is that they are protected due to the topologically non-trivial content of the system, which originates from the strong spin-orbit interaction. The latter implies that these modes will persist even in the presence of disorder as long as  $\mathcal{T}$ -symmetry is not violated. The presence of topologically protected helical modes leads to the quantum spin Hall effect (QSHE). This situation is similar to the quantum Hall effect (QHE) [26], where the Hall transport is mediated from chiral, instead of helical edge modes, due to the presence of a strong external magnetic field  $\mathcal{B}$  which selects *only one* of the two spin polarizations (chiralities) that we have in the case of helical edge modes. Essentially, the chiral edge modes are described by the dispersion  $E_\sigma(k) = \sigma k$  with **only a single** chirality present per edge, i.e.  $\sigma = +1$  ( $\sigma = -1$ ). Which of the two allowed chirality values will persist, is a matter of the orientation of the applied magnetic field  $\mathcal{B}$ .

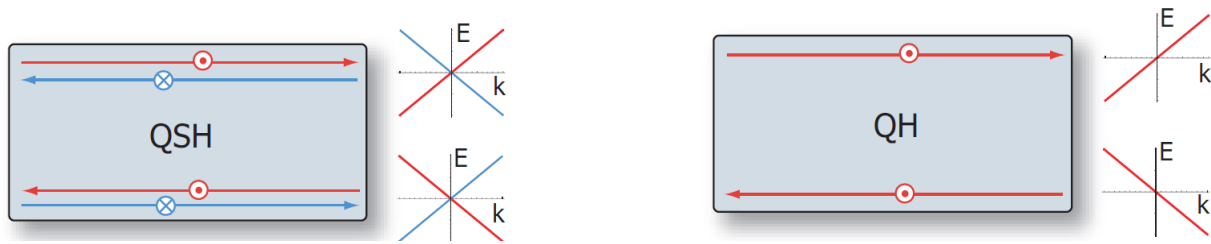


FIG. 1: **Left:** Helical edge modes in a two-dimensional topological insulator preserving  $\mathcal{T}$ -symmetry, as for instance the situation encountered in HgTe/CdTe quantum well structures [25]. **Right:** Chiral edge modes appearing in the usual quantum Hall effect case. Only one spin-polarization is accessible due to the presence of the external magnetic field which is applied perpendicular to the plane and violates  $\mathcal{T}$ -symmetry. Figure taken from X.-L. Qi *et al.*, Phys. Rev. Lett. **102**, 187001 (2009).

The discovery of topological insulators shed light on the connection of topologically non-trivial bulk systems and the appearance of protected edge modes, but more importantly, nurtured further advancements linking the topologically non-trivial properties with of symmetries. In fact, an important concept emerged, according to which: *Different systems share a number of similar properties if they are characterized by the same symmetries*. One of these properties or physical quantities can be for instance the Hall conductivity. As a matter of fact, apart from the usual setup exhibiting the QHE, one can also find completely different systems which are characterized by a quantized Hall conductivity [18, 19, 24]. In the latter case, no external magnetic field is applied and consequently no Landau levels are involved. For these reasons the related quantum Hall phenomenon is termed quantum anomalous Hall effect (QAHE). The only requirement for any QAHE system, is to violate the same symmetries as in the case of the usual QHE. This is the only constraint for obtaining a quantized Hall conductivity as in QHE. In fact, in this case, only the Hall conductivity is guaranteed to behave in a similar way, while other properties of these QAHE materials can be completely different compared to the usual QHE setup. In this manner we can distinguish two types of physical quantities: **a.** the ones that depend on the details of the single-particle Hamiltonian and **b.** the ones that depend only on the symmetries which characterize the system. The latter are the most important, since they are robust against any deformation of a given Hamiltonian and are called topological invariants. The word “topological” encodes further information. It implies that these quantities which can be common for completely different systems and are linked to symmetry, crucially depend on the dimensionality ( $d$ ) of the system. From the above we may directly infer that any candidate QAHE system has to be two-dimensional (spatial dimensionality  $d = 2$ ) and should violate intrinsically  $\mathcal{T}$ -symmetry [27] (e.g. due to ferromagnetic dopants) which is effected in the usual QHE case by the applied magnetic field.

Following the discussion above, we conclude that based solely on the symmetry properties of a system, we are in a position to predict if it can be characterized by a set of topological invariant quantities such as a quantized Hall

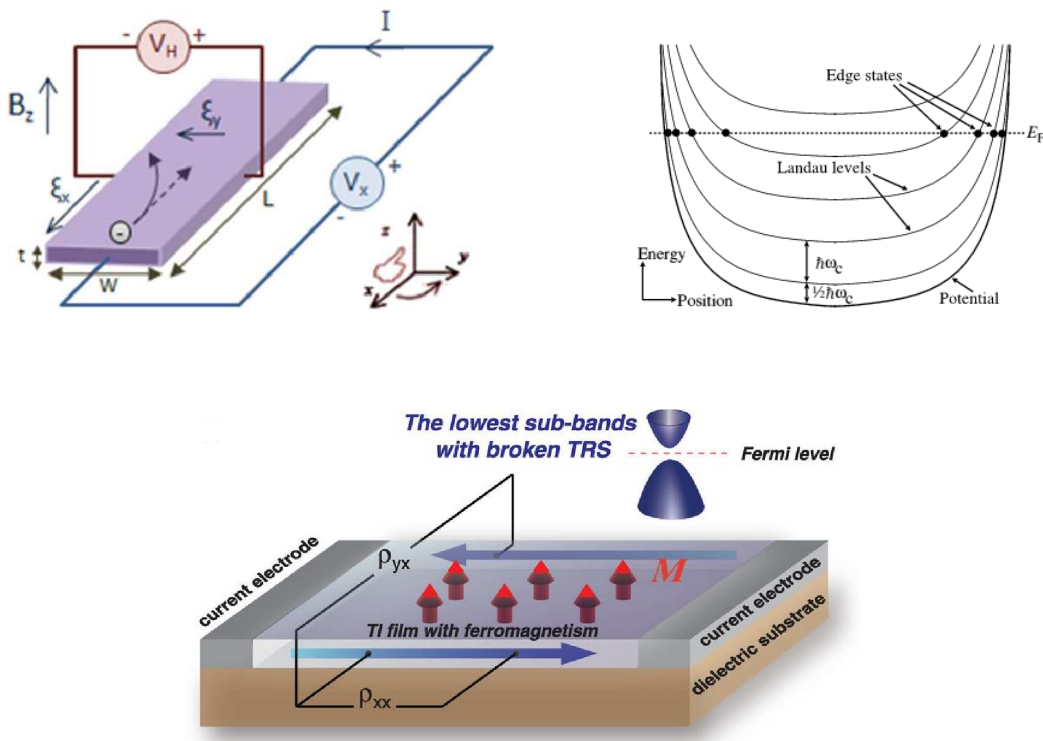


FIG. 2: **Up**: The usual QHE setup. The Hall current is transported due to the chiral edge modes which appear when the banded (due to presence of the confining potential) Landau levels cross the Fermi energy. Figures taken from *wikipedia*. **Down**: QAHE based on ferromagnetically doped topological insulator. Figure taken from the recent experiment [27].

conductivity. As a matter of fact, any single-particle Hamiltonian belongs to a particular **symmetry class** [1, 11, 12], depending on whether it preserves or violates a specific set of symmetries. For each one of these symmetry classes, there can be a topological invariant depending on the dimensionality. In order to study the related topological invariant, e.g. Hall conductivity, that characterizes the corresponding symmetry class we may study a single representative system that belongs to the class. Of course, the investigation of the representative system is useful only for understanding the topological properties of systems belonging to the same symmetry class, since no information concerning the non-topological features can be generalized. Similarly to the case of the QHE, for which the existence of a non-zero topological invariant (the Hall conductivity which is a bulk property) implies the presence of topologically protected bound states confined at the boundaries of the system, we expect topologically protected boundary solutions for all the “bulk” Hamiltonians for which we can define some kind of topological invariant quantity  $\tilde{N}$ . This generalization is termed “**bulk-boundary**” correspondence (or index theorem) and it dictates that: *For two materials with values  $\tilde{N}$  and  $\tilde{N}'$  for the corresponding topological invariant related to the given symmetry class, there should exist a number of  $|\tilde{N} - \tilde{N}'|$  topologically protected modes confined in the vicinity of the boundary separating the two materials.*

For the case of the QHE, the presence of chiral edge modes can be understood via the theory of electromagnetism. The boundaries separate the topological material, which is experiencing a finite external magnetic field, from the vacuum where the magnetic field is zero. Nonetheless, the vacuum can be also considered as a topological system with zero-Hall conductivity  $\sigma'_{xy} = 0$ . Essentially, based on electromagnetism and the boundary condition for the magnetic field  $\mathbf{n} \times (\mathbf{B} - \mathbf{B}') = \mathbf{J}_{\text{bound}}$  ( $\mathbf{n}$  the unit vector normal to the boundary), a boundary current  $\mathbf{J}_{\text{bound}}$  has to appear in order to satisfy the constraint that the electromagnetic field is zero in the vacuum. In the case that our material borders some other material (not vacuum) with quantized Hall conductivity  $\sigma'_{xy} = \tilde{N}'e^2/h$ , it is clearly understood that the continuity of the electromagnetic field would impose the appearance of  $|\tilde{N} - \tilde{N}'|$  solutions living at the boundary separating the two materials. The bulk-boundary correspondence generalizes this continuity principle of the electromagnetic field and the unavoidable appearance of boundary currents discussed above, to other topological invariant quantities and related “currents” that have to appear at the “boundaries” separating two materials with values  $\tilde{N}$  and  $\tilde{N}'$  for the corresponding topological invariant.

## II. SYMMETRIES AND TOPOLOGICAL CLASSIFICATION

In order to topologically classify single-particle Hamiltonians, we have to go through the symmetries that categorize the latter in the *ten* symmetry classes [1, 11, 12]. Generally, within the quantum mechanical description, a symmetry transformation acts on the wavefunction in the following manner

$$\phi'(\mathbf{r}) = \widehat{\mathcal{O}}\phi(\mathbf{r}), \quad (1)$$

where  $\widehat{\mathcal{O}}$  corresponds to the symmetry transformation operator. For instance if we want to translate the system by  $a$  along the direction defined by the unit vector  $\mathbf{n}$ , i.e.  $\mathbf{r}' = \mathbf{r} + a\mathbf{n}$ , we must act with the translation operator  $\hat{t}_a^{\mathbf{n}} = e^{-ian \cdot \hat{\mathbf{p}}/\hbar}$ , where  $\hat{\mathbf{p}}$  defines the momentum operator. It is straightforward to see that for an infinitesimal translation  $a$ , we have

$$\phi'(\mathbf{r}) = e^{-ian \cdot \hat{\mathbf{p}}/\hbar}\phi(\mathbf{r}) \simeq (1 - ian \cdot \hat{\mathbf{p}}/\hbar)\phi(\mathbf{r}) = (1 - a\mathbf{n} \cdot \nabla)\phi(\mathbf{r}) \simeq \phi(\mathbf{r} - a\mathbf{n}). \quad (2)$$

Note that the particular transformation property was expected, since we can equivalently write that

$$\phi'(\mathbf{r} + a\mathbf{n}) = \phi(\mathbf{r}) \quad \Rightarrow \quad \phi'(\mathbf{r}') = \phi(\mathbf{r}). \quad (3)$$

In a similar fashion, a rotation by an angle  $\theta$  about an axis with direction  $\mathbf{n}$  would be effected using the following rotation operator  $\hat{R}_\theta^{\mathbf{n}} = e^{-i\theta\mathbf{n} \cdot \hat{\mathbf{L}}/\hbar}$ , where  $\hat{\mathbf{L}} = \hat{\mathbf{r}} \times \hat{\mathbf{p}}$  defines the angular momentum operator. If the wavefunction  $\phi(\mathbf{r})$  is instead a spinor  $\hat{\phi}(\mathbf{r})$ , then a rotation will be generated by the total angular momentum  $\hat{\mathbf{J}} = \hat{\mathbf{L}} + \hat{\mathbf{S}}$ . For a spin-1/2, we have  $\hat{\mathbf{S}} = \hbar\boldsymbol{\sigma}/2$ , where  $\boldsymbol{\sigma}$  define the Pauli matrices. Since we know the transformation properties of the wave-function, we can readily determine the transformation of any operator  $\hat{A}$ , by requiring that the matrix elements remain the same. Specifically, we have:

$$\int d\mathbf{r} \phi^*(\mathbf{r})\hat{A}'\phi(\mathbf{r}) = \int d\mathbf{r} [\phi^*(\mathbf{r})]'\hat{A}[\phi(\mathbf{r})]' \Rightarrow \int d\mathbf{r} \phi^*(\mathbf{r})\hat{A}'\phi(\mathbf{r}) = \int d\mathbf{r} \phi^*(\mathbf{r})\widehat{\mathcal{O}}^\dagger\hat{A}\widehat{\mathcal{O}}\phi(\mathbf{r}) \Rightarrow \hat{A}' = \widehat{\mathcal{O}}^\dagger\hat{A}\widehat{\mathcal{O}}. \quad (4)$$

Of course for the particular description of our wavefunction (defined in coordinate space  $\mathbf{r}$ ), we may also view the position vector  $\mathbf{r}$  as an operator  $\hat{\mathbf{r}}$ . In this way we may indeed verify that for a translation  $\hat{t}_a^{\mathbf{n}}$  we obtain from the operator formula

$$\hat{\mathbf{r}}' = (\hat{t}_a^{\mathbf{n}})^\dagger \hat{\mathbf{r}} \hat{t}_a^{\mathbf{n}} = e^{ian \cdot \hat{\mathbf{p}}/\hbar} \hat{\mathbf{r}} e^{-ian \cdot \hat{\mathbf{p}}/\hbar} = \hat{\mathbf{r}} + a\mathbf{n}, \quad (5)$$

as expected. Nonetheless, all the above transformations belong to the space group transformations (translations and point group) and all share two common characteristics. The first is that in a completely disordered system they will be **all** broken. The second is that they are all **unitary**, i.e. they do not additionally effect complex-conjugation. Note that if we consider the complex number  $z$ , the effect of a unitary transformation will provide  $z' = \widehat{\mathcal{O}}_u^\dagger z \widehat{\mathcal{O}}_u = z$  while for an **anti-unitary** we have  $z' = \widehat{\mathcal{O}}_a^\dagger z \widehat{\mathcal{O}}_a = z^*$ . In fact one can introduce the complex conjugation operator  $\widehat{\mathcal{K}}$  which only effects complex conjugation and satisfies  $\widehat{\mathcal{K}}^2 = \hat{I}$ . In this manner, any anti-unitary operator can be written as a product of a unitary operator and  $\widehat{\mathcal{K}}$ . A familiar example of an anti-unitary operator, is of course time-reversal  $\widehat{\mathcal{T}}$  which has the following action on the following basic operators

$$\widehat{\mathcal{T}}^\dagger \hat{\mathbf{r}} \widehat{\mathcal{T}} = +\hat{\mathbf{r}}, \quad \widehat{\mathcal{T}}^\dagger \hat{\mathbf{p}} \widehat{\mathcal{T}} = -\hat{\mathbf{p}}, \quad \widehat{\mathcal{T}}^\dagger \hat{\mathbf{J}} \widehat{\mathcal{T}} = -\hat{\mathbf{J}}. \quad (6)$$

With the help of  $\widehat{\mathcal{K}}$ , we can write the time-reversal operator in the following way

$$\widehat{\mathcal{T}} = e^{i\pi\hat{S}_y/\hbar}\widehat{\mathcal{K}}. \quad (7)$$

For spin-1/2 fermions, like electrons, we have  $\hat{S}_y = \hbar\sigma_y/2$  and consequently  $\widehat{\mathcal{T}} = i\sigma_y\widehat{\mathcal{K}}$ . Notice that  $\widehat{\mathcal{T}}^2 = -\hat{I}$  which is characteristic for systems with half-integer spin. In contrast, for systems with integer spin, we obtain  $\widehat{\mathcal{T}}^2 = \hat{I}$ . In the first case, the negative sign yields Kramers' degeneracy, i.e. every state is doubly degenerate and the two states are connected by time-reversal symmetry. For instance for electrons in the absence of a magnetic field, the states with spin-up and spin-down are degenerate. For the second case, time-reversal operator resembles to the usual complex-conjugation operator  $\widehat{\mathcal{K}}$ . In this case, the presence of time-reversal symmetry which squares to identity, implies that the Hamiltonian can be rewritten in an appropriate basis as a real matrix-operator.

The most significant feature of anti-unitary symmetries is that in contrast to the unitary ones, they can be still preserved even in disordered systems. For every system with **no** unitary symmetries present, i.e. we cannot find an operator  $\hat{\mathcal{O}}$  satisfying  $[\hat{\mathcal{H}}(\hat{\mathbf{p}}, \hat{\mathbf{r}}), \hat{\mathcal{O}}] = 0$ , there exist only two anti-unitary symmetries: a generalized time-reversal symmetry with operator  $\hat{\Theta}$  and a generalized charge-conjugation symmetry with operator  $\hat{\Xi}$ , which if they are present they satisfy the following relations:

$$\hat{\Theta}^\dagger \hat{\mathcal{H}}(\hat{\mathbf{p}}, \hat{\mathbf{r}}) \hat{\Theta} = +\hat{\mathcal{H}}(\hat{\mathbf{p}}, \hat{\mathbf{r}}) \Rightarrow [\hat{\mathcal{H}}(\hat{\mathbf{p}}, \hat{\mathbf{r}}), \hat{\Theta}] = 0, \quad (8)$$

$$\hat{\Xi}^\dagger \hat{\mathcal{H}}(\hat{\mathbf{p}}, \hat{\mathbf{r}}) \hat{\Xi} = -\hat{\mathcal{H}}(\hat{\mathbf{p}}, \hat{\mathbf{r}}) \Rightarrow \{\hat{\mathcal{H}}(\hat{\mathbf{p}}, \hat{\mathbf{r}}), \hat{\Xi}\} = 0. \quad (9)$$

Observe that for a system with both symmetries present one can define a new symmetry which is called: chiral symmetry, with a **unitary** operator  $\hat{\Pi} \equiv \hat{\Xi} \hat{\Theta}$  which satisfies

$$\hat{\Pi}^\dagger \hat{\mathcal{H}}(\hat{\mathbf{p}}, \hat{\mathbf{r}}) \hat{\Pi} = -\hat{\mathcal{H}}(\hat{\mathbf{p}}, \hat{\mathbf{r}}) \Rightarrow \{\hat{\mathcal{H}}(\hat{\mathbf{p}}, \hat{\mathbf{r}}), \hat{\Pi}\} = 0. \quad (10)$$

Nonetheless, a Hamiltonian can have a chiral symmetry without the necessary presence of a time-reversal symmetry and a charge-conjugation symmetry. Note also that chiral symmetry is not a unitary symmetry with the usual sense, since it anti-commutes with the Hamiltonian. By taking into account the sign of  $\hat{\Xi}^2$  and  $\hat{\Theta}^2$ , one can define the **ten** symmetry classes mentioned earlier, which are presented in the following table:

| Symmetry |          |       |       | $d$            |                |                |                |                |                |                |                |
|----------|----------|-------|-------|----------------|----------------|----------------|----------------|----------------|----------------|----------------|----------------|
| AZ       | $\Theta$ | $\Xi$ | $\Pi$ | 1              | 2              | 3              | 4              | 5              | 6              | 7              | 8              |
| A        | 0        | 0     | 0     | 0              | $\mathbb{Z}$   | 0              | $\mathbb{Z}$   | 0              | $\mathbb{Z}$   | 0              | $\mathbb{Z}$   |
| AIII     | 0        | 0     | 1     | $\mathbb{Z}$   | 0              | $\mathbb{Z}$   | 0              | $\mathbb{Z}$   | 0              | $\mathbb{Z}$   | 0              |
| AI       | 1        | 0     | 0     | 0              | 0              | 0              | $\mathbb{Z}$   | 0              | $\mathbb{Z}_2$ | $\mathbb{Z}_2$ | $\mathbb{Z}$   |
| BDI      | 1        | 1     | 1     | $\mathbb{Z}$   | 0              | 0              | 0              | $\mathbb{Z}$   | 0              | $\mathbb{Z}_2$ | $\mathbb{Z}_2$ |
| D        | 0        | 1     | 0     | $\mathbb{Z}_2$ | $\mathbb{Z}$   | 0              | 0              | 0              | $\mathbb{Z}$   | 0              | $\mathbb{Z}_2$ |
| DIII     | -1       | 1     | 1     | $\mathbb{Z}_2$ | $\mathbb{Z}_2$ | $\mathbb{Z}$   | 0              | 0              | 0              | $\mathbb{Z}$   | 0              |
| AII      | -1       | 0     | 0     | 0              | $\mathbb{Z}_2$ | $\mathbb{Z}_2$ | $\mathbb{Z}$   | 0              | 0              | 0              | $\mathbb{Z}$   |
| CII      | -1       | -1    | 1     | $\mathbb{Z}$   | 0              | $\mathbb{Z}_2$ | $\mathbb{Z}_2$ | $\mathbb{Z}$   | 0              | 0              | 0              |
| C        | 0        | -1    | 0     | 0              | $\mathbb{Z}$   | 0              | $\mathbb{Z}_2$ | $\mathbb{Z}_2$ | $\mathbb{Z}$   | 0              | 0              |
| CI       | 1        | -1    | 1     | 0              | 0              | $\mathbb{Z}$   | 0              | $\mathbb{Z}_2$ | $\mathbb{Z}_2$ | $\mathbb{Z}$   | 0              |

FIG. 3: The ten symmetry classes categorized using  $\hat{\Theta}^2 = \pm \hat{I}(\pm 1)$ ,  $\hat{\Xi}^2 = \pm \hat{I}(\pm 1)$  for the cases in which the respective symmetries  $\hat{\Theta}$  and  $\hat{\Xi}$  are present. If  $\hat{\Pi}$  is present (not-present) we just have 1(0). The spatial-dimensionality is given by  $d$ . With  $\mathbb{Z}$ (integer) and  $\mathbb{Z}_2(\pm 1)$  we denote the cases where a topological invariant quantity can be defined. For the rest of the cases we cannot define a topological invariant for the given dimensionality. Note that there exist a periodicity, the so-called ‘‘Bott’’ periodicity, with respect to the dimensionality  $d$ , i.e.  $d + 8 \rightarrow d$ . Figure taken from [18].

### III. QUANTUM ANOMALOUS HALL EFFECT IN A JACKIW AND REBBI-LIKE MODEL

Here we present a simple model exhibiting non-trivial topological properties. We will consider both one- and two-dimensional cases. In  $d = 1$  this model is akin to Jackiw and Rebbi model proposed in 1976 [28] in the context of high energy physics, addressing the 1d-Dirac equation in the presence of solitons. Later it was revisited by Su, Schrieffer and Heeger (SSH model) for studying solitons in polyacetylene [29]. By extending this model to  $d = 2$ , we obtain a model exhibiting the QAHE due to emergence of chiral edge modes, which follows Haldane’s earlier proposal [24].

### A. 1d model - zero-energy bound states with fixed chirality

We will now consider the following 1d-Dirac type of Hamiltonian

$$\hat{\mathcal{H}}(\hat{p}_x, x) = v\hat{p}_x\sigma_y + M(x)\sigma_z, \quad (11)$$

which describes electrons in a Rashba spin-orbit coupled wire in the additional presence of an inhomogeneous magnetic field. Here the most important property is that the magnetic profile is chosen to satisfy the following boundary conditions (Fig. 4):

$$M(x \rightarrow \pm\infty) = -M, \quad M(x) < 0 \quad \text{for } x \in (-\infty, x_1) \cup (x_2, +\infty) \quad \text{and} \quad M(x) > 0 \quad \text{for } x \in (x_1, x_2). \quad (12)$$

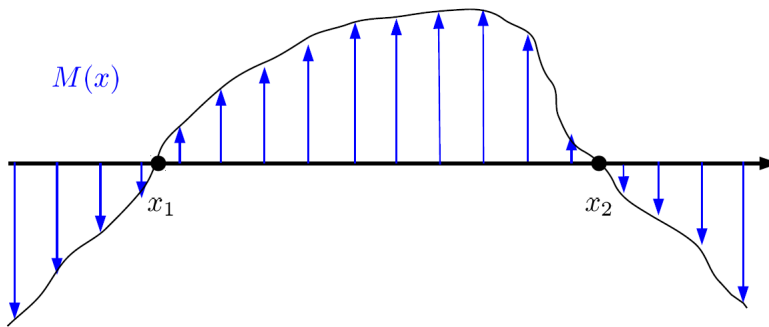


FIG. 4: A general inhomogeneous magnetization profile which leads to zero-energy solutions confined at the boundary points  $x_{1,2}$  separating areas where the magnetization changes sign.

Essentially the particular profile dictates that the magnetization is characterized by two domain walls at the points  $x_1, x_2$ . Each domain wall corresponds to a solitonic configuration of the magnetization field, where we interpolate from a solution with  $\text{sign}(M) = +1$  to a solution with  $\text{sign}(M) = -1$ . Below we will show that the particular Hamiltonian supports zero energy edge states localized at the domain walls, which play the role of boundaries for the areas with different sign of magnetization. Let us first determine the symmetries of the Hamiltonian above. First we can find an anticommuting matrix  $\hat{\Pi} = \sigma_x$  which leads to a chiral symmetry. Furthermore, we find a generalized time-reversal symmetry  $\hat{\Theta} = \hat{\mathcal{K}}$ . This also implies the presence of a generalized charge conjugation symmetry with  $\hat{\Xi} = \sigma_x \hat{\mathcal{K}}$ . Since  $\hat{\Theta}^2 = \hat{I}$  and  $\hat{\Xi}^2 = \hat{I}$ , the table of the symmetry classes of Fig. 3 yields that the symmetry class of the system is BDI. The same table tells us that for  $d = 1$  we can in principle define a  $\mathbb{Z}$  topological invariant. At some other point we will see how we can define this invariant. For now it is clear that since we are in position to define a topological invariant, it implies that the above Hamiltonian constitutes a candidate for a system exhibiting some non-trivial topological properties. These properties are clearly linked to the zero-energy states that we will show that exist.

Based on the existence of chiral symmetry we have the following property: for every solution of the Hamiltonian  $\hat{\phi}_\nu(x)$  with eigen-energy  $E_\nu$ , we will find another solution with eigen-energy  $-E_\nu$ , which is given by  $\hat{\Pi}\hat{\phi}_\nu(x) = \sigma_x\hat{\phi}_\nu(x)$ . This is easy to show by assuming that

$$\hat{\mathcal{H}}(\hat{p}_x, x)\hat{\Pi}\hat{\phi}_\nu(x) = \bar{E}_\nu\hat{\Pi}\hat{\phi}_\nu(x) \Rightarrow -\hat{\Pi}\hat{\mathcal{H}}(\hat{p}_x, x)\hat{\phi}_\nu(x) = \bar{E}_\nu\hat{\Pi}\hat{\phi}_\nu(x) \Rightarrow \hat{\mathcal{H}}(\hat{p}_x, x)\hat{\phi}_\nu(x) = -\bar{E}_\nu\hat{\phi}_\nu(x) \Rightarrow \bar{E}_\nu = -E_\nu \quad (13)$$

If there exists a non-degenerate zero-energy solution, then  $E_\nu \leftrightarrow -E_\nu$  and the same holds for the eigen-vectors  $\hat{\phi}_\nu(x) \leftrightarrow \hat{\Pi}\hat{\phi}_\nu(x)$ , implying that the zero-energy solutions constitute eigenstates of the chiral symmetry operator  $\hat{\Pi} = \sigma_x$ .

Let's now solve the above Hamiltonian for the following stepwise magnetic profile (Fig. 5):

$$M(x) = -M + 2M\Theta(x - x_1) - 2M\Theta(x - x_2), \quad (14)$$

where we assume that  $x_2 - x_1 \rightarrow \infty$ . For each region  $s = l, m, r$ , the magnetic moment is constant  $M_l = M_r = -M$  and  $M_m = +M$  and therefore we can Fourier transform and solve the corresponding partial translationally invariant Schrödinger's equations

$$\hat{\mathcal{H}}_s(k) = v\hbar k\sigma_y + M_s\sigma_z, \quad s = l, m, r. \quad (15)$$

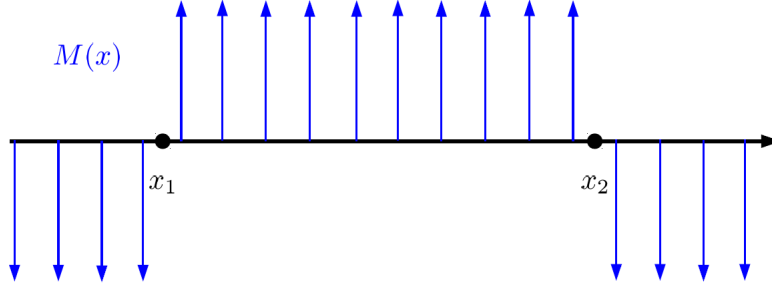


FIG. 5: A stepwise magnetization profile which leads to zero-energy solutions confined at the boundary points  $x_{1,2}$  separating areas where the magnetization changes sign.

However for these systems the wave-vector  $k$  is not a good quantum number anymore, since translational invariance is broken. Nonetheless, the energy is still a good quantum number. This implies that for the particular system instead of having  $E(k)$  we instead have  $k_s(E)$  for  $s = l, m, r$ . Using the arising relativistic energy spectrum, which has the form

$$E = \pm \sqrt{(v\hbar k_s)^2 + M_s^2}, \quad (16)$$

we find that for a specific energy  $E$ , the corresponding  $k_s$ 's are given by

$$v\hbar k_s = \pm \sqrt{E^2 - M_s^2}. \quad (17)$$

However, since for the particular selection  $M_s^2 = M^2$  for  $s = l, m, r$  we simply have for all regions that

$$v\hbar k_s = \pm \sqrt{E^2 - M^2}. \quad (18)$$

Since we are looking for zero energy states, we set  $E = 0$  which leads to the following equation per segment

$$(v\hbar k\sigma_y + M_s\sigma_z) \hat{\phi}_{0,s}(k) = 0 \Rightarrow (v\hbar k + iM_s\sigma_x) \hat{\phi}_{0,s}(k) = 0 \Rightarrow (v\hbar k + i\sigma M_s) \hat{\phi}_{0,s}^\sigma(k) = 0 \Rightarrow v\hbar k_{s,\sigma} = -i\sigma M_s, \quad (19)$$

where the quantum number  $\sigma = \pm 1$  labels the eigen-vectors of the  $\sigma_x$  matrix. We directly confirm that the zero-energy solutions of the particular model constitute eigen-vectors of the chiral symmetry operator. Now that we have found the expression for the zero-energy solutions for each segment, we use the wave-function matching technique in order to find the zero-energy solution defined in whole space. We write for every segment:

$$\hat{\phi}_{0,s}(x) = c_{s,+} e^{+\frac{M_s}{v\hbar}x} \frac{1}{\sqrt{2}} \begin{pmatrix} 1 \\ 1 \end{pmatrix} + c_{s,-} e^{-\frac{M_s}{v\hbar}x} \frac{1}{\sqrt{2}} \begin{pmatrix} 1 \\ -1 \end{pmatrix}, \quad (20)$$

while we also have to satisfy the boundary conditions  $\hat{\phi}_{0,l}(x \rightarrow -\infty) = \hat{\phi}_{0,r}(x \rightarrow +\infty) = 0$ . This yields the following expression for the wave-functions

$$\begin{aligned} \hat{\phi}_{0,l}(x) &= c_{l,-} e^{+\frac{M}{v\hbar}x} \frac{1}{\sqrt{2}} \begin{pmatrix} 1 \\ -1 \end{pmatrix}, \\ \hat{\phi}_{0,m}(x) &= c_{m,-} e^{-\frac{M}{v\hbar}x} \frac{1}{\sqrt{2}} \begin{pmatrix} 1 \\ -1 \end{pmatrix} + c_{m,+} e^{+\frac{M}{v\hbar}x} \frac{1}{\sqrt{2}} \begin{pmatrix} 1 \\ 1 \end{pmatrix}, \\ \hat{\phi}_{0,r}(x) &= c_{r,+} e^{-\frac{M}{v\hbar}x} \frac{1}{\sqrt{2}} \begin{pmatrix} 1 \\ 1 \end{pmatrix}. \end{aligned} \quad (21)$$

Now we will determine the remaining coefficients using continuity at  $x_{1,2} \Rightarrow \hat{\phi}_{0,l}(x_1) = \hat{\phi}_{0,m}(x_1), \hat{\phi}_{0,m}(x_2) = \hat{\phi}_{0,r}(x_2)$  and the normalization of the wave-function. Furthermore, we will assume that  $x_2 - x_1 \rightarrow \infty$  so that in the vicinity of  $x = x_1$  we will approximate

$$\hat{\phi}_{0,m}(x) \simeq c_{m,-} e^{-\frac{M}{v\hbar}x} \frac{1}{\sqrt{2}} \begin{pmatrix} 1 \\ -1 \end{pmatrix} \quad (22)$$

while in the vicinity of  $x = x_2$  we will approximate

$$\hat{\phi}_{0,m}(x) \simeq c_{m,+} e^{+\frac{M}{v\hbar}x} \frac{1}{\sqrt{2}} \begin{pmatrix} 1 \\ 1 \end{pmatrix}. \quad (23)$$

Under these conditions we obtain  $c_{l,-} = c_- e^{-Mx_1/(v\hbar)}$ ,  $c_{m,-} = c_- e^{Mx_1/(v\hbar)}$ ,  $c_{m,+} = c_+ e^{-Mx_2/(v\hbar)}$ ,  $c_{r,+} = c_+ e^{Mx_2/(v\hbar)}$ , with  $c_{\pm}$  to be determined by the normalization of the wave-functions. After these steps we end up with the following two localized solutions at the points  $x_1$  and  $x_2$  respectively (Fig. 6)

$$\hat{\phi}_{0,-}(x) = c_- e^{-\frac{M}{v\hbar}|x-x_1|} \frac{1}{\sqrt{2}} \begin{pmatrix} 1 \\ -1 \end{pmatrix} \quad \text{and} \quad \hat{\phi}_{0,+}(x) = c_+ e^{-\frac{M}{v\hbar}|x-x_2|} \frac{1}{\sqrt{2}} \begin{pmatrix} 1 \\ 1 \end{pmatrix}. \quad (24)$$

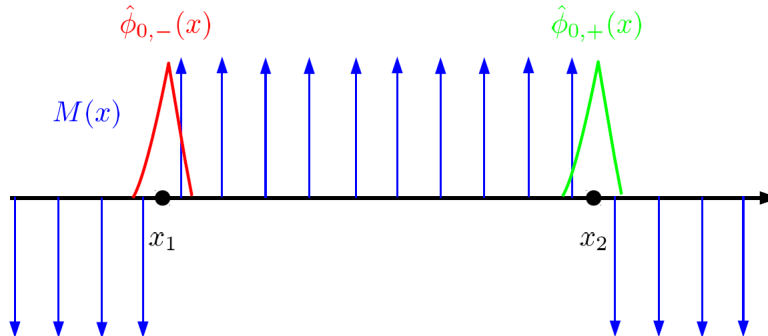


FIG. 6: Zero-energy solutions with specific chirality  $\sigma = \pm 1$  located at the boundaries separating the areas of different magnetization. In general the two solutions have an exponentially decaying overlap  $\propto e^{-\text{const} \cdot (x_2 - x_1)}$  and therefore correspond to exactly zero-energy solutions only for  $x_2 - x_1 \rightarrow \infty$ .

#### Comments:

- Note that the edge states have half the degrees of freedom of the original electrons [28], since chirality is fixed to  $\pm 1$  respectively per edge solution.
- Since edge states appear at the boundaries separating segments of different magnetic moment, this implies that there should be a topological invariant with alternating sign along successive segments of the material.
- Note that the edge states appear at the points where  $M(x) = 0$ . This corresponds to the gap closing points of the bulk spectrum  $E = \pm \sqrt{(v\hbar k_x)^2 + M^2}$  at  $k_x = 0$ .

#### B. 2d model - chiral edge modes - QAHE

We will now consider the following 2d extension of the previous Hamiltonian

$$\hat{\mathcal{H}}(\hat{\mathbf{p}}, x) = v(\hat{p}_x \sigma_y - \hat{p}_y \sigma_x) + M(x) \sigma_z, \quad (25)$$

where we have also included the remaining component of the Rashba spin-orbit interaction. We have assumed that our system is translationally invariant along the  $y$ -direction. Due to translational invariance we expect to find dispersive electronic modes running along the  $y$ -direction, since the wave-vector  $k_y$  is a good quantum number. Let's proceed with studying the symmetries of this 2d Hamiltonian. It is clear that the symmetries of the new Hamiltonian will belong to a subset of the symmetries of the 1d model. First of all the addition of the third Pauli matrix breaks chiral symmetry  $\hat{\Pi}$ . This also implies that we may only have up to one remaining anti-unitary symmetry left. It is straightforward to check that only  $\hat{\Xi} = \sigma_x \hat{\mathcal{K}}$  persists. Consequently, the Hamiltonian lies in symmetry class D. From the symmetry class table we can see that, in 2d, class D supports a  $\mathbb{Z}$  topological invariant. This implies that we can still have non-trivial topological properties for the particular Hamiltonian and they are going to be closely connected to the non-trivial topological content of the 1d model. To clearly demonstrate this, we restrict ourselves to the low

energy sector of the 1d model. Essentially we will consider the two zero-energy solutions. In the 2d model, these originally zero-energy solutions become dispersive, i.e. depend on  $k_y$ . In fact we introduce the related wave-functions

$$\hat{\phi}_{0,-,k_y}(\mathbf{r}) = c_- e^{ik_y y} e^{-\frac{M}{v\hbar}|x-x_1|} \frac{1}{\sqrt{2}} \begin{pmatrix} 1 \\ -1 \end{pmatrix} \quad \text{and} \quad \hat{\phi}_{0,+,k_y}(\mathbf{r}) = c_+ e^{ik_y y} e^{-\frac{M}{v\hbar}|x-x_2|} \frac{1}{\sqrt{2}} \begin{pmatrix} 1 \\ 1 \end{pmatrix} \quad (26)$$

and we directly observe that they satisfy the 2d Hamiltonian above

$$[v(\hat{p}_x \sigma_y - \hat{p}_y \sigma_x) + M(x) \sigma_z] \hat{\phi}_{0,\sigma,k_y}(\mathbf{r}) = E_\sigma(k_y) \hat{\phi}_{0,\sigma,k_y}(\mathbf{r}), \quad (27)$$

only if  $E_\sigma(k_y) = -\sigma v \hbar k_y$  (Fig. 7). The latter linear dispersion depends on the chirality of the eigen-state and that is why it is called **chiral**. This has to be compared with the chiral edge modes found in the quantum Hall effect. In the present case they give rise to the quantum anomalous Hall effect [27] where there is no necessity for an external magnetic field  $\mathbf{B}$ . The solution located at the left (right) edge has chirality  $\sigma = -1$  (+1) and an energy dispersion  $E^{left}(k_y) = +v \hbar k_y$  ( $E^{right}(k_y) = -v \hbar k_y$ ).

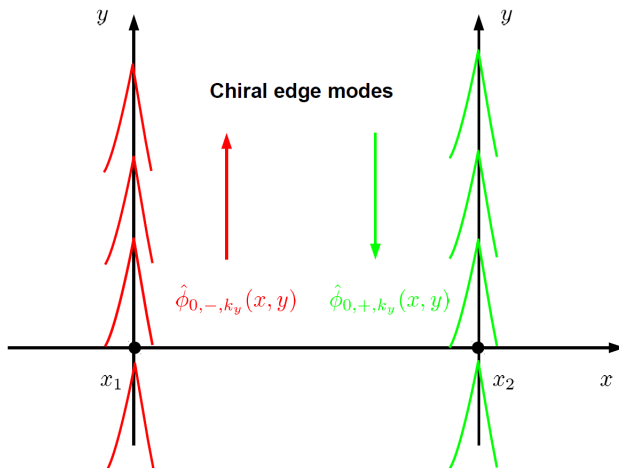


FIG. 7: The previously zero-energy solutions of the 1d model owing specific chirality become dispersive chiral edge modes in the 2d case.

### C. Non relativistic kinetic term - disorder - symmetry class transition - topological protection

In the models above, we considered a somehow artificial situation where we neglected the usual quadratic kinetic term or the presence of impurities. Let's now study the symmetry class modification that is introduced when we add the usual kinetic term or introduce disorder to the system.

- 1d model:

$$\hat{\mathcal{H}}(\hat{p}_x, x) = \frac{\hat{p}_x^2}{2m} - \mu + v \hat{p}_x \sigma_y + M(x) \sigma_z. \quad (28)$$

Due to the presence of the kinetic term, the chiral and charge-conjugation symmetries are broken, while  $\hat{\Theta} = \hat{\mathcal{K}}$  persists. We have the following symmetry class transition  $\text{BDI} \rightarrow \text{AI}$ . We observe that the latter symmetry class does not support any topological invariant in  $d = 1$  and therefore even if we can find some bound states at  $x_1, x_2$  they will not be topologically protected. We would obtain the same effect if we would add to our Hamiltonian disorder via a random potential  $V(x)$ .

- 2d model:

$$\hat{\mathcal{H}}(\hat{\mathbf{p}}, x) = \frac{\hat{\mathbf{p}}^2}{2m} - \mu + v(\hat{p}_x \sigma_y - \hat{p}_y \sigma_x) + M(x) \sigma_z. \quad (29)$$

In the absence of the non-relativistic term, the Hamiltonian above belongs to symmetry class D, with only the charge-conjugation present. Due to the presence of the kinetic term, the charge-conjugation symmetry will become broken and the system will undergo the symmetry class transition  $D \rightarrow A$  which can be also characterized by a  $\mathbb{Z}$  invariant in 2d. In this manner, we observe that the  $d = 2$  dimensionality can support topologically protected edge modes for the particular Hamiltonian. Notice that in principle the edge modes will be also protected against disorder, since the symmetry class remains the same.

#### IV. QUANTUM ANOMALOUS HALL EFFECT IN A $\mathcal{T}$ -VIOLATING TOPOLOGICAL INSULATOR MODEL

Let's now proceed with another model that exhibits bound states in 1d and chiral edge modes in 2d. On one hand the latter study will illustrate the fact that different systems belonging to the same symmetry class share a number of common properties but on the other, it will provide a direct connection to realistic models describing the bulk band structure of 2d topological insulators [4].

##### A. 1d model

The 1d model under consideration is obtained by the **bulk** 1d Jackiw-Rebbi model in Eq. (15) simply by replacing the constant magnetization  $M$  with a momentum dependent magnetization  $M(\hat{p}_x) = m - \hat{p}_x^2$ . The latter replacement leads to the Hamiltonian

$$\hat{\mathcal{H}}(\hat{p}_x) = v\hat{p}_x\sigma_y + (m - \hat{p}_x^2)\sigma_z, \quad (30)$$

with  $m$  a constant. This type of magnetization term can naturally appear for  $\mathcal{T}$ -violating semiconducting systems where  $s$ - and  $p$ - orbitals are involved for the conduction and valence bands, respectively [4]. The aforementioned Hamiltonian is particularly relevant for the QAHE observed just recently [27] in ferromagnetically doped 2d  $\mathcal{T}$ -preserving topological insulators. In fact, as we will also discuss later, the Hamiltonian describing the physics of  $\mathcal{T}$ -invariant HgTe/CdTe semiconducting quantum wells consists of two time-reversed copies [4] of the Hamiltonian appearing in Eq. (30). Since the Hamiltonian of Eq. (30) is only a function of momentum and not of the coordinate  $x$ , we can readily Fourier transform and for an infinite system we obtain the bulk Hamiltonian

$$\hat{\mathcal{H}}(k_x) = v\hbar k_x\sigma_y + (m - \hbar^2 k_x^2)\sigma_z. \quad (31)$$

Let us now study the symmetries of the particular Hamiltonian. Note that complex conjugation acts on the wave-vector in the following manner  $\hat{\mathcal{K}}^\dagger k_x \hat{\mathcal{K}} = -k_x$ . We directly observe the presence of chiral symmetry  $\hat{\Pi} = \sigma_x$ , time-reversal symmetry  $\hat{\Theta} = \hat{\mathcal{K}}$  and charge-conjugation symmetry  $\hat{\Xi} = \sigma_x \hat{\mathcal{K}}$ . Once again we encounter the symmetry class BDI and is natural to expect that also this model should exhibit zero-energy boundary solutions. Nonetheless, a question which naturally arises is what kind of boundaries should we consider in order to obtain zero-energy bound state solutions. In fact, due to the particular form of the Hamiltonian and more importantly due to the quadratic term in momentum, we have the possibility to obtain zero-energy bound state solutions by simply confining the electrons in a box. In fact, we will consider that the electrons are restricted to move in a box extended from  $x_1$  to  $x_2$ , due to the presence of an infinitely high positive confining potential  $V(x) = +\infty$  for  $x \in (-\infty, x_1] \cup [x_2, +\infty)$ . Since the electrons are confined between  $x_1$  and  $x_2$ , the electronic wave-function has to satisfy a hard-wall condition, i.e. it should be exactly zero at these points  $\hat{\phi}(x_1) = \hat{\phi}(x_2) = 0$ . One remark has to be made before proceeding. We can also obtain zero-energy edge states by considering domain walls similar to the Jackiw-Rebbi model via setting  $m(x) = -m + 2m\Theta(x - x_1) - 2m\Theta(x - x_2)$ . In this case the quadratic in momentum term becomes irrelevant since in the vicinity of the domain walls we can expand about  $k = 0$ , yielding the Jackiw-Rebbi model.

The introduction of infinitely high boundaries at  $x_1$  and  $x_2$  implies that the wave-vector is not a good quantum number. Only energy constitutes a good quantum number for labelling eigen-solutions. Since we are looking for zero-energy solutions we will consider the equation

$$[v\hbar k_x\sigma_y + (m - \hbar^2 k_x^2)\sigma_z] \hat{\phi}_0 = 0 \quad \Rightarrow \quad \hbar k_x = -i\sigma(v/2) \pm \sqrt{m - (v/2)^2}. \quad (32)$$

Similarly to the Jackiw-Rebbi model, the wave-vectors depend also here on the chirality  $\sigma = \pm 1$ . *However, we observe an important difference.* In the 1d Jackiw-Rebbi model, the zero-energy wave-vectors were strictly imaginary since  $M > 0$ . In the model considered in this paragraph, the quadratic term allows also for strictly real wave-vectors. In

the latter situation, the zero-energy states are not localized at the boundaries and leak into the bulk. Remember though that bulk-boundary correspondence dictates that a topologically non-trivial phase implies the presence of zero-energy bound state solutions. The disappearance of these bound states, while the symmetry class remains the same, signifies that the bulk system entered the topologically trivial phase. Consequently, the value of  $m$  for which a number of wave-vectors become strictly real marks the passage to the topologically trivial regime. This critical value of  $m_c$  is retrieved by setting  $\Im(k_x) = 0$ . The latter condition yields  $m_c = 0$ . Since the values of  $m$  span a 1d *parameter* space, we observe that this point in this parameter space constitutes the “boundary” separating the topologically trivial phase ( $m < m_c$ ) from the topologically non-trivial phase ( $m > m_c$ ) (see Fig. 8). One directly observes that for  $m = m_c = 0$ , the bulk spectrum exhibits a gap closing at  $k_x = 0$ . This gap closing for the infinite (bulk) system leads to a zero-energy mode which is the analog of the zero-energy bound state solution for the finite system. This is essentially the manifestation of bulk-boundary correspondence in this system, which should also be understood via the introduction of an appropriate topological invariant quantity, which should be finite only for  $m > m_c$ .

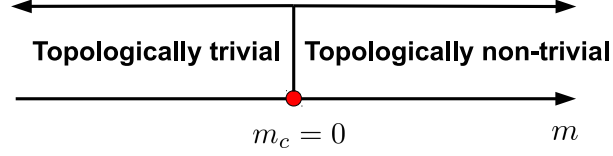


FIG. 8: Topological phase diagram in the parameter space spanned by the values of  $m$ . For  $m > m_c$  the systems becomes topologically non-trivial with zero-energy bound state solutions. For  $m < m_c$  the system lies in the topologically trivial phase. For  $m = m_c = 0$  the bulk spectrum exhibit a gap closing for  $k_x = 0$ . The passage from the topologically trivial to the topologically non-trivial phase (and vice versa) is realized through the gap closing of the bulk spectrum. In the bulk, the  $k_x = 0$  for  $m = m_c = 0$  constitutes a zero-energy mode, which is the analog of the zero-energy bound state solution in the finite size system.

We proceed now with retrieving the zero-energy bound state solutions. In the topologically non-trivial phase  $m > 0$  and we set  $k_x \equiv -i\sigma/l \pm a$  with  $a = \sqrt{m - (v/2)^2}/\hbar$  and  $1/l = v/(2\hbar) > 0$ . Note that the wave-vectors corresponding to zero-energy owe a specific decaying behaviour depending on the chirality  $\sigma = \pm 1$ . This directly yields at which boundary side, is a solution of specific chirality located. Since for  $\sigma = +1$  the wave-vector has a negative imaginary part, this chirality zero-energy solution lies on the right boundary ( $x = x_2$ ). Consequently, the  $\sigma = -1$  chirality solution lies on the left boundary ( $x = x_1$ ). By considering that  $x_2 - x_1 \rightarrow +\infty$  we can write the two solutions separately for the left and right boundaries:

$$\hat{\phi}_{0,-}(x) = \left[ c_{-,+} e^{ia(x-x_1)} + c_{-,-} e^{-ia(x-x_1)} \right] e^{-(x-x_1)/l} \frac{1}{\sqrt{2}} \begin{pmatrix} 1 \\ -1 \end{pmatrix}, \quad (33)$$

$$\hat{\phi}_{0,+}(x) = \left[ c_{+,+} e^{ia(x-x_2)} + c_{+,-} e^{-ia(x-x_2)} \right] e^{+(x-x_2)/l} \frac{1}{\sqrt{2}} \begin{pmatrix} 1 \\ 1 \end{pmatrix}. \quad (34)$$

Note that for  $m > (v/2)^2$  we obtain  $a = 1/\xi$  while if  $0 < m < (v/2)^2$  then  $a \equiv -i/\xi$  with  $\xi = \hbar/\sqrt{|m - (v/2)^2|} \in \mathbb{R}^+$ . By applying the hard-wall boundary condition we have  $\hat{\phi}_{0,-}(x_1) = 0$  and  $\hat{\phi}_{0,+}(x_2) = 0$  which is satisfied only if  $c_{\sigma,-} = -c_{\sigma,+}$  (Fig. 9). This leads to the cases (see also Fig. 10)

- $m > (v/2)^2 > 0$ :

$$\hat{\phi}_{0,-}(x) \propto \sin[(x - x_1)/\xi] e^{-(x-x_1)/l} \frac{1}{\sqrt{2}} \begin{pmatrix} 1 \\ -1 \end{pmatrix}, \quad (35)$$

$$\hat{\phi}_{0,+}(x) \propto \sin[(x - x_2)/\xi] e^{+(x-x_2)/l} \frac{1}{\sqrt{2}} \begin{pmatrix} 1 \\ 1 \end{pmatrix}. \quad (36)$$

- $0 < m < (v/2)^2$ :

$$\hat{\phi}_{0,-}(x) \propto \sinh[(x - x_1)/\xi] e^{-(x-x_1)/l} \frac{1}{\sqrt{2}} \begin{pmatrix} 1 \\ -1 \end{pmatrix}, \quad (37)$$

$$\hat{\phi}_{0,+}(x) \propto \sinh[(x - x_2)/\xi] e^{+(x-x_2)/l} \frac{1}{\sqrt{2}} \begin{pmatrix} 1 \\ 1 \end{pmatrix}. \quad (38)$$

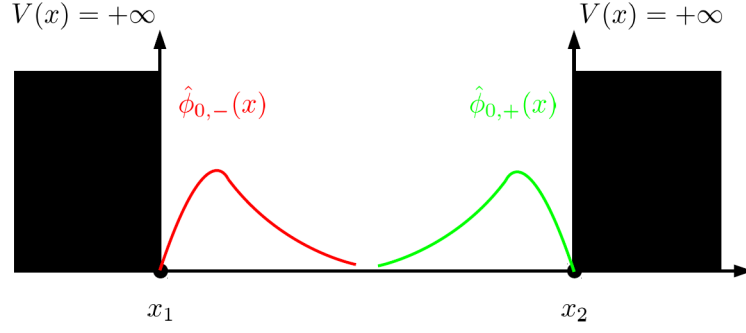


FIG. 9: Zero-energy bound states of opposite chirality  $\sigma = \pm 1$  (green, red). The latter zero energy bound state solutions are present only for  $m > 0$  and satisfy the hard-wall conditions  $\hat{\phi}_{0,-}(x_1) = 0$  and  $\hat{\phi}_{0,+}(x_2) = 0$ .

- $m = m_c = 0$ :

$$\hbar k_x = -iv \frac{\sigma \pm 1}{2}. \quad (39)$$

This shows that for  $m = 0$  one solution per chirality extends through the whole bulk since it corresponds to  $k_x = 0$  and becomes not “bound” any more.

- $m < 0$ : We observe that for each chirality the two related solutions have a decay factor that locates them in opposite boundaries. This implies that the hard wall conditions can be only satisfied if the corresponding eigen-vectors are the null vectors. In this case we transit to the topologically trivial phase with no zero-energy bound states. The latter situation is completely different compared to the case  $m > 0$  where solutions of the same chirality lie on the same boundary side.

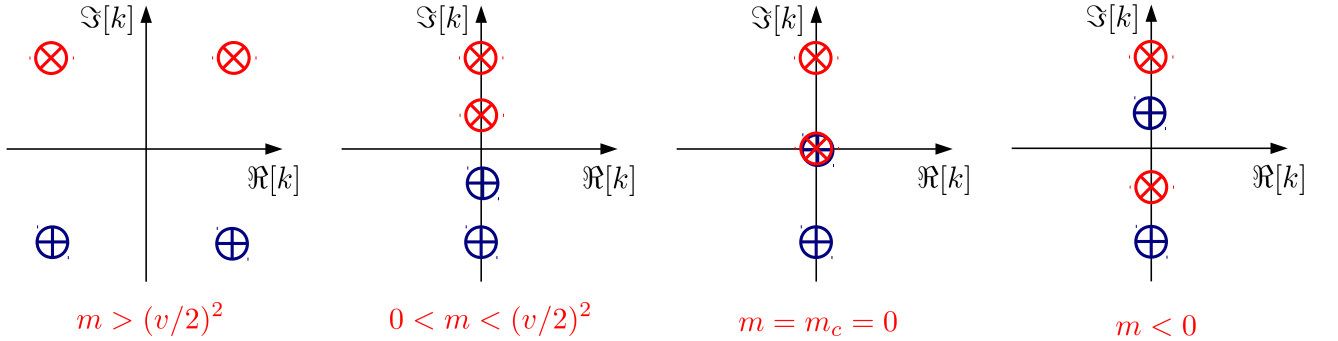


FIG. 10: Wave-vector solutions of Eq. (32) in the complex  $k$ -plane. The solutions in the upper (lower) half-plane lead to zero-energy bound states localized at the left (right) boundary. Blue and red symbols distinguish the two chiralities. The passage from the topologically non-trivial ( $m > 0$ ) to the trivial ( $m < 0$ ) phase is accompanied by the vanishing of the zero-energy bound states and occurs when  $k_x = 0$  and  $m_c = 0$ . For the latter values the bulk gap closes. This constitutes a direct consequence of the bulk-boundary correspondence.

## B. 2d model

The 2d model is obtained by adding the remaining component of Rashba spin-orbit coupling as previously:

$$\hat{\mathcal{H}}(\hat{\mathbf{p}}) = v(\hat{p}_x \sigma_y - \hat{p}_y \sigma_x) + (m - \hat{\mathbf{p}}^2) \sigma_z. \quad (40)$$

Note that we added a quadratic  $\hat{p}_y^2$  dependence in  $M(\hat{\mathbf{p}})$ . Since in the low energy limit a gap closing can occur only for small momenta, the most significant term is  $\hat{p}_y \sigma_x$  which is linear in momentum compared to the  $\hat{p}_y^2 \sigma_z$  term that is quadratic in momentum. By neglecting the latter, the eigen-functions for the chiral edge modes are directly retrieved

- $m > (v/2)^2 > 0$ :

$$\hat{\phi}_{0,-,k_y}(\mathbf{r}) \propto \sin[(x-x_1)/\xi] e^{-(x-x_1)/l} e^{ik_y y} \frac{1}{\sqrt{2}} \begin{pmatrix} 1 \\ -1 \end{pmatrix}, \quad (41)$$

$$\hat{\phi}_{0,+,k_y}(\mathbf{r}) \propto \sin[(x-x_2)/\xi] e^{+(x-x_2)/l} e^{ik_y y} \frac{1}{\sqrt{2}} \begin{pmatrix} 1 \\ 1 \end{pmatrix}. \quad (42)$$

- $0 < m < (v/2)^2$ :

$$\hat{\phi}_{0,-,k_y}(\mathbf{r}) \propto \sinh[(x-x_1)/\xi] e^{-(x-x_1)/l} e^{ik_y y} \frac{1}{\sqrt{2}} \begin{pmatrix} 1 \\ -1 \end{pmatrix}, \quad (43)$$

$$\hat{\phi}_{0,+,k_y}(\mathbf{r}) \propto \sinh[(x-x_2)/\xi] e^{+(x-x_2)/l} e^{ik_y y} \frac{1}{\sqrt{2}} \begin{pmatrix} 1 \\ 1 \end{pmatrix}. \quad (44)$$

In both cases the energy reads

$$E_{\sigma,k_y} = -\sigma v \hbar k_y. \quad (45)$$

The spectrum above is chiral, since each chirality solution is located at **different** boundaries. In a completely analogous way as in the 2d extension of the Jackiw and Rebbi model we have that the solution located at the left (right) edge has chirality  $\sigma = -1$  ( $+1$ ) and an energy dispersion  $E^{left}(k_y) = +v\hbar k_y$  ( $E^{right}(k_y) = -v\hbar k_y$ ) (Fig. 7). Finally, if we also consider the originally neglected term  $\hat{p}_y^2 \sigma_z$ , we see that in the  $\hat{\phi}_{0,\pm,k_y}(\mathbf{r})$  subspace it acts as an interaction with a matrix form

$$\langle \hat{p}_y^2 \sigma_z \rangle = (\hbar k_y)^2 \begin{pmatrix} 0 & t \\ t & 0 \end{pmatrix} \quad \text{with} \quad t \propto e^{-\frac{x_2-x_1}{l}} \frac{a(x_2-x_1) \cos[a(x_2-x_1)] - \sin[a(x_2-x_1)]}{2a}, \quad (46)$$

where  $t$  defines the overlap of the chiral edge modes which decays exponentially with  $x_2 - x_1$ . For  $x_2 - x_1 \rightarrow +\infty$  and small momenta  $\hbar k_y$ , this term leads to a negligible mixing of the two edge modes.

### C. Quantized Hall conductivity of the 2d bulk system - topological invariant

We have already mentioned that bulk-boundary correspondence implies the presence of topologically protected edge solutions. In the case under consideration, the system exhibits the QAHE. We expect from the bulk Hall conductivity to be quantized  $\sigma_{xy} = \tilde{N}e^2/h$ . The confirmation of this fact will be the final proof for the validity of the bulk-correspondence (at least for this system) from a bulk perspective. Therefore our next step will be to calculate the Hall conductivity. In the general case the Hall conductivity is calculated via Kubo's formula [30]. Of course, there exist other approaches based for instance on the Boltzmann equation and Fermi's Golden Rule which despite their phenomenological character, they still reproduce in a simpler manner the results derived using Kubo's method. Here, we will consider an adiabatic approach [31] for the calculation of the Hall conductivity, which is suitable for insulating materials. The same results can be obtained using Kubo's formula with real time, thermal (Matsubara) or non-equilibrium (Keldysh) Green's functions [32-37]. As a matter of fact, the adiabatic approach which we will follow, is based upon the modified adiabatic eigenstates of the 2d model due to the influence of an external electric field.

#### 1. Bulk eigen-states

We Fourier transform the bulk Hamiltonian of Eq. (40) and obtain

$$\begin{aligned} \hat{\mathcal{H}}(\mathbf{k}) &= v\hbar(k_x \sigma_y - k_y \sigma_x) + (m - \hbar^2 \mathbf{k}^2) \sigma_z = \begin{pmatrix} (m - \hbar^2 \mathbf{k}^2) & -v\hbar(k_y + ik_x) \\ -v\hbar(k_y - ik_x) & -(m - \hbar^2 \mathbf{k}^2) \end{pmatrix} \\ &\equiv E(\mathbf{k}) \begin{pmatrix} \cos \vartheta_{\mathbf{k}} & -i \sin \vartheta_{\mathbf{k}} e^{-i\varphi_{\mathbf{k}}} \\ i \sin \vartheta_{\mathbf{k}} e^{i\varphi_{\mathbf{k}}} & -\cos \vartheta_{\mathbf{k}} \end{pmatrix} \\ &= E(\mathbf{k}) \hat{\mathbf{g}}(\mathbf{k}) \cdot \boldsymbol{\sigma}, \end{aligned} \quad (47)$$

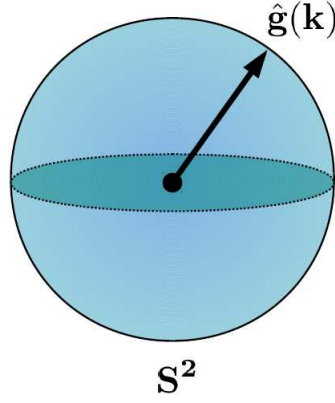


FIG. 11: The unit vector  $\hat{\mathbf{g}}(\mathbf{k})$  parametrizing the Hamiltonian takes values on a two-dimensional sphere  $S^2$ .

with  $E(\mathbf{k}) = \sqrt{\mathbf{g}(\mathbf{k}) \cdot \mathbf{g}(\mathbf{k})} = \sqrt{(v\hbar\mathbf{k})^2 + (m - \hbar^2\mathbf{k}^2)^2}$  where we have introduced the  $\mathbf{g}$ -vector and the angles  $\varphi_{\mathbf{k}}, \vartheta_{\mathbf{k}}$ :

$$\mathbf{g}(\mathbf{k}) = (-v\hbar k_y, v\hbar k_x, m - \hbar^2\mathbf{k}^2) = E(\mathbf{k}) (-\sin\varphi_{\mathbf{k}} \sin\vartheta_{\mathbf{k}}, \cos\varphi_{\mathbf{k}} \sin\vartheta_{\mathbf{k}}, \cos\vartheta_{\mathbf{k}}). \quad (48)$$

The corresponding eigen-vectors read

$$|+, \mathbf{k}\rangle = \begin{pmatrix} \cos\left(\frac{\vartheta_{\mathbf{k}}}{2}\right) \\ i \sin\left(\frac{\vartheta_{\mathbf{k}}}{2}\right) e^{i\varphi_{\mathbf{k}}} \end{pmatrix} \quad \text{and} \quad |-, \mathbf{k}\rangle = \begin{pmatrix} i \sin\left(\frac{\vartheta_{\mathbf{k}}}{2}\right) e^{-i\varphi_{\mathbf{k}}} \\ \cos\left(\frac{\vartheta_{\mathbf{k}}}{2}\right) \end{pmatrix}. \quad (49)$$

The above bulk eigen-states satisfy  $\widehat{\mathcal{H}}(\mathbf{k})|\nu, \mathbf{k}\rangle = E_{\nu}(\mathbf{k})|\nu, \mathbf{k}\rangle$  with  $E_{\nu}(\mathbf{k}) = \nu E(\mathbf{k})$  where  $\nu = \pm$ .

### 2. Coupling to an external constant electric field - Adiabatic eigen-states

In order to study the QAHE from a bulk perspective, we need to apply a constant electric field  $\mathcal{E}_x$  and calculate the electric current  $J_y = \sigma_H \mathcal{E}_x$ , where  $\sigma_H$  corresponds to  $\sigma_H = \sigma_{yx} = -\sigma_{xy}$ . Since in general the electric field can be written in terms of the scalar ( $V$ ) and vector ( $\mathbf{A}$ ) potentials as  $\mathcal{E} = -\nabla V - \partial_t \mathbf{A}$ , we can include it in our 2d Hamiltonian through the minimal coupling, i.e.  $\hat{\mathbf{p}} \rightarrow \hat{\mathbf{p}} + e\mathbf{A}(t)$  which translates to  $\mathbf{k} \rightarrow \mathbf{k} + e\mathbf{A}(t)/\hbar$  ( $e > 0$ ). Essentially, the presence of a finite electric field renders the wave-vector time-dependent, satisfying

$$\hbar \dot{\mathbf{k}}(t) = -e\mathcal{E}(t), \quad (50)$$

which describes Newton's second law. Note that for a constant electric field  $\mathbf{k}(t) = \mathbf{k}(t_0) - e\mathcal{E}(t - t_0)/\hbar$ . The crucial point in the manner that the electric field enters the Hamiltonian, is that the form of the latter remains the same, i.e. we can write  $\widehat{\mathcal{H}}(\mathbf{k}, t) \equiv \widehat{\mathcal{H}}(\mathbf{k}(t))$ . For the case of an insulating system and under the condition that the rate  $\dot{\mathbf{k}}$  is small, one can consider that the system evolves adiabatically in the presence of the time-dependent vector potential. This assumption implies that the eigen-states of the system follow the adiabatically varying  $\mathbf{k}(t)$ . In this manner, the adiabatic or instantaneous eigen-states are simply  $|\pm, \mathbf{k}(t)\rangle$ .

### 3. Time-dependent perturbation theory based on adiabatic eigen-states

The adiabatic eigen-states can constitute a useful basis for formulating a time-dependent perturbation theory [31], in the case of a slowly varying external field. In the presence of the external field, Schrödinger's equation obtains the form

$$i\hbar \frac{\partial}{\partial t} |\nu, \mathbf{k}, t\rangle = \widehat{\mathcal{H}}(\mathbf{k}, t) |\nu, \mathbf{k}, t\rangle, \quad (51)$$

where  $|\nu, \mathbf{k}, t\rangle$  correspond to the exact eigen-states of  $\widehat{\mathcal{H}}(\mathbf{k}, t)$ . We would like now to set up a perturbation theory, for which the exact eigen-states will coincide with the adiabatic eigen-states at zero-th order. We write

$$\left(i\hbar\frac{\partial}{\partial t} - E_\nu[\mathbf{k}(t)]\right)|\nu, \mathbf{k}, t\rangle + E_\nu[\mathbf{k}(t)]|\nu, \mathbf{k}, t\rangle = \widehat{\mathcal{H}}(\mathbf{k}, t)|\nu, \mathbf{k}, t\rangle \quad (52)$$

where the first term will be considered as the *perturbation* on the adiabatic eigen-states  $|\nu, \mathbf{k}(t)\rangle$ . At this point we expand  $|\nu, \mathbf{k}, t\rangle$  perturbatively, in the following sense  $|\nu, \mathbf{k}, t\rangle = |\nu, \mathbf{k}, t\rangle^{(0)} + |\nu, \mathbf{k}, t\rangle^{(1)} + \dots \equiv |\nu, \mathbf{k}(t)\rangle + \delta|\nu, \mathbf{k}(t)\rangle + \dots$ . By plugging this expression in the equation above, we obtain:

$$|\nu, \mathbf{k}, t\rangle = |\nu, \mathbf{k}(t)\rangle + i\hbar \sum_{\lambda \neq \nu} |\lambda, \mathbf{k}(t)\rangle \frac{\langle \lambda, \mathbf{k}(t) | \partial_t |\nu, \mathbf{k}(t)\rangle}{E_\lambda[\mathbf{k}(t)] - E_\nu[\mathbf{k}(t)]} + \text{h.o.t.} \quad (53)$$

With the help of the chain rule for derivatives we have

$$|\nu, \mathbf{k}, t\rangle = |\nu, \mathbf{k}(t)\rangle + i\hbar \dot{\mathbf{k}}(t) \cdot \sum_{\lambda \neq \nu} |\lambda, \mathbf{k}(t)\rangle \frac{\langle \lambda, \mathbf{k}(t) | \nabla_{\mathbf{k}(t)} |\nu, \mathbf{k}(t)\rangle}{E_\lambda[\mathbf{k}(t)] - E_\nu[\mathbf{k}(t)]} + \text{h.o.t.} \quad (54)$$

Using Newton's law Eq. (50), we obtain

$$|\nu, \mathbf{k}, t\rangle = |\nu, \mathbf{k}(t)\rangle - ie\mathcal{E}(t) \cdot \sum_{\lambda \neq \nu} |\lambda, \mathbf{k}(t)\rangle \frac{\langle \lambda, \mathbf{k}(t) | \nabla_{\mathbf{k}(t)} |\nu, \mathbf{k}(t)\rangle}{E_\lambda[\mathbf{k}(t)] - E_\nu[\mathbf{k}(t)]} + \text{h.o.t.} \quad (55)$$

For a constant electric field the above eigen-states are simply linear combinations of the adiabatic eigen-states. Consequently they are also adiabatic eigen-states and therefore we can write  $|\tilde{\nu}, \mathbf{k}(t)\rangle \equiv |\nu, \mathbf{k}, t\rangle^{(0)} + |\nu, \mathbf{k}, t\rangle^{(1)}$ . Furthermore, we may suppress the time-dependence in  $\mathbf{k}$  and simply write

$$|\tilde{\nu}, \mathbf{k}\rangle \simeq |\nu, \mathbf{k}\rangle - ie\mathcal{E} \cdot \sum_{\lambda \neq \nu} |\lambda, \mathbf{k}\rangle \frac{\langle \lambda, \mathbf{k} | \nabla_{\mathbf{k}} |\nu, \mathbf{k}\rangle}{E_\lambda(\mathbf{k}) - E_\nu(\mathbf{k})}. \quad (56)$$

#### 4. Adiabatic current

In order to retrieve the Hall conductivity, we have to define the current operator. We will start from the microscopic equation of continuity for the electric charge

$$\dot{\hat{\rho}}(\mathbf{q}, t) + i\mathbf{q} \cdot \hat{\mathbf{j}}(\mathbf{q}, t) = 0, \quad (57)$$

where  $\hat{\rho}(\mathbf{q}, t)$  and  $\hat{\mathbf{j}}(\mathbf{q}, t)$  define second-quantized Heisenberg operators evolving with the general second-quantized Hamiltonian in Schrödinger's picture

$$\widehat{\mathcal{H}}(t) = \int d\mathbf{k} \widehat{\Psi}_{\mathbf{k}}^\dagger \widehat{\mathcal{H}}(\mathbf{k} + e\mathbf{A}(t)/\hbar) \widehat{\Psi}_{\mathbf{k}}, \quad (58)$$

where we have introduced the spinor  $\widehat{\Psi}_{\mathbf{k}}^\dagger = (c_{\mathbf{k}, \uparrow}^\dagger, c_{\mathbf{k}, \downarrow}^\dagger)$ . The electric charge density operator in Heisenberg's picture reads

$$\hat{\rho}(\mathbf{q}, t) = -e \int \frac{d\mathbf{k}}{(2\pi)^d} \sum_{\sigma=\uparrow, \downarrow} \hat{c}_{\mathbf{k}, \sigma}^\dagger(t) \hat{c}_{\mathbf{k}+\mathbf{q}, \sigma}(t) \equiv -e \int \frac{d\mathbf{k}}{(2\pi)^d} \widehat{\Psi}_{\mathbf{k}}^\dagger(t) \hat{I}_\sigma \widehat{\Psi}_{\mathbf{k}+\mathbf{q}}(t), \quad (59)$$

where the time-dependence of the field operators is a result of the Heisenberg description. In order to determine the current we have to calculate  $\dot{\hat{\rho}}$ , which is given as

$$\dot{\hat{\rho}}(\mathbf{q}, t) = \frac{i}{\hbar} \left[ \widehat{\mathcal{H}}(t), \hat{\rho}(\mathbf{q}, t) \right] = e^{i \int_{t_0}^t \widehat{\mathcal{H}}(t') dt' / \hbar} \left[ \widehat{\mathcal{H}}(t), \hat{\rho}(\mathbf{q}) \right] e^{-i \int_{t_0}^t \widehat{\mathcal{H}}(t') dt' / \hbar}, \quad (60)$$

where  $\hat{\rho}(\mathbf{q})$  defines the corresponding Schrödinger operator, yielding

$$\begin{aligned} \left[ \widehat{\mathcal{H}}(t), \hat{\rho}(\mathbf{q}) \right] &= -e \iint \frac{d\mathbf{k} d\mathbf{k}'}{(2\pi)^d} \left[ \widehat{\Psi}_{\mathbf{k}}^\dagger \widehat{\mathcal{H}}(\mathbf{k} + e\mathbf{A}(t)/\hbar) \widehat{\Psi}_{\mathbf{k}}, \widehat{\Psi}_{\mathbf{k}'}^\dagger \hat{I}_\sigma \widehat{\Psi}_{\mathbf{k}'+\mathbf{q}} \right] \\ &= -e \int \frac{d\mathbf{k}}{(2\pi)^d} \widehat{\Psi}_{\mathbf{k}}^\dagger \left[ \widehat{\mathcal{H}}(\mathbf{k} + e\mathbf{A}(t)/\hbar) - \widehat{\mathcal{H}}(\mathbf{k} + \mathbf{q} + e\mathbf{A}(t)/\hbar) \right] \widehat{\Psi}_{\mathbf{k}+\mathbf{q}}. \end{aligned} \quad (61)$$

Using the equation of continuity we obtain the Schrödinger current operator

$$\hat{\mathbf{j}}(\mathbf{q}, t) = -\frac{e}{\hbar} \int \frac{d\mathbf{k}}{(2\pi)^d} \hat{\Psi}_{\mathbf{k}}^\dagger \frac{\partial \hat{\mathcal{H}}(\mathbf{k} + e\mathbf{A}(t)/\hbar)}{\partial \mathbf{k}} \hat{\Psi}_{\mathbf{k}+\mathbf{q}}. \quad (62)$$

Note that in general the current operator depends also on the external vector potential. This can become more transparent for a quadratic dispersion  $\hat{\mathcal{H}}(\mathbf{k}) = (\hbar\mathbf{k})^2/2m$  where we obtain  $\partial \hat{\mathcal{H}}(\mathbf{k} + e\mathbf{A}(t)/\hbar)/\partial \mathbf{k} = \hbar(\hbar\mathbf{k}/m + e\mathbf{A}(t))$ . The current consists of the paramagnetic and diamagnetic contributions, respectively. In the case under consideration we are interested in the linear response where  $\mathbf{A}(t)$  is small. In this case, only the paramagnetic current becomes relevant and reads

$$\hat{\mathbf{j}}(\mathbf{q}) = -\frac{e}{\hbar} \int \frac{d\mathbf{k}}{(2\pi)^d} \hat{\Psi}_{\mathbf{k}}^\dagger \frac{\partial \hat{\mathcal{H}}(\mathbf{k})}{\partial \mathbf{k}} \hat{\Psi}_{\mathbf{k}+\mathbf{q}}. \quad (63)$$

For a homogeneous electric field, only the  $\mathbf{q} = \mathbf{0}$  component is relevant (homogeneous current), which reads

$$\hat{\mathbf{j}} = -\frac{e}{\hbar} \int \frac{d\mathbf{k}}{(2\pi)^d} \hat{\Psi}_{\mathbf{k}}^\dagger \frac{\partial \hat{\mathcal{H}}(\mathbf{k})}{\partial \mathbf{k}} \hat{\Psi}_{\mathbf{k}}. \quad (64)$$

It is obvious that the above equation will hold also for the adiabatic situation similar to the one considered in the previous paragraph. In terms of the single-particle eigen-states  $|\tilde{\nu}, \mathbf{k}\rangle$  with corresponding creation (annihilation) operator  $\hat{\psi}_{\mathbf{k}, \tilde{\nu}}^\dagger$  ( $\hat{\psi}_{\mathbf{k}, \tilde{\lambda}}$ ) we obtain

$$\hat{\mathbf{j}} = -\frac{e}{\hbar} \int \frac{d\mathbf{k}}{(2\pi)^d} \sum_{\tilde{\nu}, \tilde{\lambda}} \left\langle \tilde{\nu}, \mathbf{k} \left| \frac{\partial \hat{\mathcal{H}}(\mathbf{k})}{\partial \mathbf{k}} \right| \tilde{\lambda}, \mathbf{k} \right\rangle \hat{\psi}_{\mathbf{k}, \tilde{\nu}}^\dagger \hat{\psi}_{\mathbf{k}, \tilde{\lambda}}. \quad (65)$$

### 5. Hall conductivity formula

We are now in a position to evaluate the expectation value of the current operator up to first order in the electric field. Based on the adiabatic eigen-states  $|\tilde{\nu}, \mathbf{k}\rangle$  we have

$$\begin{aligned} J_a = \langle \hat{j}_a \rangle &= -\frac{e}{\hbar} \int \frac{d\mathbf{k}}{(2\pi)^d} \sum_{\tilde{\nu}} \left\langle \tilde{\nu}, \mathbf{k} \left| \frac{\partial \hat{\mathcal{H}}(\mathbf{k})}{\partial k_a} \right| \tilde{\nu}, \mathbf{k} \right\rangle n_F[E_{\tilde{\nu}}(\mathbf{k})] \simeq -\frac{e}{\hbar} \int \frac{d\mathbf{k}}{(2\pi)^d} \sum_{\nu} \left\langle \nu, \mathbf{k} \left| \frac{\partial \hat{\mathcal{H}}(\mathbf{k})}{\partial k_a} \right| \nu, \mathbf{k} \right\rangle n_F[E_{\nu}(\mathbf{k})] \\ &- \frac{e^2 \mathcal{E}_b}{i\hbar} \int \frac{d\mathbf{k}}{(2\pi)^d} \sum_{\nu, \lambda}^{\nu \neq \lambda} \frac{\left\langle \nu, \mathbf{k} \left| \frac{\partial \hat{\mathcal{H}}(\mathbf{k})}{\partial k_a} \right| \lambda, \mathbf{k} \right\rangle \left\langle \lambda, \mathbf{k} \left| \frac{\partial}{\partial k_b} \right| \nu, \mathbf{k} \right\rangle - \left\langle \lambda, \mathbf{k} \left| \frac{\partial \hat{\mathcal{H}}(\mathbf{k})}{\partial k_a} \right| \nu, \mathbf{k} \right\rangle \left\langle \lambda, \mathbf{k} \left| \frac{\partial}{\partial k_b} \right| \nu, \mathbf{k} \right\rangle^*}{E_{\lambda}(\mathbf{k}) - E_{\nu}(\mathbf{k})} n_F[E_{\nu}(\mathbf{k})], \end{aligned} \quad (66)$$

where  $n_F(\epsilon)$  denotes the Fermi-Dirac distribution for energy  $\epsilon$  and  $a, b = x, y$ . For systems which are not characterized by a finite current flow in the ground state for  $\mathcal{E} = \mathbf{0}$ , only the last term can lead to a finite current. For the rest we will focus only on the second term. Using now the formulae

$$\left\langle \nu, \mathbf{k} \left| \frac{\partial \hat{\mathcal{H}}(\mathbf{k})}{\partial \alpha} \right| \lambda, \mathbf{k} \right\rangle = [E_{\lambda}(\mathbf{k}) - E_{\nu}(\mathbf{k})] \left\langle \nu, \mathbf{k} \left| \frac{\partial}{\partial \alpha} \right| \lambda, \mathbf{k} \right\rangle \quad (67)$$

and

$$\left\langle \nu, \mathbf{k} \left| \frac{\partial}{\partial \mathbf{k}} \right| \lambda, \mathbf{k} \right\rangle = - \left\langle \lambda, \mathbf{k} \left| \frac{\partial}{\partial \mathbf{k}} \right| \nu, \mathbf{k} \right\rangle^*, \quad (68)$$

we have

$$\begin{aligned} J_a &= -\frac{e^2 \mathcal{E}_b}{i\hbar} \int \frac{d\mathbf{k}}{(2\pi)^d} \sum_{\nu, \lambda}^{\nu \neq \lambda} \frac{\left\langle \nu, \mathbf{k} \left| \frac{\partial \hat{\mathcal{H}}(\mathbf{k})}{\partial k_a} \right| \lambda, \mathbf{k} \right\rangle \left\langle \lambda, \mathbf{k} \left| \frac{\partial}{\partial k_b} \right| \nu, \mathbf{k} \right\rangle - \left\langle \nu, \mathbf{k} \left| \frac{\partial \hat{\mathcal{H}}(\mathbf{k})}{\partial k_a} \right| \lambda, \mathbf{k} \right\rangle^* \left\langle \lambda, \mathbf{k} \left| \frac{\partial}{\partial k_b} \right| \nu, \mathbf{k} \right\rangle^*}{E_{\lambda}(\mathbf{k}) - E_{\nu}(\mathbf{k})} n_F[E_{\nu}(\mathbf{k})] \\ &= -\frac{e^2 \mathcal{E}_b}{i\hbar} \int \frac{d\mathbf{k}}{(2\pi)^d} \sum_{\nu, \lambda}^{\nu \neq \lambda} \left[ \left\langle \nu, \mathbf{k} \left| \frac{\partial}{\partial k_a} \right| \lambda, \mathbf{k} \right\rangle \left\langle \lambda, \mathbf{k} \left| \frac{\partial}{\partial k_b} \right| \nu, \mathbf{k} \right\rangle - \left\langle \nu, \mathbf{k} \left| \frac{\partial}{\partial k_a} \right| \lambda, \mathbf{k} \right\rangle^* \left\langle \lambda, \mathbf{k} \left| \frac{\partial}{\partial k_b} \right| \nu, \mathbf{k} \right\rangle^* \right] n_F[E_{\nu}(\mathbf{k})]. \end{aligned} \quad (69)$$

The conductivity reads

$$\sigma_{ab} = -\frac{e^2}{\hbar} \sum_{\nu} \int \frac{d\mathbf{k}}{(2\pi)^d} \Omega_{ab}^{\nu}(\mathbf{k}) n_F[E_{\nu}(\mathbf{k})], \quad (70)$$

where we introduced the so-called *Berry's curvature* [31, 38]

$$\Omega_{ab}^{\nu}(\mathbf{k}) = -i \sum_{\lambda \neq \nu} \left[ \left\langle \nu, \mathbf{k} \left| \frac{\partial}{\partial k_a} \right| \lambda, \mathbf{k} \right\rangle \left\langle \lambda, \mathbf{k} \left| \frac{\partial}{\partial k_b} \right| \nu, \mathbf{k} \right\rangle - \left\langle \nu, \mathbf{k} \left| \frac{\partial}{\partial k_b} \right| \lambda, \mathbf{k} \right\rangle \left\langle \lambda, \mathbf{k} \left| \frac{\partial}{\partial k_a} \right| \nu, \mathbf{k} \right\rangle \right], \quad (71)$$

which satisfies  $\Omega_{ab}^{\nu}(\mathbf{k}) = -\Omega_{ba}^{\nu}(\mathbf{k})$ . Furthermore the summand

$$\left\langle \nu, \mathbf{k} \left| \frac{\partial}{\partial k_a} \right| \lambda, \mathbf{k} \right\rangle \left\langle \lambda, \mathbf{k} \left| \frac{\partial}{\partial k_b} \right| \nu, \mathbf{k} \right\rangle - \left\langle \nu, \mathbf{k} \left| \frac{\partial}{\partial k_b} \right| \lambda, \mathbf{k} \right\rangle \left\langle \lambda, \mathbf{k} \left| \frac{\partial}{\partial k_a} \right| \nu, \mathbf{k} \right\rangle \quad (72)$$

is identically **zero** for  $\nu = \lambda$  which implies that we can remove the constraint of the sum appearing in the expression for the Berry curvature. Then using the completeness relation  $\sum_{\nu} |\nu, \mathbf{k}\rangle \langle \nu, \mathbf{k}| = \hat{I}_{\sigma}$  along with the orthogonality condition

$$\langle \lambda, \mathbf{k} | \nu, \mathbf{k} \rangle = \delta_{\nu, \lambda} \quad \Rightarrow \quad \frac{\partial \langle \lambda, \mathbf{k} |}{\partial \alpha} | \nu, \mathbf{k} \rangle = - \langle \lambda, \mathbf{k} | \frac{\partial | \nu, \mathbf{k} \rangle}{\partial \alpha}, \quad (73)$$

we obtain

$$\begin{aligned} \Omega_{ab}^{\nu}(\mathbf{k}) &= -i \sum_{\lambda} \left[ \left\langle \nu, \mathbf{k} \left| \frac{\partial}{\partial k_a} \right| \lambda, \mathbf{k} \right\rangle \left\langle \lambda, \mathbf{k} \left| \frac{\partial}{\partial k_b} \right| \nu, \mathbf{k} \right\rangle - \left\langle \nu, \mathbf{k} \left| \frac{\partial}{\partial k_b} \right| \lambda, \mathbf{k} \right\rangle \left\langle \lambda, \mathbf{k} \left| \frac{\partial}{\partial k_a} \right| \nu, \mathbf{k} \right\rangle \right] \\ &= -i \sum_{\lambda} \left[ \frac{\partial \langle \nu, \mathbf{k} |}{\partial k_b} | \lambda, \mathbf{k} \rangle \langle \lambda, \mathbf{k} | \frac{\partial | \nu, \mathbf{k} \rangle}{\partial k_a} - \frac{\partial \langle \nu, \mathbf{k} |}{\partial k_a} | \lambda, \mathbf{k} \rangle \langle \lambda, \mathbf{k} | \frac{\partial | \nu, \mathbf{k} \rangle}{\partial k_b} \right] \\ &= i \left( \frac{\partial \langle \nu, \mathbf{k} |}{\partial k_a} \frac{\partial | \nu, \mathbf{k} \rangle}{\partial k_b} - \frac{\partial \langle \nu, \mathbf{k} |}{\partial k_b} \frac{\partial | \nu, \mathbf{k} \rangle}{\partial k_a} \right) \equiv \frac{\partial \mathcal{A}_b^{\nu}(\mathbf{k})}{\partial k_a} - \frac{\partial \mathcal{A}_a^{\nu}(\mathbf{k})}{\partial k_b}, \end{aligned} \quad (74)$$

where we introduced Berry's vector potential

$$\mathcal{A}^{\nu}(\mathbf{k}) = \langle \nu, \mathbf{k} | i \nabla_{\mathbf{k}} | \nu, \mathbf{k} \rangle. \quad (75)$$

In fact  $\mathcal{A}^{\nu}(\mathbf{k})$  is a gauge potential since under a gauge transformation  $|\nu, \mathbf{k}\rangle \rightarrow e^{-i\alpha(\mathbf{k})} |\nu, \mathbf{k}\rangle$  it transforms as  $\mathcal{A}^{\nu} \rightarrow \mathcal{A}^{\nu}(\mathbf{k}) + \nabla_{\mathbf{k}} \alpha(\mathbf{k})$ . With the use of Berry's vector potential the Hall conductivity reads

$$\sigma_H = \sigma_{yx} = \frac{e^2}{\hbar} \sum_{\nu} \int \frac{d\mathbf{k}}{(2\pi)^2} \left[ \frac{\partial \mathcal{A}_y^{\nu}(\mathbf{k})}{\partial k_x} - \frac{\partial \mathcal{A}_x^{\nu}(\mathbf{k})}{\partial k_y} \right] n_F[E_{\nu}(\mathbf{k})] \equiv \frac{e^2}{\hbar} \sum_{\nu} \int \frac{d\mathbf{k}}{(2\pi)^2} \Omega_z^{\nu}(\mathbf{k}) n_F[E_{\nu}(\mathbf{k})], \quad (76)$$

where we introduced Berry's curvature

$$\Omega_z^{\nu}(\mathbf{k}) \equiv \Omega_{xy}^{\nu}(\mathbf{k}) = (\nabla_{\mathbf{k}} \times \mathcal{A}(\mathbf{k}))_z, \quad (77)$$

where we labelled the Berry curvature  $\Omega_{xy}^{\nu}(\mathbf{k})$  with the  $z$ -axis which is perpendicular to the  $xy$ -plane, since  $\Omega_{ab}^{\nu}(\mathbf{k}) \propto \varepsilon_{abc}$  with  $\varepsilon_{abc}$  the completely anti-symmetric tensor with  $a, b, c = \{x, y, z\}$ . Notice that the Hall conductivity is proportional to the integral of the Berry curvature along the  $z$ -axis which is similar to the QHE. Essentially,  $\Omega_z^{\nu}(\mathbf{k})$  plays the role of the external  $\mathcal{B}_z$  field in the QHE. Consequently,  $\Omega_z^{\nu}(\mathbf{k})$  should be *odd* under  $\mathcal{T}$ , which can occur only for systems which violate  $\mathcal{T}$ -symmetry.

### 6. Quantized Hall conductivity in a $\mathcal{T}$ -violating topological insulator

For the Hamiltonian under consideration (Eq. (47)) we obtain

$$\Omega_z^{\nu}(\mathbf{k}) = -\frac{\nu}{2} \hat{\mathbf{g}}(\mathbf{k}) \cdot \left( \frac{\partial \hat{\mathbf{g}}(\mathbf{k})}{\partial k_x} \times \frac{\partial \hat{\mathbf{g}}(\mathbf{k})}{\partial k_y} \right), \quad (78)$$

where we have made use of the unit vector  $\hat{\mathbf{g}}(\mathbf{k}) = \mathbf{g}(\mathbf{k})/|\mathbf{g}(\mathbf{k})|$ . The Hall conductivity becomes

$$\sigma_H = \frac{e^2}{h} \frac{1}{4\pi} \int d\mathbf{k} \hat{\mathbf{g}}(\mathbf{k}) \cdot \left( \frac{\partial \hat{\mathbf{g}}(\mathbf{k})}{\partial k_x} \times \frac{\partial \hat{\mathbf{g}}(\mathbf{k})}{\partial k_y} \right) \left\{ n_F[-E(\mathbf{k})] - n_F[E(\mathbf{k})] \right\}. \quad (79)$$

For zero temperature, only the lowest band is occupied and due to the fact that the Fermi-Dirac distribution becomes a step function, we obtain

$$\sigma_H = \frac{e^2}{h} \frac{1}{4\pi} \int d\mathbf{k} \hat{\mathbf{g}}(\mathbf{k}) \cdot \left( \frac{\partial \hat{\mathbf{g}}(\mathbf{k})}{\partial k_x} \times \frac{\partial \hat{\mathbf{g}}(\mathbf{k})}{\partial k_y} \right) \equiv \frac{e^2}{h} \tilde{N}, \quad (80)$$

where we will argue that the following quantity

$$\tilde{N} = \frac{1}{4\pi} \int d\mathbf{k} \hat{\mathbf{g}}(\mathbf{k}) \cdot \left( \frac{\partial \hat{\mathbf{g}}(\mathbf{k})}{\partial k_x} \times \frac{\partial \hat{\mathbf{g}}(\mathbf{k})}{\partial k_y} \right), \quad (81)$$

is an integer ( $\mathbb{Z}$ ) and constitutes a topological invariant [13]. To show why this integral takes only quantized values, we have to understand better the behavior of the integrand, and particularly investigate the behavior of  $\hat{\mathbf{g}}(\mathbf{k})$  towards infinity. Since we have

$$\hat{\mathbf{g}}(\mathbf{k}) = \left( -\frac{v\hbar k_y}{\sqrt{(v\hbar\mathbf{k})^2 + (m - \hbar^2\mathbf{k}^2)^2}}, \frac{v\hbar k_x}{\sqrt{(v\hbar\mathbf{k})^2 + (m - \hbar^2\mathbf{k}^2)^2}}, \frac{m - \hbar^2\mathbf{k}^2}{\sqrt{(v\hbar\mathbf{k})^2 + (m - \hbar^2\mathbf{k}^2)^2}} \right), \quad (82)$$

we will now examine the behavior of this unit vector at the origin  $\mathbf{k} = \mathbf{0}$  and towards infinity  $|\mathbf{k}| \rightarrow +\infty$ . We have

$$\hat{\mathbf{g}}(\mathbf{0}) = (0, 0, \text{sign}(m)) \quad \text{and} \quad \hat{\mathbf{g}}(|\mathbf{k}| \rightarrow +\infty) = (0, 0, -1). \quad (83)$$

Note that for  $m > 0$  ( $m < 0$ ) the orientation of the  $\hat{\mathbf{g}}(\mathbf{k})$  at the origin and at infinity are the opposite (same), leading to a skyrmion (trivial) configuration (Fig. 12). Since the  $\hat{\mathbf{g}}(\mathbf{k})$  vector is oriented along the same direction at all points of the 2d space at infinity, all these points become essentially equivalent. In this sense our 2d space is not any more  $\mathbb{R}^2$  but compactifies to  $S^2$ , which corresponds to the usual sphere.

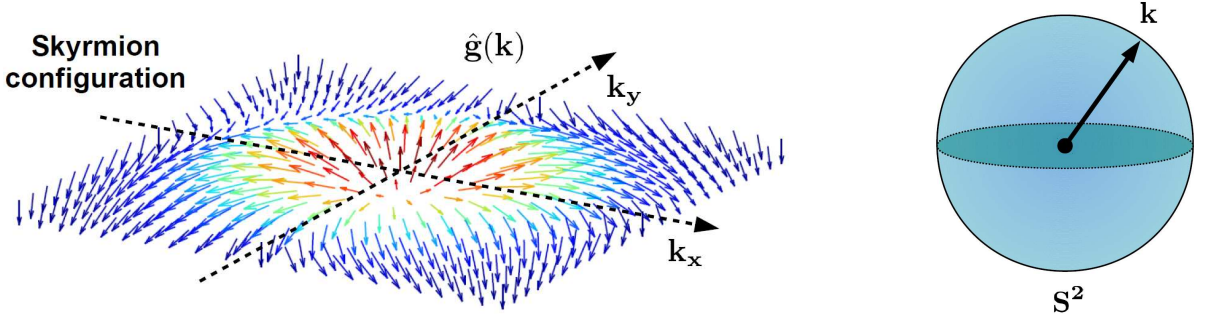


FIG. 12: **Left:** Skyrmion configuration [39] of the unit vector  $\hat{\mathbf{g}}(\mathbf{k})$ . In this topologically non-trivial configuration, the  $\hat{\mathbf{g}}$  vector changes continuously its orientation in such a manner so that the orientation at the “center” of  $\mathbf{k}$ -space is anti-parallel to the orientation at the boundary (infinity). Note that the  $\hat{\mathbf{g}}(\mathbf{k})$  obtains exactly the same orientation at infinity rendering the whole boundary equivalent to a single point. This essentially compactifies  $\mathbf{k}$ -space from  $\mathbb{R}^2$  to a two-sphere  $S^2$ . **Right:** The compactified  $\mathbf{k}$ -space into an  $S^2$ .

On the other hand, the term  $\hat{\mathbf{g}} \cdot (d_x \hat{\mathbf{g}} \times d_y \hat{\mathbf{g}})$  provides the infinitesimal solid angle covered upon an infinitesimal variation of  $\hat{\mathbf{g}}(\mathbf{k})$ , since

$$\tilde{N} = \frac{1}{4\pi} \int d\mathbf{k} \sin \vartheta_{\mathbf{k}} \left( \frac{\partial \varphi_{\mathbf{k}}}{\partial k_y} \frac{\partial \vartheta_{\mathbf{k}}}{\partial k_x} - \frac{\partial \varphi_{\mathbf{k}}}{\partial k_x} \frac{\partial \vartheta_{\mathbf{k}}}{\partial k_y} \right) = \frac{1}{4\pi} \iint d\vartheta d\varphi \sin \vartheta. \quad (84)$$

Due to the boundary condition at infinity, when we integrate over the whole  $\mathbf{k}$ -space, the  $\hat{\mathbf{g}}(\mathbf{k})$  will vary and cover an integer number of a complete solid angle,  $4\pi$ , providing in the general case a total solid angle of  $4\pi\mathbb{Z}$ . In this manner,  $\tilde{N} = \mathbb{Z}$  and yields the expected quantized Hall conductivity. One may directly observe that for  $m > 0$  we obtain  $\tilde{N} = 1$  which would correspond to a single chiral edge mode per boundary of the material. Clearly this is another different aspect of the bulk-boundary correspondence. The topological invariant quantity is the result of the homotopy mapping of a  $S^2 \rightarrow S^2$  [13, 14] (see Fig. 13).

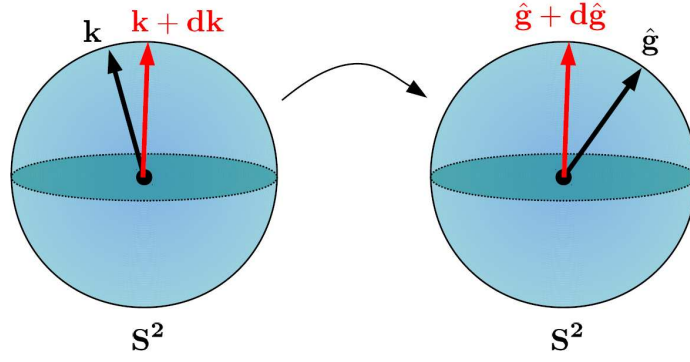


FIG. 13: The topological invariant  $\tilde{N}$  responsible for the quantization of the Hall conductivity is an  $\mathbb{Z}$  performing the mapping of the compactified  $\mathbf{k}$ -space,  $S^2$ , to the manifold of the unit vector  $\hat{\mathbf{g}}(\mathbf{k})$  which also a two sphere  $S^2$ . Generally any mapping of two spheres of the same dimensionality is an integer  $\mathbb{Z}$ .

### 7. The first encounter of space compactification in physics: Kaluza - Klein theory

The concept of compactification has appeared almost one century ago in high energy physics, in terms of the Kaluza-Klein theory [40, 41] which was aiming at the unification of gravity and electromagnetism. Although unsuccessful, it led to a breakthrough since it opened new routes in including additional dimensions beyond the usual Minkowski spacetime, which consists of a single time-dimension ( $t$ ) and three Euclidean spatial dimensions ( $\mathbf{r}$ ). The current developments in high energy physics suggest that we live in an 11-dimensional world where 10 of them correspond to spatial dimensions. However, the additional 7-dimensions are not directly visible to us since their fingerprints lie in higher energies. In fact, the latter concept was exactly the fundamental step in Kaluza-Klein theory. The additional dimensions are not visible to us because they are compact, i.e. for instance circles, spheres or more complicated structures. Kaluza and Klein considered a five-dimensional space where the fifth dimension ( $\zeta$ ) is a circle of radius  $R$ . In this manner, space-time can be visualized as a “cylinder” (Fig. 14). Due to the compactification of the extra dimension, a particle described by a classical field  $\Phi(t, \mathbf{r}, \zeta)$  which satisfies the five-dimensional Klein-Gordon equation

$$\left( \frac{\partial^2}{\partial t^2} - \nabla^2 - \frac{1}{R^2} \frac{\partial^2}{\partial \zeta^2} + M^2 \right) \Phi(t, \mathbf{r}, \zeta) = 0 \quad \Rightarrow \quad \left[ \frac{\partial^2}{\partial t^2} - \nabla^2 + M^2 + \left( \frac{n}{R} \right)^2 \right] \Phi_n(t, \mathbf{r}) = 0, \quad (85)$$

can be viewed as a particle living in the usual 4-dimensional space with an effective mass originating from the plane wave-solutions  $\Phi(t, \mathbf{r}, \zeta) = \Phi_n(t, \mathbf{r})e^{in\zeta}$  of the additional dimension. Due to the compactification and the single-valuedness of  $e^{in\zeta}$ , one obtains the allowed values of  $n$ , i.e.  $n = 0, 1, 2, \dots$ . In this manner, we obtain an infinite number of solutions, particles of different masses, the so-called Kaluza-Klein tower. The relativistic spectrum in this case reads  $E^2 = \mathbf{p}^2 + m_n^2$  with the allowed masses  $m_n = \sqrt{m^2 + (n/R)^2}$ . Note that the smaller the radius for the compactified  $\zeta$ -space, the higher in energy we can observe the effects of the fifth dimension.

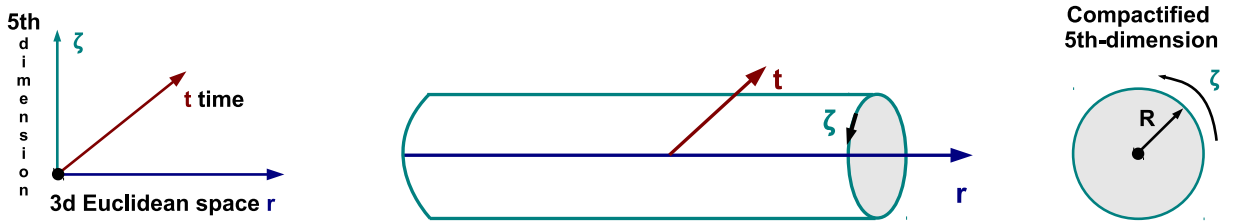


FIG. 14: **Left:** The five-dimensional spacetime considered within the Kaluza-Klein theory. In our case, the additional dimension defines a spatial dimension on top of the usual Minkowski spacetime. **Middle:** The extra dimension is assumed to be compact and in our case a circle. As a result, the five-dimensional space resembles a cylinder. **Right:** The compactified  $\zeta$ -space is a circle of radius  $R$ .

### D. Topological invariant for the 1d bulk system from dimensional reduction

We can directly obtain the topological invariant for the 1d-model, which belongs to class BDI and is expected to be an integer. The  $\hat{\mathbf{g}}(\mathbf{k})$  simply reduces to

$$\mathbf{g}(k) = (0, v\hbar k, m - (\hbar k)^2) = E(k) (0, \sin \vartheta_k, \cos \vartheta_k), \quad (86)$$

where for simplicity we set  $k \equiv k_x$ . Once again, we study the boundary values of  $\hat{\mathbf{g}}(k)$ . We have  $\hat{\mathbf{g}}(|k| \rightarrow +\infty) = -1$  leading to the compactification of  $k$ -space from  $\mathbb{R}$  to a circle  $S^1$ . As previously,  $\hat{\mathbf{g}}(k=0) = \text{sign}(m)$  and the sign of  $m$  will define if we lie in the topologically trivial or not phase. Particularly for  $m < 0$  we may deform our Hamiltonian so to be constant  $\hat{\mathbf{g}}(k) = (0, 0, -1)$  while for  $m > 0$  we obtain a twist of the  $\hat{\mathbf{g}}$  vector (see Fig. 15).

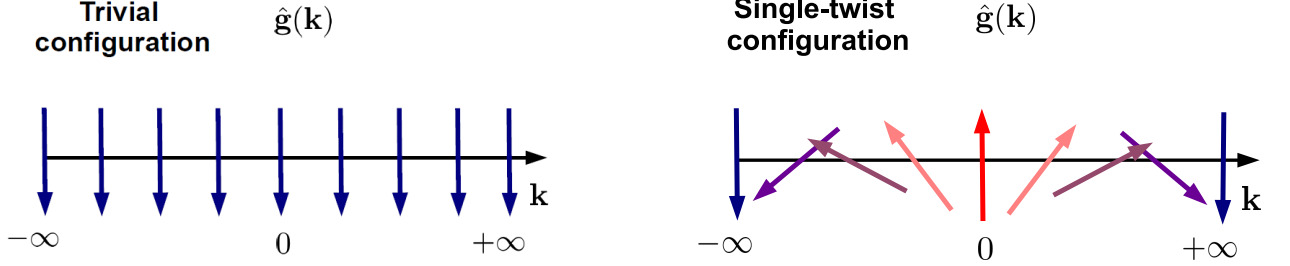


FIG. 15: **Left:** Trivial configuration of the topologically deformed  $\hat{\mathbf{g}}(k)$ -vector. **Right:** Topologically non-trivial configuration of the unit  $\hat{\mathbf{g}}(k)$ -vector with a single twist. In both cases the  $\hat{\mathbf{g}}(k)$  has the same orientation at  $\pm\infty$  leading to a compactification of the 1d  $k$ -space from  $\mathbb{R}$  to  $S^1$ .

From Fig. 16 it is clear that a topological invariant quantity can be obtained from the mapping of  $S^1 \rightarrow S^1$ . Similar to the  $S^2 \rightarrow S^2$  case this also an integer. It is obvious that two spheres of the same dimensionality are always linked via an integer. The topological invariant in the present 1d case coincides with the angle  $\vartheta_k$  which is covered when we cover an angle of  $2\pi$  in the  $S^1$  compactified  $k$ -space. We may readily introduce the so-called winding number [12–14]

$$\tilde{w} = \frac{1}{2\pi} \int d\vartheta \equiv \frac{1}{2\pi} \int dk \frac{d\vartheta}{dk} = -\frac{1}{2\pi} \int dk \left( \hat{\mathbf{g}}(\mathbf{k}) \times \frac{\partial \hat{\mathbf{g}}(\mathbf{k})}{\partial k} \right)_x. \quad (87)$$

For the case considered here, it is straightforward to see that  $\tilde{w} = 1$ . At this point it is useful to make the following remarks:

- We have already mentioned that the quantities  $\tilde{N}$  and  $\tilde{w}$  constitute topological invariant quantities, robust under smooth deformations of the Hamiltonian. Smooth implies that the changes which we subject the Hamiltonian to, are such that they do not close the bulk gap since this would lead to an indefinite  $\hat{\mathbf{g}}(\mathbf{k})$ -vector. Furthermore, the symmetry class of the Hamiltonian should remain the same during this deformation procedure. Here we will prove this property for  $\tilde{w}$  (similarly for  $\tilde{N}$ ). We start from the expression for the topological invariant

$$\tilde{w}' = -\frac{1}{2\pi} \int dk \left( \hat{\mathbf{g}}'(\mathbf{k}) \times \frac{\partial \hat{\mathbf{g}}'(\mathbf{k})}{\partial k} \right)_x, \quad (88)$$

where we have smoothly deformed our Hamiltonian by infinitesimally deforming the  $\hat{\mathbf{g}}(k)$ -vector in the following manner  $\hat{\mathbf{g}}'(k) = \hat{\mathbf{g}}(k) + \delta\hat{\mathbf{g}}(k)$ , with  $\hat{\mathbf{g}}(k) \cdot \delta\hat{\mathbf{g}}(k) = 0$ . The latter constraint implies that we add a genuinely different contribution to the previous Hamiltonian, which allows to  $\hat{\mathbf{g}}'(k)$  to be a unit vector, i.e.  $\hat{\mathbf{g}}'(k) \cdot \hat{\mathbf{g}}'(k) = 1 \rightarrow \hat{\mathbf{g}}(k) \cdot \delta\hat{\mathbf{g}}(k) = 0$ . In order to assure that we remain in the same symmetry class we have to satisfy simultaneously the additional constraints:  $\delta g_x(k) = 0$ ,  $\delta g_y(k) = -\delta g_y(-k)$  and  $\delta g_z(k) = \delta g_z(-k)$ . By replacing we have

$$\tilde{w}' = \tilde{w} - \frac{1}{\pi} \int dk \left( \delta\hat{\mathbf{g}}(\mathbf{k}) \times \frac{\partial \hat{\mathbf{g}}(\mathbf{k})}{\partial k} \right)_x + \text{h.o.t} = \tilde{w}, \quad (89)$$

where we used the antisymmetry of the external product and the following relations

$$\hat{\mathbf{g}}(k) \cdot \hat{\mathbf{g}}(k) = 1 \rightarrow \hat{\mathbf{g}}(k) \cdot \frac{\partial \hat{\mathbf{g}}(k)}{\partial k} = 0 \Rightarrow \frac{\partial \hat{\mathbf{g}}(k)}{\partial k} \parallel \delta\hat{\mathbf{g}}(k) \Rightarrow \frac{\partial \hat{\mathbf{g}}(k)}{\partial k} \times \delta\hat{\mathbf{g}}(k) = \mathbf{0}. \quad (90)$$

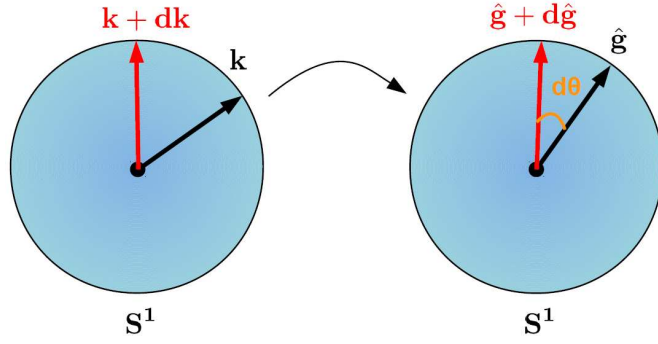


FIG. 16: The two  $S^1$  spheres are homotopically mapped with the winding number  $\tilde{w}$  counting how many times an angle of  $2\pi$  has been covered in  $\hat{\mathbf{g}}$ -space, when an angle of  $2\pi$  has been covered in the compactified  $k$ -space.

- If we calculate the topological invariant quantities,  $\tilde{N}$  and  $\tilde{w}$ , for the bulk Hamiltonians of the Jackiw-Rebbi model discussed earlier (see Eq. (15) and Eq. (25)) we will observe that  $\tilde{N} = \tilde{w} = 1/2$ . According to our discussion,  $\tilde{N}$  enters in the expression of the conductivity and its fractionalization implies that a fractional number of electrons carry the electric current. However, this is not physical for a *non-interacting* system. The reason for this contradiction is related to the fact that Hamiltonians which are linear in momenta as for instance  $\hat{\mathcal{H}} = v(\hat{p}_x\sigma_y - \hat{p}_y\sigma_x) - M\sigma_z$  are pathological as far these invariants are concerned [13], since  $\hat{\mathbf{g}}(\mathbf{k})$  does not satisfy the appropriate boundary conditions. In fact,  $\hat{\mathbf{g}}(\mathbf{k})$  does not point along the same direction for all  $|\mathbf{k}| \rightarrow +\infty$ . Consequently,  $\mathbf{k}$ -space cannot be compactified into a sphere and therefore we cannot define a topologically invariant quantity. This is essentially the reason why the latter model cannot exhibit edge modes without the consideration of an  $M(x)$ . Specifically for the stewise double domain wall magnetization profile, each bulk phase is characterized by a fractional topological invariant, so that the changes of the topological invariant yield an integer number. This is exactly the way that integer nature of the invariant is restored. Consequently we have to define domain walls, i.e. pairs of bulk phases which are characterized by a fractional topological invariant, in order to obtain a well defined integer number of zero-energy bound states (see Fig. 17). In this case the sign of the difference of the topological invariants characterizing two consecutive segments provides the chirality ( $\sigma_x$  eigen-value) characterizing the bound state solution.

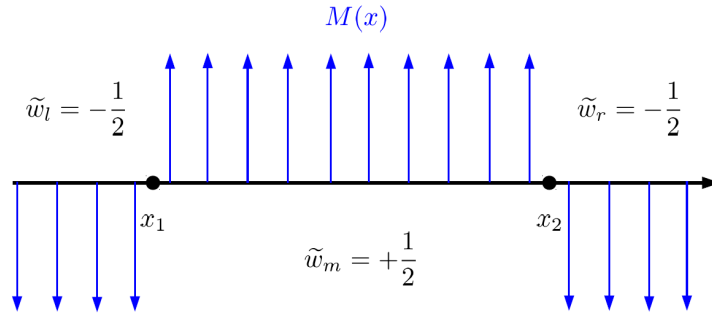


FIG. 17: The calculated winding number  $\tilde{w}$  for each of the three bulk segments within the Jackiw-Rebbi model. The calculated invariant has a sign which depends on the sign of the magnetization. Moreover, it is fractionalized as a consequence of the fact that the Hamiltonian is linear in momentum. However, the difference of the winding number along a domain wall is an integer and equals the number of zero-energy bound state solutions appearing at the interface. The sign of the difference of the winding number along the domain wall provides the chirality of the zero-energy bound state.

- The above remark sets constraints to the models that can describe a physical system. Any relativistic theory of the Jackiw-Rebbi family must consist of a direct sum of an even number of block Hamiltonians of the following type  $\hat{\mathcal{H}} = v(\hat{p}_x\sigma_y - \hat{p}_y\sigma_x) - M\sigma_z$ . However, as we have already observed, any model of the latter type becomes topologically “regular” when it attains non-relativistic corrections, like the terms which are quadratic in momenta. In the latter case, the required boundary conditions for the  $\hat{\mathbf{g}}$ -vector are fulfilled and we can define a topological invariant quantity.

## V. $\mathcal{T}$ -INVARIANT TOPOLOGICAL INSULATORS

Having studied the 1d and 2d models for a  $\mathcal{T}$ -violating topological insulator, it is straightforward to construct related  $\mathcal{T}$ -invariant models for topological insulators, by simply doubling the degrees of freedom. In the simplest case this is achieved by adding the  $\mathcal{T}$ -reversed copy of the block Hamiltonian presented in Eq. (40). Moreover,  $\mathcal{T}$ -invariant topological insulators were also predicted to exist in 3d [10, 42, 43, 45], which was later experimentally confirmed [46–52]. The latter owe similar but also distinct properties compared to their lower dimensional analogs.

### 1. 2d $\mathcal{T}$ -invariant topological insulators

Let's start with the 2d model Hamiltonian for a  $\mathcal{T}$ -invariant topological insulator [4]

$$\begin{pmatrix} \hat{\mathcal{H}}(\mathbf{k}) & 0 \\ 0 & \hat{\mathcal{H}}^*(-\mathbf{k}) \end{pmatrix} \quad \text{with} \quad \hat{\mathcal{H}}(\mathbf{k}) = v\hbar(k_x\sigma_y - k_y\sigma_x) + (m - \hbar^2\mathbf{k}^2)\sigma_z, \quad (91)$$

At this point we have to clarify the basis on which the Hamiltonian above, acts on. So far we have naturally associated the Pauli matrices  $\boldsymbol{\sigma}$  with the electronic spin-1/2. Here however, the four eigen-states on which the Hamiltonian acts on, correspond to the eigen-states of the total angular momentum  $\hat{\mathbf{J}} = \hat{\mathbf{L}} + \hat{\mathbf{S}}$  with  $j = 3/2$ , i.e.  $|j = 3/2; m_j = +3/2\rangle$ ,  $|j = 3/2; m_j = +1/2\rangle$ ,  $|j = 3/2; m_j = -3/2\rangle$  and  $|j = 3/2; m_j = -1/2\rangle$  (here there is a slight difference compared to the Bernevig-Hughes-Zhang model (BHZ) [4]). The angular momentum  $j = 3/2$  originates from the hybridization of the conduction  $\Gamma_6$  and valence  $\Gamma_8$  bands encountered in the typical semiconducting  $\mathcal{T}$ -invariant 2d topological insulators, involving  $l = 1$  and  $s = 1/2$ . As shown in Fig. 18, the band structure of HgTe is inverted compared to the usual motif encountered for instance in CdTe. By fabricating HgTe/CdTe quantum wells of different width  $d$ , one can impose the one or the other type of band structure. In the Hamiltonian of Eq. (91) the only parameter which depends on  $d$  is  $m$ . However, we have already shown that the parameter  $m$  controls the topological properties of these systems. The dependence of  $m$  with respect to  $d$  is such that, for  $d > d_c \rightarrow m > 0$ , the quantum well structure is exhibiting the inverted band structure characteristics typical to HgTe and as a result the system transits to the topologically non-trivial phase. As a matter of fact, the transition to the topologically non-trivial phase by tuning the width of the quantum well was theoretically predicted by [4] and experimentally confirmed by [25].

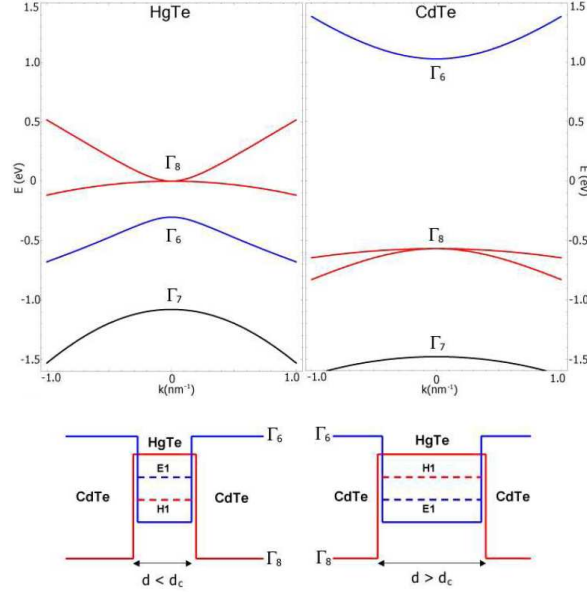


FIG. 18: Band structure in HgTe/CdTe quantum wells. The band structure of bulk HgTe is inverted compared to the typical case encountered in bulk CdTe. In the former, the  $\Gamma_6$  band lies below the  $\Gamma_8$  band, which constitute the conduction and valence bands for CdTe. The width of the middle region determines if the HgTe band structure characteristics will dominate, leading to a topologically non-trivial phase. Note that the  $\Gamma$ 's correspond to irreducible representations of the relevant point group.

We observe that the complete Hamiltonian is block diagonal and the system belongs to the symmetry class  $\text{BDI} \oplus \text{BDI}$ . Note that there is an artificial chiral symmetry which can be always lifted with the inclusion of a finite chemical

potential or disorder, leading to class  $A \oplus A$ . In the latter case, the Hamiltonian is characterized by two  $\mathbb{Z}$  topological invariants  $\tilde{N}_\sigma$ , with  $\sigma = \uparrow, \downarrow$  labelling the sign of the  $m_j$  of the eigen-states of the two blocks. In order for the system to be  $\mathcal{T}$ -symmetric, the two invariants have to satisfy  $\tilde{N}_\sigma = \sigma \tilde{N}$ . The electric Hall conductivity will be proportional to  $\tilde{N}_\uparrow + \tilde{N}_\downarrow$  and will be zero in this case. In contrast, the difference  $\tilde{N}_\uparrow - \tilde{N}_\downarrow = 2\tilde{N} \neq 0$  leading to the so called quantum spin Hall effect. Note that in the latter case, we have a number of  $\tilde{N}$  helical modes per edge.

We have to remark that there exist further terms that we can add in the Hamiltonian above, which preserve  $\mathcal{T}$ -symmetry but mix the two blocks. In the latter case, the Hamiltonian transits to symmetry class AII that supports a  $\mathbb{Z}_2$  topological invariant. The result of this symmetry class transition is to allow to the system to exhibit only a single pair of topologically protected helical solutions per edge. Essentially, in the presence of infinitesimally small terms which lead to class AII, the  $\mathbb{Z}_2$  topological invariant coincides with  $(\tilde{N}_\uparrow - \tilde{N}_\downarrow)/2 \bmod 2 = \tilde{N} \bmod 2$ , providing  $\mathbf{0}$  for a topologically trivial phase and  $\mathbf{1}$  for a non-trivial [9, 18, 19].

## 2. Interlude: 2d topological semi-metals - graphene

So far we have examined 2d *insulating* systems which violate or preserve  $\mathcal{T}$ -symmetry. Nonetheless, graphene is quite similar to a 2d  $\mathcal{T}$ -invariant insulator but does not have a band gap. It is natural to ask if a system like graphene can have any non-trivial topological properties, arising from the Dirac spectrum. Before answering this question, let's first discuss the band structure of graphene [53], which in the low energy limit can be described by two block diagonal  $2 \times 2$  Hamiltonians of the form

$$\begin{pmatrix} \hat{\mathcal{H}}_{\mathbf{K}}(\mathbf{q}) & 0 \\ 0 & \hat{\mathcal{H}}_{\mathbf{K}'}(\mathbf{q}) \end{pmatrix} \quad \text{with} \quad \hat{\mathcal{H}}_{\mathbf{K}}(\mathbf{q}) = v\hbar\mathbf{q} \cdot \boldsymbol{\sigma} \quad \text{and} \quad \hat{\mathcal{H}}_{\mathbf{K}'}(\mathbf{q}) = v\hbar\mathbf{q} \cdot \boldsymbol{\sigma}^*, \quad (92)$$

where we have introduced the reciprocal lattice vectors

$$\mathbf{K} = \left( \frac{2\pi}{3a}, \frac{2\pi}{3\sqrt{3}a} \right) \quad \text{and} \quad \mathbf{K}' = \left( \frac{2\pi}{3a}, -\frac{2\pi}{3\sqrt{3}a} \right). \quad (93)$$

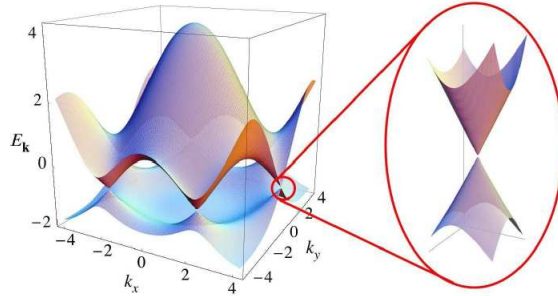


FIG. 19: The two  $S^1$  spheres are homotopically mapped with the winding number  $\tilde{w}$  counting how many times an angle of  $2\pi$  has been covered in  $\hat{\mathbf{g}}$ -space, when an angle of  $2\pi$  has been covered in the compactified  $k$ -space. The two  $S^1$  spheres are homotopically mapped with the winding number  $\tilde{w}$  counting how many times an angle of  $2\pi$  has been covered in  $\hat{\mathbf{g}}$ -space, when an angle of  $2\pi$  has been covered in the compactified  $k$ -space.

At these two inequivalent points of the 2d  $\mathbf{k}$ -space, the energy spectrum shows zeros. Therefore, for investigating the low energy properties of graphene, we can focus in the vicinity of these two points by expanding the wave-vectors in the following sense  $\mathbf{k} = \mathbf{K} + \mathbf{q}$  in terms of small momenta  $\mathbf{q}$ , i.e.  $|\mathbf{q}| \ll |\mathbf{K}|$ . Since the two vectors  $\mathbf{K}$  and  $\mathbf{K}'$  are connected by the mirror symmetry  $y \rightarrow -y$ , which for the particular case is equivalent to acting with the time reversal operator  $\mathcal{T}$ , the Hamiltonians at these two points are related by taking  $\sigma \rightarrow -\sigma_y$ . Note also, that in the present case we have a system with an even (two) number of Dirac points. In the previous section we discussed that it is necessary for the Jackiw-Rebbi type of models to contain an even number of Dirac copies, in order to circumvent the pathology of the Dirac equation which is linear in momentum and is not compact. In the graphene case, the system is not an insulator and therefore we cannot extend the same reasoning since the invariant  $\tilde{N}$  cannot be defined. Nonetheless, we observe that graphene's Hamiltonian includes an even number of Dirac type Hamiltonians  $v\hbar\mathbf{q} \cdot \boldsymbol{\sigma}$ , leading to an even number of independent Dirac zero-energy points. The necessity of an even number of Dirac points originates in

this case from  $\mathcal{T}$ -symmetry. The latter constraint can be also viewed as a consequence of the Nielsen-Ninomiya no-go theorem [54], forbidding an odd number of Dirac points for any *bulk* system which preserves  $\mathcal{T}$ -symmetry.

In order to explore possible non-trivial topological properties of the Hamiltonian above let us recall that in the topological non-trivial insulating systems examined earlier, the quantum anomalous Hall conductivity was expressed in terms of the properties of each band and specifically it depended on the Berry curvature (Eq. (77)) and the related gauge potential  $\mathcal{A}^\nu(\mathbf{k})$  Eq. (75). It is useful to investigate these quantities for the semimetallic case. Similarly to the situation in Eq. (47), the eigen-vectors of  $\hat{\mathcal{H}}_{\mathbf{K}}(\mathbf{q})$  and  $\hat{\mathcal{H}}_{\mathbf{K}'}(\mathbf{q})$  are given from the following expressions:

$$|\pm, \mathbf{q}, \mathbf{K}\rangle = \frac{1}{\sqrt{2}} \begin{pmatrix} \pm 1 \\ e^{+i\varphi_{\mathbf{q}}} \end{pmatrix}, \quad \text{and} \quad |\pm, \mathbf{q}, \mathbf{K}'\rangle = \frac{1}{\sqrt{2}} \begin{pmatrix} \pm 1 \\ e^{-i\varphi_{\mathbf{q}}} \end{pmatrix}, \quad (94)$$

where we introduced  $q_x = |\mathbf{q}| \cos \varphi_{\mathbf{q}}$ ,  $q_y = |\mathbf{q}| \sin \varphi_{\mathbf{q}}$  with eigen-energies  $E_\nu(\mathbf{q}) = \nu v \hbar |\mathbf{q}|$ . We readily obtain

$$\mathcal{A}^\nu(\mathbf{q}) = -\frac{1}{2} \frac{\partial \varphi_{\mathbf{q}}}{\partial \mathbf{q}} \quad \text{and} \quad \mathcal{A}'^\nu(\mathbf{q}) = +\frac{1}{2} \frac{\partial \varphi_{\mathbf{q}}}{\partial \mathbf{q}}, \quad (95)$$

for the points  $\mathbf{K}$  and  $\mathbf{K}'$  respectively. We observe that the Berry gauge field is non-zero and independent of the band index. Furthermore, it is straightforward to confirm with the use of Eq. (77), that  $\Omega_z^\nu(\mathbf{k}) = 0$ . The latter is consistent with the preservation of  $\mathcal{T}$ -symmetry which requires the vanishing of the coefficient of the third Pauli matrix. We can rewrite the result for the gauge field in a more illustrative form

$$\mathcal{A}^\nu(\mathbf{q}) = \frac{1}{2} \left( \frac{q_y}{|\mathbf{q}|^2}, -\frac{q_x}{|\mathbf{q}|^2} \right) \quad \text{and} \quad \mathcal{A}'^\nu(\mathbf{q}) = \frac{1}{2} \left( -\frac{q_y}{|\mathbf{q}|^2}, \frac{q_x}{|\mathbf{q}|^2} \right). \quad (96)$$

By transferring to the circular coordinates  $(q_x, q_y) \rightarrow (|\mathbf{q}|, \varphi_{\mathbf{q}})$  we obtain  $\mathcal{A}_\varphi^\nu(\mathbf{q}) = -1/(2|\mathbf{q}|)$  and  $\mathcal{A}'_\varphi(\mathbf{q}) = +1/(2|\mathbf{q}|)$ , implying that the radial component of  $\mathcal{A}$  is zero. From the above expression we directly observe that the gauge-field has a finite circulation, i.e.  $\oint_C d\mathbf{l} \cdot \mathcal{A}^\nu(\mathbf{q}) = -\pi$  and  $\oint_C d\mathbf{l} \cdot \mathcal{A}'^\nu(\mathbf{q}) = \pi$ . However, according to Stokes theorem  $\oint_C d\mathbf{l} \cdot \mathcal{A}^\nu(\mathbf{q}) = \oint_{\sigma(C)} d\sigma \hat{\mathbf{n}} \cdot \Omega^\nu(\mathbf{q}) = -\pi$ , implying  $\Omega_z^\nu(\mathbf{q}) = -\pi \delta(\mathbf{q})$  (similar for  $\mathbf{K}'$ ). This contradiction is quite common in electromagnetism when we encounter point-like charges. For instance for an electric point-charge  $e$  sitting at the origin of the 3d-coordinate space  $\mathbf{r} = \mathbf{0}$  the Poisson equation reads  $\nabla^2 V = 0$  despite the fact that  $V(\mathbf{r}) = -e/r$  up to a multiplying constant. In the latter case, the expression for the scalar potential can be found via the Gauss law and the related divergence theorem  $\int_\sigma d\sigma \hat{\mathbf{n}} \cdot \mathcal{E} = e \Rightarrow \int_{u(\sigma)} du \nabla \cdot \mathcal{E}(\mathbf{r}) = e \Rightarrow 4\pi \int dr r^2 \nabla^2 V(r) = -e \Rightarrow V(\mathbf{r}) = -e/r$ . In the present case, the Dirac point where the upper and lower bands touch, behaves like a magnetic point-like source (vortex) providing a finite circulation for the vector potential and a singular Berry curvature, which is non-zero exactly at the singularity  $\mathbf{q} = \mathbf{0}$ . The finite  $\pi$ -circulation of  $\mathcal{A}$  is also called  $\pi$ -Berry's phase. In fact, in  $\mathcal{T}$ -invariant 2d systems the Berry phase can be either  $0, \pi$ , i.e. a  $\mathbb{Z}_2$  number, similar in a sense to the  $\mathbb{Z}_2$ -invariant characterizing the 2d  $\mathcal{T}$ -invariant topological insulators. As a consequence, one expects that graphene could also demonstrate some type of edge modes. Indeed, in the zig-zag (but not in the armchair) configuration, graphene nanoribbons support dispersionless edge states [53] which could be also viewed as a limiting case of the dispersive helical edge modes of a  $\mathcal{T}$ -invariant 2d topological insulator [55].

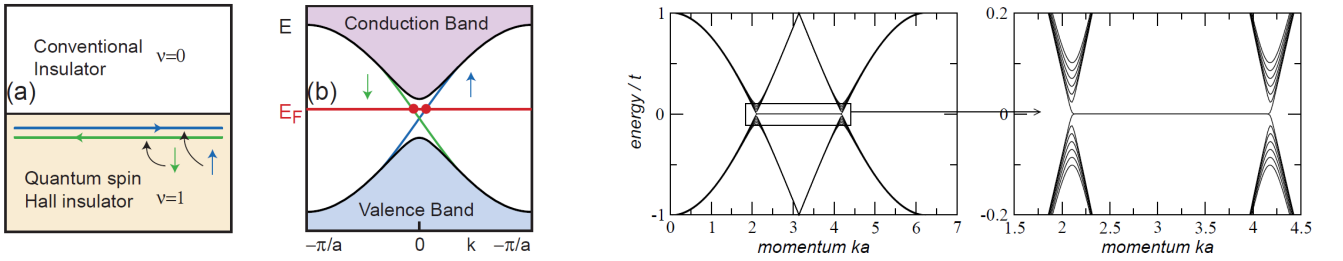


FIG. 20: **Left:** Helical edge modes at the boundary separating a 2d  $\mathcal{T}$ -invariant topological insulator from vacuum. The edge states appear within the bulk, are dispersive and merge with the bulk states away from  $k = 0$  where the bulk gap closing occurs. Figure taken from [18]. **Right:** Dispersionless edge states in a graphene nanoribbon, arranged in the zig-zag configuration. The dispersionless graphene edge states can be viewed as a limiting case of the helical edge modes shown in the left panel when the bulk gap of the insulator goes to zero. Figure taken from [53].

### 3. 3d topological insulators - topologically protected Dirac surface modes

We will conclude the discussion of  $\mathcal{T}$ -invariant topological insulators with a short description of the 3d systems. Similar to their 2d analogs, a simple extension for a 3d topological insulator [56] can have the form

$$\hat{\mathcal{H}}(\hat{\mathbf{p}}) = v(\hat{p}_x\sigma_y - \hat{p}_y\sigma_x) + v\hat{p}_z\lambda_x\sigma_z + (m - \hat{\mathbf{p}}^2)\lambda_y\sigma_z, \quad (97)$$

where we have enlarged the spinor dimension to four. For the present discussion, we can consider that the  $\sigma$  Pauli matrices correspond to the usual electronic spin-1/2 and the  $\lambda$  Pauli matrices correspond to a band index. Every element of the Hamiltonian above is a Kronecker product  $\lambda_\mu \otimes \sigma_\nu$  of the respective Pauli matrices  $\mu, \nu = x, y, z$  and the related unit matrices  $\mu, \nu = 0$ . As we have already followed in Eq. (97) we will suppress the Kronecker symbol and the unit matrices. Under  $\hat{\mathcal{T}}$  we have  $\hat{\mathcal{T}}^\dagger \sigma \hat{\mathcal{T}} = -\sigma$  while we assume  $\hat{\mathcal{T}}^\dagger(\lambda_x, \lambda_y, \lambda_z)\hat{\mathcal{T}} = (\lambda_x, -\lambda_y, \lambda_z)$ . Due to the properties of the  $\lambda$  matrices the Hamiltonian under investigation is characterized by the usual  $\mathcal{T}$ -symmetry, i.e.  $\hat{\Theta} = \hat{\mathcal{T}} = i\sigma_y\hat{\mathcal{K}}$ , as also by a chiral symmetry  $\hat{\Pi} = \lambda_z\sigma_z$  and a concomitant charge-conjugation symmetry with  $\hat{\Xi} = \lambda_z\sigma_x\hat{\mathcal{K}}$ . The symmetry class of the system is DIII, since  $\hat{\Theta}^2 = -\hat{I}$  and  $\hat{\Xi}^2 = +\hat{I}$ . The particular class is characterized by a  $\mathbb{Z}$  invariant in 3d. Note that in the presence of a non-zero chemical potential that would be added via the introduction of a constant diagonal term in the above Hamiltonian, the symmetry would change to AII which is characterized by a  $\mathbb{Z}_2$  invariant in 3d. The situation is completely similar to the 2d  $\mathcal{T}$ -invariant topological insulators where in the presence of chiral symmetry we have a  $\mathbb{Z}$  number of protected helical modes appear per edge, while when it is broken only a single pair of helical solutions appears per edge. The only difference is that in the present case we do not have helical edge modes but helical surface modes, or as we will see Dirac surface modes.

In order to explicitly demonstrate the existence of helical surface modes in the model above, we will follow the procedure discussed in the context of  $\mathcal{T}$ -violating topological insulators and confine the system in a box ( $z \in [z_1, z_2]$ ) along the  $z$ -axis. Along the other two spatial dimensions,  $x$  and  $y$ , we will assume translational invariance. We Fourier transform and set  $k_x = k_y = 0$ . The Hamiltonian obtains the form

$$\hat{\mathcal{H}}(k_x = k_y = 0, k_z) = v\hbar k_z\lambda_x\sigma_z + (m - \hbar^2 k_z^2)\lambda_y\sigma_z, \quad (98)$$

which is similar to Eq. (40). The zero-energy solutions will be eigen-states of  $\hat{\Pi} = \lambda_z\sigma_z$  and have the form

- $m > (v/2)^2 > 0$ :

$$\hat{\phi}_{0,-,\sigma}(z) \propto \sin[(z - z_1)/\xi]e^{-(z-z_1)/l} \begin{pmatrix} 0 \\ 1 \end{pmatrix}, \quad (99)$$

$$\hat{\phi}_{0,+,\sigma}(z) \propto \sin[(z - z_2)/\xi]e^{+(z-z_2)/l} \begin{pmatrix} 1 \\ 0 \end{pmatrix}. \quad (100)$$

- $0 < m < (v/2)^2$ :

$$\hat{\phi}_{0,-,\sigma}(z) \propto \sinh[(z - z_1)/\xi]e^{-(z-z_1)/l} \begin{pmatrix} 0 \\ 1 \end{pmatrix}, \quad (101)$$

$$\hat{\phi}_{0,+,\sigma}(z) \propto \sinh[(z - z_2)/\xi]e^{+(z-z_2)/l} \begin{pmatrix} 1 \\ 0 \end{pmatrix}, \quad (102)$$

with  $\xi = \hbar/\sqrt{|m - (v/2)^2|} \in \mathbb{R}^+$  and  $1/l = v/(2\hbar) > 0$ . The eigen-solutions are labelled by the eigen-values of  $\lambda_z = \pm 1$  and the eigen-values of  $\sigma_z = \pm 1$  ( $\sigma$ ). Note that there is a double degeneracy, since each zero-energy solution sitting at  $z_{1,2}$  is labelled by the eigen-values of  $\sigma_z$ ,  $\sigma = \pm 1$ . This is the Kramers degeneracy and constitutes a direct consequence of  $\mathcal{T}$ -symmetry and  $\hat{\mathcal{T}}^2 = -\hat{I}$ . As a matter of fact, the two solutions at each side have opposite spin polarizations. At this point we may retrieve the helical surface modes by first allowing  $k_x$  and  $k_y$  to be non-zero and then letting the related terms to act on the truncated space spanned by the four wave-functions above. We directly obtain that close to the  $z = z_1$  boundary the Hamiltonian becomes  $\hat{\mathcal{H}}_-(z_1, \mathbf{k}_{||}) = v\hbar(k_x\sigma_y - k_y\sigma_x)$  while close to the  $z = z_2$  boundary the Hamiltonian becomes  $\hat{\mathcal{H}}_+(z_2, \mathbf{k}_{||}) = v\hbar(k_x\sigma_y - k_y\sigma_x)$ , where we neglected the Hamiltonian part which is quadratic in momenta and leads to an exponentially decaying mixing term (see Eq. (46)). The same procedure can be carried out if we assume confinement along the  $x$  and  $y$  directions, yielding helical surface modes with different wave-functions. The helical surface modes are present only for  $m > 0$ . Note that the Nielsen-Ninomiya theorem still holds, since there is a single Dirac cone on a surface, and not in the bulk. Moreover, the Dirac cones

### 3d T-invariant topological insulator

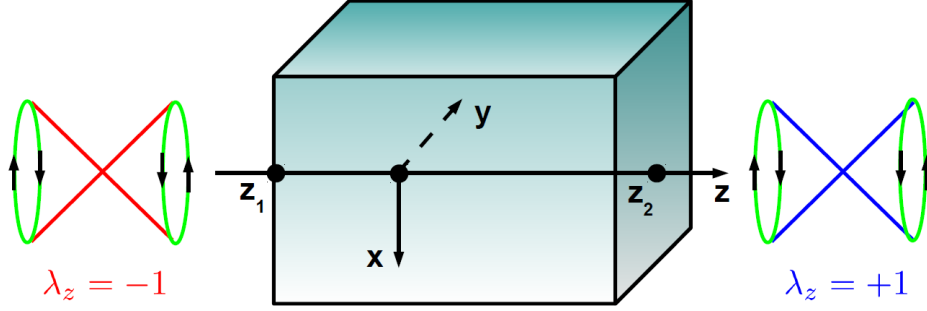


FIG. 21: 3d  $\mathcal{T}$ -invariant topological insulator confined along the  $z$ -direction between  $z_1$  and  $z_2$ . For  $m > 0$  the system resides in the topologically non-trivial phase exhibiting topologically protected Dirac-like surface modes. Each surface solution is labelled by the eigen-states of the chiral symmetry operator  $\lambda_z \sigma_z$ . In accordance with Nielsen-Ninomiya's theorem, a *single* Dirac cone is allowed on the surface and could lead to a fractional quantum anomalous Hall effect if  $\mathcal{T}$ -symmetry is broken near the surface. A similar confinement procedure can be applied for the other faces of the 3d system, leading to surface modes with different quantum numbers compared to the case examined here.

necessarily appear in pairs, *though non-locally*, in order to assure that we do not have any global fractionalization effects.

The appearance of a single Dirac cone on a surface leads to important ramifications when  $\mathcal{T}$ -symmetry is violated near the surface without closing the bulk gap. This could be the case where we place a ferromagnet in proximity to the topological surface. In this case, the helical surface modes are no longer protected, while at the same time a gap  $F$  will open in the surface spectrum. Consequently, the surface Hamiltonian will obtain the form of the 2d model  $\hat{\mathcal{H}}_-(z_1, \mathbf{k}_{||}) = v\hbar(k_x \sigma_y - k_y \sigma_x) + F\sigma_z$  which can exhibit the fractional quantum anomalous Hall effect, as discussed earlier. However, a Hall measurement will unavoidably involve also the opposite side leading to an integer quantum anomalous Hall effect. Nonetheless, optical measurements could in principle detect this fractional behavior [57].

We may now proceed with understanding the bulk topological properties of the system. First of all we directly observe that the Hamiltonian can be parametrized in the following manner

$$\hat{\mathcal{H}}(\mathbf{k}) = v\hbar(k_x \sigma_y - k_y \sigma_x) + v\hbar k_z \lambda_x \sigma_z + (m - \hbar^2 \mathbf{k}^2) \lambda_y \sigma_z = E(\mathbf{k}) \hat{\mathbf{g}}(\mathbf{k}) \cdot \mathbf{\Gamma}, \quad (103)$$

where we introduced the five-component vector

$$\begin{aligned} \mathbf{g}(\mathbf{k}) &= (-v\hbar k_y, v\hbar k_x, m - \hbar^2 \mathbf{k}^2, v\hbar k_z, 0) \\ &\equiv E(\mathbf{k}) (-\sin \chi_{\mathbf{k}} \sin \varphi_{\mathbf{k}} \sin \vartheta_{\mathbf{k}}, \sin \chi_{\mathbf{k}} \cos \varphi_{\mathbf{k}} \sin \vartheta_{\mathbf{k}}, \sin \chi_{\mathbf{k}} \cos \vartheta_{\mathbf{k}}, \cos \chi_{\mathbf{k}}, 0) \equiv E(\mathbf{k}) \hat{\mathbf{g}}(\mathbf{k}) \cdot \mathbf{\Gamma}, \end{aligned} \quad (104)$$

with  $E(\mathbf{k}) = |\mathbf{g}(\mathbf{k})| = \sqrt{(v\hbar \mathbf{k})^2 + [m - (\hbar \mathbf{k})^2]^2}$  and  $\mathbf{\Gamma} = (\sigma_x, \sigma_y, \lambda_y \sigma_z, \lambda_x \sigma_z, \lambda_z \sigma_z)$ . Note that the five  $\mathbf{\Gamma}$  matrices span an SO(5) Clifford algebra, similar to the SO(3) Clifford algebra that the usual Pauli matrices  $\boldsymbol{\sigma}$  do. This implies that the anticommutator relations  $\{\Gamma_a, \Gamma_b\} = 2\delta_{ab} \hat{I}$  which the  $\mathbf{\Gamma}$  matrices satisfy, allow us to define a five-dimensional intrinsic space. The unit vector  $\hat{\mathbf{g}}(\mathbf{k})$  will be constrained to take values on a three sphere  $S^3$ . Since the  $\hat{\mathbf{g}}(\mathbf{k})$  has the following behaviour at infinity  $\hat{\mathbf{g}}(|\mathbf{k}| \rightarrow +\infty) = (0, 0, -1, 0, 0)$  we can compactify the  $\mathbb{R}^3$   $\mathbf{k}$ -space into a three sphere  $S^3$ . According to the previous sections we expect that the topological invariant will be an  $\mathbb{Z}$  and will be connected to the mapping of  $S^3 \rightarrow S^3$  effected by  $\hat{\mathbf{g}}(\mathbf{k})$ . We introduce the following topological invariant

$$\widetilde{\mathcal{W}} = \frac{1}{2\pi^2} \int d\mathbf{k} \varepsilon_{abcd5} \hat{g}_a(\mathbf{k}) \frac{\partial \hat{g}_b(\mathbf{k})}{\partial k_x} \frac{\partial \hat{g}_c(\mathbf{k})}{\partial k_y} \frac{\partial \hat{g}_d(\mathbf{k})}{\partial k_z}, \quad (105)$$

where we have introduced the totally antisymmetric symbol  $\varepsilon_{abcde}$ , assumed Einstein's convention of summing the repeated indices and  $a, b, c, d, e = 1, 2, 3, 4, 5$ . For the model under consideration the topological invariant is non-zero for  $m > 0$  and is equal to  $\widetilde{\mathcal{W}} = 1$ . We can always construct a  $\mathbb{Z}_2$  invariant starting from a  $\mathbb{Z}$  invariant, in the following manner  $\mathbb{Z}_2 \equiv e^{-i\pi \widetilde{\mathcal{W}}} = (-1)^{\widetilde{\mathcal{W}}}$ . If chiral symmetry  $\hat{\Pi}$  and charge-conjugation become infinitesimally broken, but  $\hat{\Theta}$ -symmetry persists, then the above  $\mathbb{Z}_2$  will be the only allowed invariant of the system since now the system lies in class AII.

## VI. TOPOLOGICAL SUPERCONDUCTORS

So far we have studied insulating materials with a special band-structure which leads to a number of topological phenomena, including the quantum anomalous Hall effect and the quantum spin Hall effect. Transport in the QAHE (QSHE) system is mediated by chiral (helical) edge modes which can disperse *without any dissipation*. The latter feature is certainly quite appealing for nano-electronic applications. Evenmore, these edge modes were shown to be characterized by half-the quantum numbers of the bulk electrons, for instance specific chirality or spin projection. However, it is interesting to explore up to which point we are able to divide an electron into halves. For that one has to realize which are the available degrees of freedom of electrons. As we already know, an electron is an electrically charged spin-1/2 particle. The solutions that we have already examined had half-of the spin degrees of freedom, but none of them had half of the charge degrees of freedom. Essentially, a bound state solution of this type is called Majorana [58–60] and would imply that the corresponding wave-function would be inert to local charge sources and fluctuations. Only non-local charge sources or fields which can see both halves can interact with the system. Moreover, if this solution would correspond to zero-energy, the ground state of the system would exhibit a degeneracy. The topological protection, the immunity to charge noise and the ground state degeneracy constitute a triad of properties which are particularly attractive for topological quantum computing [61, 62] which is a prominent way of bypassing the obstacle of noise and decoherence encountered in quantum bits (qubits) based on spin [63] or superconducting systems [64].

### A. Majorana fermions and topological quantum computing

In the previous paragraph, we suggested that finding zero-energy bound state solutions of the Majorana type, would be advantageous for several aspects including the potential application in the field of topological quantum computing. In reality, Majorana fermions are not that “rare”, at least from the condensed matter perspective, but mostly kept well hidden inside every electron. To understand the latter claim, let’s mathematically formulate the above picture in terms of the creation ( $c_\alpha^\dagger(\mathbf{r})$ ) and annihilation ( $\hat{c}_\alpha(\mathbf{r})$ ) operators of electrons, satisfying the anti-commutation relation  $\{\hat{c}_\alpha(\mathbf{r}), \hat{c}_\beta^\dagger(\mathbf{r}')\} = \delta(\mathbf{r} - \mathbf{r}')\delta_{\alpha\beta}$  and  $\{\hat{c}_\alpha(\mathbf{r}), \hat{c}_\beta^\dagger(\mathbf{r})\} = 0$ . One can always formally rewrite the above operators into following fashion  $\hat{c}_\alpha(\mathbf{r}) = (\hat{\gamma}_\alpha(\mathbf{r}) + i\hat{\tilde{\gamma}}_\alpha(\mathbf{r}))/\sqrt{2}$ :

$$c_\alpha(r) = \frac{\gamma_\alpha(r) + i\tilde{\gamma}_\alpha(r)}{\sqrt{2}} = \frac{\gamma_\alpha(r)}{\tilde{\gamma}_\alpha(r)} \left( \begin{array}{c} \bullet \\ \bullet \end{array} \right) \leftarrow \text{MFs}$$

FIG. 22: Every electronic operator can be decomposed into two self-conjugate Majorana fermion operators.

where the new operators are self-conjugate (or simply real), since  $\hat{\gamma}_\alpha(\mathbf{r}) = \hat{\gamma}_\alpha^\dagger(\mathbf{r})$  and they are called *Majorana fermion* operators (for simplicity we will suppress the “ $\hat{\phantom{x}}$ ” from the operators, for the rest of the discussion). The name is coined after Ettore Majorana who first showed in 1937 [58] the possibility of real solutions of the Dirac equations leading to the proposal of Majorana particles. As a matter of fact, the neutrino has been considered the most prominent candidate of a Majorana particle. Majorana fermion (MF) operators additionally satisfy  $\{\gamma_\alpha(\mathbf{r}), \gamma_\beta(\mathbf{r}')\} = \{\tilde{\gamma}_\alpha(\mathbf{r}), \tilde{\gamma}_\beta(\mathbf{r}')\} = \delta(\mathbf{r} - \mathbf{r}')\delta_{\alpha\beta}$  and  $\{\gamma_\alpha(\mathbf{r}), \tilde{\gamma}_\beta(\mathbf{r}')\} = 0$ . Note that each of these operators also fulfills  $\gamma_\alpha^2(\mathbf{r}) = 2$  in contrast to the usual fermionic operators for which  $c_\alpha^2(\mathbf{r}) = 0$ . The latter property demonstrates that a  $\gamma$  operator alone cannot create or annihilate a particle. Only a pair of Majorana fermions can combine into an electron. Basically, these operators constitute the two neutral halves comprising a charged fermion (the electron). Although we can always express an electron in terms of two Majorana fermions this does not imply that they can be experimentally accessible. This happens because any local charge source will see simultaneously both MFs because they exist at the same point of space. Only if we can find a way to split the electron into two spatially separated Majorana fermions, we could isolate them and in principle observe them.

According to the previous sections, we have encountered topologically protected boundary solutions of the Schrödinger equation, carrying half of the electronic degrees of freedom. The latter suggests that there could be an appropriate topologically non-trivial system which can support zero-energy bound state solutions  $\hat{\phi}(\mathbf{r})$  and lead to MF operators  $\gamma(\mathbf{r}) = \gamma^\dagger(\mathbf{r})$ . Our aim is to figure out what type of topologically non-trivial system could support MFs. So far the topological systems that we have considered were described by a second quantized Hamiltonian of the following form  $\mathcal{H} = \sum_{\mathbf{k}} \hat{\Psi}_{\mathbf{k}}^\dagger \hat{\mathcal{H}}(\mathbf{k}) \hat{\Psi}_{\mathbf{k}}$  with  $\hat{\Psi}_{\mathbf{k}}^\dagger = (c_{\mathbf{k},\uparrow}^\dagger, c_{\mathbf{k},\downarrow}^\dagger)$ . We can diagonalize the corresponding single particle

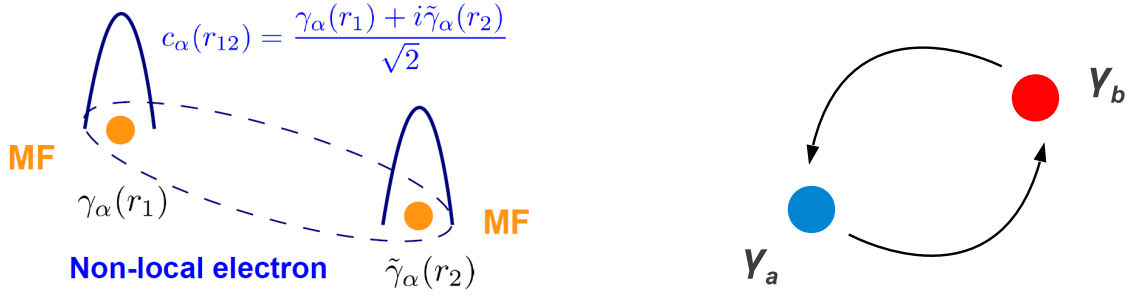


FIG. 23: **Left:** Non-local electron built up by two spatially separated Majorana fermion operators corresponding to a Majorana bound state wave-function. **Right:** Exchanging Majorana fermions in real space leads to a protected single topological qubit rotation termed braiding. In qubit space, this corresponds to a gate operation where the qubit states pick up a relative  $\pi/2$  phase.

Hamiltonian by introducing the Bogoliubov operators  $\gamma_{\mathbf{k},\alpha}$

$$\gamma_{\mathbf{k},\alpha} = u_{\mathbf{k}}c_{\mathbf{k},\alpha} + v_{\mathbf{k}}c_{\mathbf{k},-\alpha}. \quad (106)$$

Note that even if we set  $u_{\mathbf{k}} = v_{\mathbf{k}}$  the operator  $\gamma_{\mathbf{k},\alpha} \neq \gamma_{\mathbf{k},\alpha}^\dagger$ , i.e. it can never become a MF operator. The reason is that this operator is a linear combination only of electronic (particle) operators. To tackle this problem, the only route is to find a system where the Bogoliubov eigen-operators are made out of linear combinations of electron ( $c_{\mathbf{k},\alpha}$ ) and hole ( $c_{\mathbf{k},\alpha}^\dagger$ ) operators. A suitable system whose quasiparticle excitations are linear combinations of electrons and holes is a superconductor. For a conventional superconductor, the mean-field decoupled second quantized Hamiltonian has the form

$$\mathcal{H} = \int d\mathbf{k} \sum_{\alpha=\uparrow,\downarrow} \varepsilon_{\alpha}(\mathbf{k})c_{\mathbf{k},\alpha}^\dagger c_{\mathbf{k},\alpha} + \int d\mathbf{k} \left( \Delta c_{\mathbf{k},\uparrow}^\dagger c_{-\mathbf{k},\downarrow}^\dagger + \Delta^* c_{-\mathbf{k},\downarrow} c_{\mathbf{k},\uparrow} \right), \quad (107)$$

where  $\Delta$  defines the superconducting order parameter. In the particular case a Bogoliubov transformation where

$$\gamma_{\mathbf{k},\uparrow} = u_{\mathbf{k}}c_{\mathbf{k},\uparrow} + v_{\mathbf{k}}c_{-\mathbf{k},\downarrow}^\dagger, \quad (108)$$

can diagonalize the single particle Hamiltonian. Note that once again,  $\gamma_{\mathbf{k},\uparrow}^\dagger \neq \gamma_{\mathbf{k},\uparrow}$  even if we set  $u_{\mathbf{k}} = v_{\mathbf{k}}$ . Although we have managed to obtain linear combinations of particles and holes, the latter correspond to different spin projection, not allowing us to construct MF operators. The problem can be completely circumvented only for a superconducting system which also involves pairing for the same spin projections, i.e. leading to Cooper pairs of the form  $c_{\mathbf{k},\uparrow}^\dagger c_{-\mathbf{k},\downarrow}^\dagger$ . For this unconventional type of a superconductor, the Bogoliubov transformation will have the form

$$\gamma_{\mathbf{k},\alpha} = u_{\mathbf{k},\alpha}c_{\mathbf{k},\alpha} - v_{\mathbf{k},\alpha}c_{-\mathbf{k},\alpha}^\dagger + u_{\mathbf{k},-\alpha}c_{\mathbf{k},-\alpha} - v_{\mathbf{k},-\alpha}c_{-\mathbf{k},-\alpha}^\dagger. \quad (109)$$

In the case shown above, if there can be for instance a wave-function of the form  $u_{\mathbf{k},\pm\alpha} = -v_{\mathbf{k},\pm\alpha} \in \mathbb{R}$  then

$$\gamma_{\mathbf{k},\alpha} = u_{\mathbf{k},\alpha} \left( c_{\mathbf{k},\alpha} + c_{-\mathbf{k},\alpha}^\dagger \right) + u_{\mathbf{k},-\alpha} \left( c_{\mathbf{k},-\alpha} + c_{-\mathbf{k},-\alpha}^\dagger \right) \quad (110)$$

and one observes that for the inversion-symmetric points  $\mathbf{k}_T$  satisfying  $\mathbf{k} \equiv -\mathbf{k}$ , we indeed obtain MFs  $\gamma_{\mathbf{k}_T,\alpha} = \gamma_{\mathbf{k}_T,\alpha}^\dagger$ . Apparently the required recipe in order to obtain MFs, is to obtain an unconventional superconducting pairing which leads to Cooper pairs consisting of electrons having the same spin-projection. This type of superconductivity is called spin-triplet and the most common example is a p-wave superconductor which we will examine in the next paragraphs.

Before proceeding let us comment on the importance of retrieving MF operators located at different points of coordinate space. As we have already mentioned, two zero-energy bound state solutions of the MF type, lead to the corresponding operators  $\gamma_a$  and  $\gamma_b$  from which we can construct a non-local electron with an annihilation operator  $c_0 = (\gamma_a + i\gamma_b)/\sqrt{2}$ . Since the corresponding energy of the  $c_0$  electron is zero, occupying or not-occupying the particular electronic state does not modify the energy of the total system. Consequently the state where this electron is not-occupied  $|\mathbf{0}\rangle$ , satisfying  $c_0|\mathbf{0}\rangle = 0$ , and the state with an occupied electron  $|\mathbf{1}\rangle = c_0^\dagger|\mathbf{0}\rangle$  are degenerate. Note that the particular degeneracy is topologically protected as long as the zero-energy MF solutions are also

protected. The arising doubly degenerate two-state subspace can define a topological qubit, which constitutes the fundamental building block for performing topological quantum information processing [62]. Rotations in this qubit space correspond to single-qubit operations. For the topological qubit, there exist a single operation called *braiding*, which is topologically protected and corresponds to  $(|0\rangle, |1\rangle) \rightarrow (e^{i\pi/4}|0\rangle, e^{-i\pi/4}|1\rangle)$ . This operation can be effected by exchanging adiabatically the two MFs building up the non-local electron. As a matter of fact, this is the only topologically protected operation against noise and decoherence that one can define within this qubit space. Other operations are also possible but not protected. As a result, universal topological quantum computing is not accessible in terms of MFs and further solutions have to be found [65].

## B. Unconventional superconductivity

As we have already mentioned, the mean-field decoupled Hamiltonian describing a conventional superconductor as it was originally proposed by Bardeen-Cooper-Schrieffer (BCS) [66], has the form of Eq. (107). The mean-field theory approximation is crucial for decoupling the attractive electron-electron interaction (phonon-mediated)

$$\mathcal{V}_{int} = -\frac{g}{(2\pi)^d} \iint d\mathbf{k}d\mathbf{k}' c_{\mathbf{k},\uparrow}^\dagger c_{-\mathbf{k},\downarrow}^\dagger c_{-\mathbf{k}',\downarrow} c_{\mathbf{k}',\uparrow}, \quad (111)$$

into a solvable non-interacting theory for quasiparticles which are superpositions of electrons and holes. The mean-field theory approximation is the consideration that specific operators can be replaced by their expectation values. In general, which operator should be selected for the mean-field approximation depends on the type of phase transition. In the case of superconductivity, particle number conservation will be spontaneously broken, when entering the superconducting phase. Therefore, we can consider

$$c_{\mathbf{k},\uparrow}^\dagger c_{-\mathbf{k},\downarrow}^\dagger = \langle c_{\mathbf{k},\uparrow}^\dagger c_{-\mathbf{k},\downarrow}^\dagger \rangle + \left( c_{\mathbf{k},\uparrow}^\dagger c_{-\mathbf{k},\downarrow}^\dagger - \langle c_{\mathbf{k},\uparrow}^\dagger c_{-\mathbf{k},\downarrow}^\dagger \rangle \right), \quad (112)$$

where the term in the parenthesis denotes the fluctuation of the operator around this mean value. After neglecting the second order terms in the fluctuations and leaving aside the arising term  $|\Delta|^2/g$ , which is irrelevant for examining the quasiparticle properties, we retrieve Eq. (107). To obtain the BCS Hamiltonian we introduced the superconducting order parameter

$$\Delta = -g \int \frac{d\mathbf{k}}{(2\pi)^d} \langle c_{-\mathbf{k},\downarrow} c_{\mathbf{k},\uparrow} \rangle \quad \text{and} \quad \Delta^* = -g \int \frac{d\mathbf{k}}{(2\pi)^d} \langle c_{\mathbf{k},\uparrow}^\dagger c_{-\mathbf{k},\downarrow}^\dagger \rangle. \quad (113)$$

The particular superconducting order parameter is a complex scalar number. It is the so-called conventional or s-wave superconducting order parameter discussed within the BCS theory. Since it corresponds to a Cooper pair of zero momentum, where the electrons involved have anti-parallel spins, it is additionally termed a spin-singlet superconducting order parameter. Due to the fermionic anti-commutation relations the superconducting order parameter has to be anti-symmetric under the exchange of the two electrons. The spin-singlet configuration of two electrons is odd under spin-exchange since it has the form  $|S=0; m_s=0\rangle = (|\uparrow\downarrow\rangle - |\downarrow\uparrow\rangle)/\sqrt{2}$ . Since the order parameter essentially constitutes the wave-function of the Cooper pair, in order to be completely antisymmetric it has to be even under inversion  $\mathbf{k} \leftrightarrow -\mathbf{k}$ . Generally, we can write  $\Delta_{\uparrow\downarrow}(\mathbf{k}) = -\Delta_{\downarrow\uparrow}(-\mathbf{k})$ . We directly confirm that for the spin-singlet pairing, the superconducting order parameter has to satisfy  $\Delta_{\text{singlet}}(\mathbf{k}) = \Delta_{\text{singlet}}(-\mathbf{k})$ . However, another possibility opens up. For two electrons with spin-1/2 the total spin can also take the quantum number  $S=1$ . This is the triplet case where  $|S=1; m_s=+1\rangle = |\uparrow\uparrow\rangle$ ,  $|S=1; m_s=0\rangle = (|\uparrow\downarrow\rangle + |\downarrow\uparrow\rangle)/\sqrt{2}$  and  $|S=1; m_s=-1\rangle = |\downarrow\downarrow\rangle$ . All these states are symmetric under the exchange of the two particles. As a matter of fact the three possible order parameters which correspond to this spin-triplet Cooper pairing, must be an odd function of momentum. In the most general case we can introduce the order parameters  $\Delta_{\alpha\beta}(\mathbf{k})$  in terms of the spin projections of the two electrons. These matrix elements have to satisfy  $\Delta_{\alpha\beta}(\mathbf{k}) = -\Delta_{\beta\alpha}(-\mathbf{k})$ . However, these order parameters can be visualized as elements of a matrix  $\hat{\Delta}(\mathbf{k})$ , defined in spin-space. The antisymmetry condition now reads  $\hat{\Delta}(\mathbf{k}) = -\hat{\Delta}^T(-\mathbf{k})$ , with  $T$  denoting matrix transposition. The order parameter can be decomposed into spin-singlet  $\psi(\mathbf{k})$  and triplet parts  $\mathbf{d}(\mathbf{k})$  in the following manner:  $\hat{\Delta}(\mathbf{k}) = \psi(\mathbf{k})i\sigma_y + \mathbf{d}(\mathbf{k})i\sigma_y\boldsymbol{\sigma}$ . The singlet and triplet order parameters satisfy the constraints  $\psi(\mathbf{k}) = \psi(-\mathbf{k})$  and  $\mathbf{d}(\mathbf{k}) = -\mathbf{d}(-\mathbf{k})$  [67].

For a rotationally invariant normal phase, one can expand the order parameters in spherical harmonics  $Y_{lm}(\mathbf{k})$  defined in momentum space. Since  $Y_{lm}(-\mathbf{k}) = (-1)^l Y_{lm}(\mathbf{k})$  one observes that singlet (triplet) superconducting order parameters can take only even (odd) harmonics. For  $l=0$  we obtain the spin singlet s-wave superconductivity,  $\psi(\mathbf{k}) = \Delta_s$ , conventional superconductivity. For  $l=2$  we have five possible types of d-wave superconductivity.

Among them one finds  $\psi(\mathbf{k}) = \Delta_d(k_x^2 - k_y^2)$  which is related to the type of superconductivity encountered in high-Tc cuprate superconductors [68]. Which type of superconducting order parameter will become preferred depends on one hand on the type of the interaction and on the other on the energy dispersion and particularly the Fermi surface of the electrons in the normal phase. If the FS is isotropic, then an s-wave order parameter will be preferred. If the Fermi surface is anisotropic in  $\mathbf{k}$ -space, it is possible but not necessary that an anisotropic order parameter can be stabilized, but the exact outcome is related to the microscopic details of the system. Apart from the singlet order parameters, we also have triplet. For example in the  $l = 1$  case we have the following harmonics  $k_x + ik_y, k_z, k_x - ik_y$  corresponding to a particular  $m_l = +1, 0, -1$ . Within a real basis we simply have  $Y_{l=1} \sim \mathbf{k}$ . Depending on the combination of the p-wave harmonics in the  $\mathbf{d}(\mathbf{k})$ -vector one can break spontaneously additional symmetries apart from the electromagnetic  $U(1)$  symmetry. The important difference of the conventional order parameter compared to the rest, it is that it shows no zeros. Instead unconventional order parameters can become zero at some  $\mathbf{k}$ -space points, lines or surfaces. The latter characteristic is very important for obtaining MFs.

### C. Majorana fermions in chiral p-wave superconductors

In this section we will focus on a particular model for p-wave superconductivity which will allow the discussion of topologically protected edge states and edge modes of the Majorana type. The most general model of a mean-field decoupled Hamiltonian for a p-wave superconductor has the following form

$$\mathcal{H} = \int d\mathbf{k} \sum_{\alpha} \varepsilon_{\alpha}(\mathbf{k}) c_{\mathbf{k}\alpha}^{\dagger} c_{\mathbf{k}\alpha} + \int d\mathbf{k} \left[ c_{\mathbf{k},\alpha}^{\dagger} \mathbf{d}(\mathbf{k}) \cdot (\boldsymbol{\sigma} i \sigma_y)_{\alpha\beta} c_{-\mathbf{k},\beta}^{\dagger} + \text{h.c.} \right]. \quad (114)$$

In the particular case we will consider the following structure for the order parameter:  $\mathbf{d}(\mathbf{k}) = (0, -\Delta_p(\mathbf{k}), 0)$ , yielding

$$\mathcal{H} = \int d\mathbf{k} \sum_{\alpha} \varepsilon_{\alpha}(\mathbf{k}) c_{\mathbf{k}\alpha}^{\dagger} c_{\mathbf{k}\alpha} - \frac{1}{2} \int d\mathbf{k} \sum_{\alpha} \left[ 2i\Delta_p(\mathbf{k}) c_{\mathbf{k},\alpha}^{\dagger} c_{-\mathbf{k},\alpha}^{\dagger} - 2i\Delta_p(\mathbf{k}) c_{-\mathbf{k},\alpha} c_{\mathbf{k},\alpha} \right]. \quad (115)$$

At this point we can make use of the Nambu formalism and rewrite the above Hamiltonian in the following manner  $\mathcal{H} = \frac{1}{2} \int d\mathbf{k} \sum_{\alpha} \hat{\Psi}_{\mathbf{k},\alpha}^{\dagger} \hat{\mathcal{H}}_{\alpha}(\mathbf{k}) \hat{\Psi}_{\mathbf{k},\alpha}$ , with

$$\mathcal{H} = \frac{1}{2} \int d\mathbf{k} \sum_{\alpha} \begin{pmatrix} c_{\mathbf{k},\alpha}^{\dagger} & c_{-\mathbf{k},\alpha} \end{pmatrix} \begin{pmatrix} \varepsilon_{\alpha}(\mathbf{k}) & -2i\Delta_p(\mathbf{k}) \\ 2i\Delta_p^*(\mathbf{k}) & -\varepsilon_{\alpha}(-\mathbf{k}) \end{pmatrix} \begin{pmatrix} c_{\mathbf{k},\alpha} \\ c_{-\mathbf{k},\alpha}^{\dagger} \end{pmatrix}, \quad (116)$$

where the factor of 1/2 is crucial for not double-counting the degrees of freedom. After including the  $\boldsymbol{\tau}$  Pauli matrices defined in particle-hole space, we observe that the above single particle Hamiltonian  $\hat{\mathcal{H}}(\mathbf{k})$  is characterized by the charge-conjugation symmetry  $\hat{\Xi}^{\dagger} \hat{\mathcal{H}}(\mathbf{k}) \hat{\Xi} = -\hat{\mathcal{H}}(\mathbf{k})$  with  $\hat{\Xi} = \tau_x \hat{\mathcal{K}}$ . This arises due to the antisymmetry of the order parameter  $\Delta_p(\mathbf{k}) = -\Delta_p(-\mathbf{k})$ . Note however that the particular symmetry is quite fundamental and therefore quite robust. As long as the system is in the p-wave superconducting phase, the particular symmetry is always present. The consequence of this symmetry is that the allowed symmetry classes for the particular type of systems, are only DIII, D, BDI. The presence of the aforementioned charge-conjugation symmetry can be reflected in the following property of the Hamiltonian: if  $\hat{\phi}_{\mathbf{k}}$  is a two-component solution with energy  $E_{\mathbf{k}}$ , satisfying

$$\hat{\mathcal{H}}(\mathbf{k}) \hat{\phi}_{\mathbf{k}} = E(\mathbf{k}) \hat{\phi}_{\mathbf{k}}, \quad (117)$$

then also the wave-function  $\hat{\Xi} \hat{\phi}_{\mathbf{k}} = \tau_x \hat{\phi}_{-\mathbf{k}}^*$  satisfies

$$\hat{\mathcal{H}}(\mathbf{k}) \hat{\Xi} \hat{\phi}_{\mathbf{k}} = \bar{E}(\mathbf{k}) \hat{\Xi} \hat{\phi}_{\mathbf{k}} \Rightarrow \hat{\Xi}^{\dagger} \hat{\mathcal{H}}(\mathbf{k}) \hat{\Xi} \hat{\phi}_{\mathbf{k}} = \bar{E}(-\mathbf{k}) \hat{\phi}_{\mathbf{k}} \Rightarrow \hat{\mathcal{H}}(\mathbf{k}) \hat{\phi}_{\mathbf{k}} = -\bar{E}(-\mathbf{k}) \hat{\phi}_{\mathbf{k}} \Rightarrow \bar{E}(\mathbf{k}) = -E(-\mathbf{k}). \quad (118)$$

As a result, a zero energy solution satisfies  $\hat{\phi}_{\mathbf{k}} = \tau_x \hat{\phi}_{-\mathbf{k}}^*$ . Due to the antisymmetry of the superconducting order parameter, this zero solution can only occur for the inversion symmetric points  $\mathbf{k}_{\mathcal{I}}$  satisfying  $\mathbf{k} \equiv -\mathbf{k}$ . In this case  $\hat{\phi}_{\mathbf{k}_{\mathcal{I}}} = \tau_x \hat{\phi}_{\mathbf{k}_{\mathcal{I}}}^*$  which is exactly the Majorana condition. The latter wave-function is self-conjugate which allows us to define Majorana operators. To better understand this we can diagonalize the single particle Hamiltonian for each  $\alpha$ , with a Bogoliubov transformation. For the rest of the discussion we will focus for simplicity on a single spin-projection  $\alpha$ . The transformation reads

$$\begin{pmatrix} c_{\mathbf{k}} \\ c_{-\mathbf{k}}^{\dagger} \end{pmatrix} = \begin{pmatrix} u_{\mathbf{k}} & v_{-\mathbf{k}}^* \\ v_{\mathbf{k}} & u_{-\mathbf{k}}^* \end{pmatrix} \begin{pmatrix} \gamma_{\mathbf{k}} \\ \gamma_{-\mathbf{k}}^{\dagger} \end{pmatrix} \quad \text{and} \quad \begin{pmatrix} \gamma_{\mathbf{k}} \\ \gamma_{-\mathbf{k}}^{\dagger} \end{pmatrix} = \begin{pmatrix} u_{-\mathbf{k}}^* & -v_{-\mathbf{k}}^* \\ -v_{\mathbf{k}} & u_{\mathbf{k}} \end{pmatrix} \begin{pmatrix} c_{\mathbf{k}} \\ c_{-\mathbf{k}}^{\dagger} \end{pmatrix}. \quad (119)$$

Note that for gap closings at the inversion symmetric points  $\hat{\phi}_{\mathbf{k}_I} = \tau_x \hat{\phi}_{\mathbf{k}_I}^* \rightarrow u_{\mathbf{k}_I} = \pm v_{\mathbf{k}_I}^*$ . If we consider for instance the second case with  $u_{\mathbf{k}_I} \in \mathbb{R}$ , we obtain  $\gamma_{\mathbf{k}_I} = u_{\mathbf{k}_I} (c_{\mathbf{k}_I} + c_{\mathbf{k}_I}^\dagger) = \gamma_{\mathbf{k}_I}^\dagger$ .

Let us now consider the following particular expressions for the energy dispersion and p-wave superconducting gap:

$$\varepsilon(\mathbf{k}) = \frac{(\hbar\mathbf{k})^2}{2m} - \mu \quad \text{and} \quad \Delta_p(\mathbf{k}) = \Delta_p(k_x - ik_y), \quad (120)$$

where  $\mu$  denotes the chemical potential. The latter expression for the p-wave superconducting order parameter corresponds to the so-called *chiral* p-wave superconducting order parameter. In fact this type of unconventional superconductivity has been proposed for  $\text{Sr}_2\text{RuO}_4$  [69]. Nevertheless, this scenario still remains experimentally unsettled, which also constitutes an obstacle for using these materials for MF-based applications. The single-particle Hamiltonian corresponding to Eq. (120) reads

$$\hat{\mathcal{H}}(\mathbf{k}) = 2\Delta_p(k_x\tau_y - k_y\tau_x) + \left[ \frac{(\hbar\mathbf{k})^2}{2m} - \mu \right] \tau_z. \quad (121)$$

The Hamiltonian above has exactly the same structure as the  $\mathcal{T}$ -violating Hamiltonian Eq. (40) considered earlier for a 2d topological insulator. It is therefore straightforward to conclude that the chiral p-wave system enters the topologically non-trivial regime when  $\mu > 0$ , which is the usual case. In the topologically non-trivial phase we find Majorana chiral edge modes in the 2d case and Majorana zero-energy edge states in the 1d case. The appearance of Majorana fermions is connected to the gap closing that occurs for  $\mu_c = 0$  at the inversion symmetric  $\mathbf{k} = \mathbf{0}$  point.

#### D. Kitaev's lattice model for a 1d p-wave superconductor - unpaired Majorana fermions

A particularly useful analysis of the 1d model presented in Eq. (121) was performed by Kitaev [70], which provided transparent understanding of the emergence of MFs in these systems and stimulated further theoretical developments. Below we present a slightly modified version of Kitaev's model

$$\hat{\mathcal{H}}(k) = 2\Delta_p \sin(ka)\tau_y + \{2t[1 - \cos(ka)] - \mu\} \tau_z, \quad (122)$$

which describes a p-wave superconductor for a periodic chain of lattice sites, of lattice constant  $a$ . Due to the periodicity, the wave-vector  $k \equiv k_x$  is confined in the Brillouin zone, i.e.  $k \in (-\pi/a, \pi/a]$ . The energy spectrum of the Hamiltonian above reads

$$E(k) = \pm \sqrt{\{2t[1 - \cos(ka)] - \mu\}^2 + 4\Delta_p^2 \sin^2(ka)}. \quad (123)$$

As we have already noted, the continuum 1d model of Eq. (121) exhibits a Majorana mode for the inversion symmetric  $k = 0$  point. In the vicinity of  $k = 0$ , which is crucial for the investigation the emergent Majorana fermion physics, the Hamiltonian of Eq. (122) is identically mapped to Eq. (121), with  $t = \hbar^2/2ma^2$ . Consequently, a gap closing at  $\mu = 0$  will lead to a Majorana mode at  $k = 0$  and a Majorana bound state in coordinate space per edge of the finite size system. However, in this model another option appears. The remaining inversion symmetric point  $k = \pi/a$  can also show a gap closing. This happens for  $\mu = 4t$ . This situation didn't take place for the continuum model because the corresponding inversion point to  $\pi/a$ , is  $\lim_{a \rightarrow 0} \pi/a = +\infty$ , for which the energy goes to  $+\infty$  not allowing for a gap closing. In this manner, if we can achieve  $\mu > 4t$  we can access another phase. However, its topological character is not known a priori. To determine the latter we may directly calculate the corresponding topological invariant. The symmetry class of the system is BDI and it can be characterized by the winding number

$$\tilde{w} = -\frac{1}{2\pi} \int dk \left( \hat{\mathbf{g}}(\mathbf{k}) \times \frac{\partial \hat{\mathbf{g}}(\mathbf{k})}{\partial k} \right)_x. \quad (124)$$

For the above we properly expressed the single particle Hamiltonian of Eq. (122) as  $\hat{\mathcal{H}}(k) = \mathbf{g}(k) \cdot \boldsymbol{\tau}$ , with the help of

$$\mathbf{g}(k) = (0, 2\Delta_p \sin(ka), 2t[1 - \cos(ka)] - \mu). \quad (125)$$

By direct calculation of the winding number we obtain  $\tilde{w} = 0$  for  $\mu > 4t$ . This implies that there is only a restricted regime  $0 < \mu < 4t$  where the system resides in the topologically non-trivial phase supporting MFs.

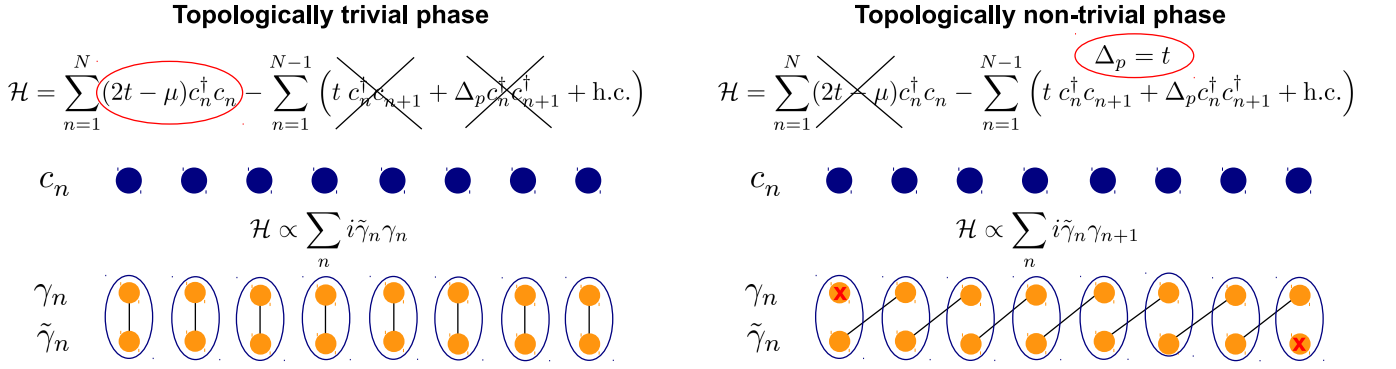


FIG. 24: **Left:** Topologically trivial metallic phase within the Kitaev model. A special case with  $\mu \neq 0$  and  $t = \Delta_p$  is depicted. Both Majorana fermion operators comprising a local electronic operator are coupled. **Right:** Topologically non-trivial superconducting phase within the Kitaev model. For the specific choice  $2t = \mu$  and  $t = \Delta_p$ , we obtain two *unpaired* Majorana fermions, one per edge (marked with red).

Let us now verify these bulk results by transferring to a finite chain of  $N$  sites. The second quantized Hamiltonian corresponding to Eq. (122) is now rewritten in the following manner

$$\mathcal{H} = \sum_{n=1}^N (2t - \mu) c_n^\dagger c_n - \sum_{n=1}^{N-1} t (c_n^\dagger c_{n+1} + c_{n+1}^\dagger c_n) - \frac{\Delta_p}{2} \sum_{n=1}^{N-1} (c_n^\dagger c_{n+1}^\dagger - c_{n+1}^\dagger c_n^\dagger + c_{n+1} c_n - c_n c_{n+1}). \quad (126)$$

According to the bulk criterion, for  $\mu = 2t$  the system lies in the topologically non-trivial superconducting phase with zero-energy edge Majorana fermions. Following Kitaev, we will consider exactly this particular case, in order to demonstrate that for this value the MF bound state wave-functions become localized at the very edges of the system, i.e. at sites  $n = 1$  and  $n = N$ . Away from  $\mu = 2t$ , but still within the appropriate MF regime, the bound state wave-function will acquire a finite spread within the bulk of the system. For  $\mu = 2t$  and by additionally setting  $\Delta_p = t$ , which is always allowed and does not affect the emergence of MFs, we obtain

$$\mathcal{H} = -t \sum_{n=1}^{N-1} (c_n^\dagger c_{n+1} - c_n c_{n+1}^\dagger + c_n^\dagger c_{n+1}^\dagger - c_n c_{n+1}) = 2ti \sum_{n=1}^{N-1} \frac{c_n - c_n^\dagger}{\sqrt{2}i} \frac{c_{n+1} + c_{n+1}^\dagger}{\sqrt{2}} = 2ti \sum_{n=1}^{N-1} \tilde{\gamma}_n \gamma_{n+1}. \quad (127)$$

We directly notice that the MF operators  $\gamma_1$  and  $\tilde{\gamma}_N$  are missing from the above Hamiltonian, i.e. they are unpaired (Fig. 24). These two operators are defined exactly at the edge points of the system and together they build up the non local zero-energy electron  $c_0 = (\tilde{\gamma}_N + i\gamma_1)/\sqrt{2}$ .

The concept of unpaired MFs is particular useful for studying the topological properties of these systems in a simplified manner. In fact the hallmark of topological superconductors constitutes the  $4\pi$ -periodic Josephson effect [70, 71]. This effect concerns the coupling of two edge MFs belonging to two *identical* adjacent 1d p-wave superconductors  $s = l, r$  (left, right) with different superconducting phases  $\varphi_s \rightarrow \Delta_p e^{i\varphi_s} c_{n,s}^\dagger c_{n+1,s}^\dagger$ , with  $s = l, r$ . Each superconducting phase can be gauged away  $c_{n,s} \rightarrow e^{i\varphi_s/2} c_{n,s}$ , recovering in this manner the previous result. The neighboring electrons sitting at the edges of the two 1d superconductors, can tunnel into the other superconductor via the tunneling Hamiltonian  $\mathcal{H}_T = -T(c_{N,l}^\dagger c_{1,r} + c_{1,r}^\dagger c_{N,l})$ . After the gauge transformation, the tunneling Hamiltonian becomes  $\mathcal{H}_T = -T[e^{i(\varphi_r - \varphi_l)/2} c_{N,l}^\dagger c_{1,r} + e^{-i(\varphi_r - \varphi_l)/2} c_{1,r}^\dagger c_{N,l}]$ . In the low energy limit, the electronic operators can be replaced by the unpaired MF operators  $c_{N,l} \simeq i\tilde{\gamma}_{N,l}/\sqrt{2}$  and  $c_{1,r} \simeq \gamma_{1,r}/\sqrt{2}$ , providing  $\mathcal{H}_T = iT \cos(\delta\varphi/2) \tilde{\gamma}_{N,l} \gamma_{1,r}$ , with  $\delta\varphi = \varphi_r - \varphi_l$ . By introducing the electron annihilation operator which can be constructed using the two neighboring unpaired MF operators,  $c_T = (\tilde{\gamma}_{N,l} + i\gamma_{1,r})/\sqrt{2}$  we obtain  $\mathcal{H}_T = \frac{T}{2} \cos(\delta\varphi/2) (2c_T^\dagger c_T - 1)$ . Note that the operator  $c_T$  does not correspond to zero-energy due to the presence of the tunneling Hamiltonian. Otherwise, in the absence of the tunneling Hamiltonian  $c_T \rightarrow c_0$ . We now proceed with calculating the related supercurrent, which is given by

$$J_s = -\frac{2e}{\hbar} \frac{\partial \langle \mathcal{H}_T \rangle}{\partial \delta\varphi} = \frac{eT}{\hbar} \frac{1}{2} \sin\left(\frac{\delta\varphi}{2}\right) \mathcal{P}_T, \quad (128)$$

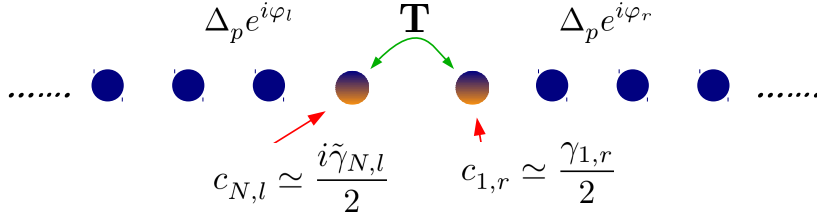


FIG. 25: Hopping between two unpaired Majorana fermions, residing at the edges of two identical 1d p-wave superconductors with different superconducting phase. A Josephson current mediated by Majorana fermions appears, with a  $4\pi$ -periodicity with respect to the phase difference  $\varphi_r - \varphi_l$ , in contrast to the  $2\pi$ -periodicity encountered in topologically non-trivial superconductors.

where we also introduced the parity of the zero-energy state  $\mathcal{P}_T = \langle 2c_T^\dagger c_T - 1 \rangle = 2n_F[E(\delta\varphi)] - 1$ , with the energy  $E(\delta\varphi) = T \cos(\delta\varphi/2)$ . The fermion parity takes the value  $+1(-1)$  if the zero-energy state is occupied (empty). If the number of electrons on the two superconductors is fixed, so will be the fermion parity. This yields to the  $4\pi$ -periodic Josephson current  $J_s \sim \sin(\delta\varphi/2)$ . In topologically trivial superconductors, where MFs are not present, the Josephson current [72] is proportional to  $J_s \sim \sin(\delta\varphi)$ . This crucial periodicity difference, is in principle detectable in experiments.

Before proceeding to the next section, it is useful to comment on a very important difference between the continuum and lattice models of Eqs. (121) and (122), respectively. Although we demonstrated that both of them support a single MF per edge, the lattice model can provide a richer topological phase diagram by including terms not only connecting the nearest neighbors. For instance, in the case where we only have next-nearest-neighbor terms the Hamiltonian in coordinate space would read

$$\mathcal{H} = \sum_{n=1}^N (2t - \mu) c_n^\dagger c_n - \sum_{n=1}^{N-2} t (c_n^\dagger c_{n+2} + c_{n+2}^\dagger c_n) - \frac{\Delta_p}{2} \sum_{n=1}^{N-2} (c_n^\dagger c_{n+2}^\dagger - c_{n+2}^\dagger c_n^\dagger + c_{n+2} c_n - c_n c_{n+2}). \quad (129)$$

In the particular case, we obtain two interpenetrating chains, each of them residing in the topologically non-trivial phase for  $0 < \mu < 4t$ . As a result each of them should host a MF per edge, leading to the following edge MFs:  $\gamma_1, \gamma_2, \tilde{\gamma}_{N-1}$  and  $\tilde{\gamma}_N$ . The possibility of more than a single MF per edge, can be naturally understood in terms of the chiral symmetry which is present. Class BDI allows for a  $\mathbb{Z}$  topological invariant, identified previously with the winding number  $\tilde{w}$  [73]. By transferring to momentum space, the Hamiltonian of Eq. (129) has the usual form  $\hat{\mathcal{H}}(k) = \mathbf{g}(k) \cdot \boldsymbol{\tau}$ , with

$$\mathbf{g}(k) = (0, 2\Delta_p \sin(2ka), 2t[1 - \cos(2ka)] - \mu). \quad (130)$$

The calculation of the winding number for the particular  $\mathbf{g}$ -vector yields  $|\tilde{w}| = 2$  leading to 2 MFs per edge. This result is easy to visualize if we plot the winding of the  $\mathbf{g}$ -vector in  $k$ -space (Fig. 26). This is in stark contrast to the continuum model where the  $\mathbf{g}$ -vector shows only a single twist (Fig. 15).

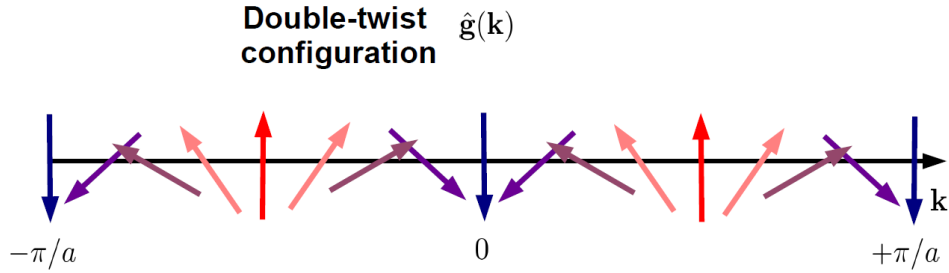


FIG. 26: A configuration of  $\hat{\mathbf{g}}(k)$  with a double-twist from  $-\pi/a$  to  $\pi/a$ . This double winding in momentum space implies the appearance of two Majorana fermion operators per edge for the finite-size system. The presence of more than one Majorana fermions per edge is allowed due to chiral symmetry.

### E. Majorana fermions in engineered 1d p-wave superconductors

As we discussed in the previous section, p-wave superconductivity is an attractive quantum phase of matter, but still remains elusive. The possibility that it intrinsically appears in  $\text{Sr}_2\text{RuO}_4$  continues to be under investigation. Nonetheless, even if p-wave superconductivity will be confirmed in Sr-Ruthenates, it will be still difficult to implement topological quantum information processes, with the current experimental techniques. The reason is that these systems are governed by strong correlations, which lead to many complications when it comes to their control and manipulation. Therefore, alternative proposals appeared recently, discussing the possibility of engineering a p-wave superconductor using more conventional ways. Based on the symmetry arguments presented earlier, it is understood that if we manage to develop a hybrid system which will belong to the same symmetry class as a p-wave superconductor, then we will have the same topological properties. This is exactly the idea that motivated a number of authors to propose a number of platforms [74–76] which fulfill this requirement, stimulating a number of experiments [77, 78]. Among them one can distinguish a hybrid structure consisting of a semiconducting wire with strong Rashba spin-orbit coupling in proximity to a conventional *spin-singlet* bulk superconductor [75]. Due to the proximity effects, a superconducting gap is induced in the semiconducting wire. By further applying a sufficiently large Zeeman field, with orientation perpendicular to the polarization of the spin-orbit coupling, we can manage to bring this hybrid system to a topologically non-trivial superconducting phase harboring a single MF per edge Fig. 27. The critical value of the Zeeman energy  $E_Z \sim \mathcal{B}$  that has to be achieved is given by  $E_Z^{\text{crit}} = \sqrt{\Delta^2 + \mu^2}$ , where  $\Delta$  defines the proximity induced superconducting gap on the wire and  $\mu$  the chemical potential of the wire. For magnetic fields yielding  $E_Z > E_Z^{\text{crit}}$  the system resides in the topologically non-trivial superconducting phase. Below, we will demonstrate that for high magnetic fields, the Hamiltonian describing the particular hybrid system can be mapped to the Hamiltonian Eq. (121) of a p-wave superconductor [62].

The Hamiltonian describing a Rashba semiconducting wire, in the presence of an external Zeeman field and proximity induced superconductivity, reads

$$\mathcal{H}(k) = \left[ \frac{(\hbar k)^2}{2m} - \mu \right] \tau_z + v\hbar k \sigma_z - E_Z \tau_z \sigma_x - \Delta \tau_y \sigma_y, \quad (131)$$

where the above Hamiltonian acts on the four-component spinor  $\hat{\Psi}_k^\dagger = (c_{k,\uparrow}^\dagger, c_{k,\downarrow}^\dagger, c_{-k,\uparrow}, c_{-k,\downarrow})$ , while  $\boldsymbol{\tau}$  and  $\boldsymbol{\sigma}$  matrices act on Nambu and spin spaces, respectively. Note that here we have chosen the  $xz$ -plane as the plane for the corresponding 2d version of the Rashba interaction:  $v(\hat{p}_x \sigma_z - \hat{p}_z \sigma_x)$ . The Hamiltonian belongs to symmetry class BDI, with time-reversal symmetry  $\hat{\Theta} = \tau_z \sigma_x \hat{\mathcal{K}}$ , charge-conjugation  $\hat{\Xi} = \tau_x \hat{\mathcal{K}}$  and chiral symmetry  $\hat{\Pi} = \tau_y \sigma_x$ . The gap closing at  $k = 0$  occurs when  $E_Z^{\text{crit}} = \sqrt{\Delta^2 + \mu^2}$ , as mentioned earlier.

To demonstrate the connection to the p-wave superconducting Hamiltonian of Eq. (121), we will consider the Rashba spin-orbit interaction and the superconducting gap as small perturbations. Furthermore, we will focus in the vicinity of  $k = 0$ , implying that  $\varepsilon(k) \equiv [(\hbar k)^2/2m - \mu] \neq 0$ . In order to perform the required perturbative expansion, we will adopt the Schrieffer-Wolff canonical transformation method. Specifically, we will consider that there exists a unitary transformation which can transform  $\mathcal{H} = \frac{1}{2} \sum_k \hat{\Psi}_k^\dagger \hat{\mathcal{H}}(k) \hat{\Psi}_k$  to a new Hamiltonian  $\tilde{\mathcal{H}} = e^{+iS} \mathcal{H} e^{-iS}$ . We will

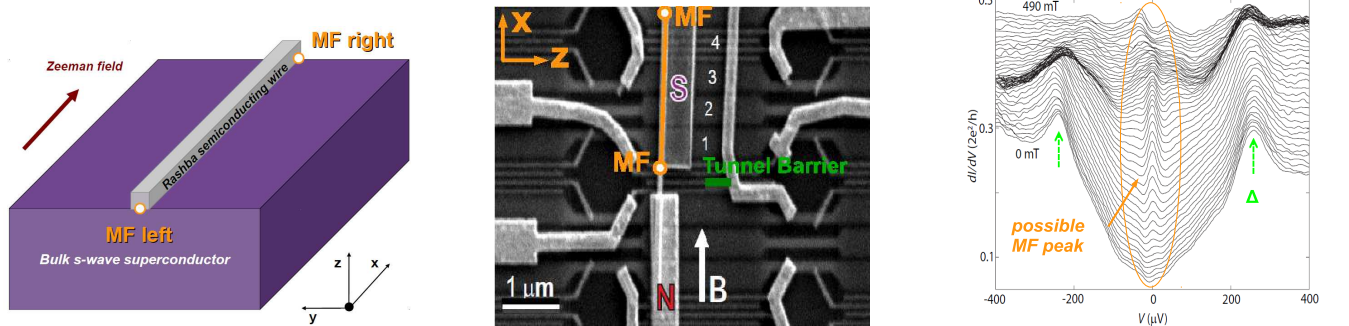


FIG. 27: **Left:** Cartoon of a hybrid structure consisting of a semiconducting wire with strong Rashba spin-orbit coupling in proximity to a conventional bulk superconductor. The system behaves as a topologically non-trivial superconductor with a single Majorana fermion per edge. **Middle:** The experimental implementation of the hybrid structure presented in the left panel. **Right:** According to tunneling measurements, a zero-bias peak anomaly hints the presence of Majorana fermions in this setup. Middle and Right figures taken from [77].

split the Hamiltonian into two parts,  $\mathcal{H} = \mathcal{H}_0 + \mathcal{V}$  where the second part defines the perturbation. The operator  $\mathcal{S}$  is considered to be of the same order as  $\mathcal{V}$ . In this way we obtain

$$\begin{aligned}\tilde{\mathcal{H}} &= e^{+i\mathcal{S}}\mathcal{H}e^{-i\mathcal{S}} = \mathcal{H} + i[\mathcal{S}, \mathcal{H}] - \frac{1}{2!}[\mathcal{S}, [\mathcal{S}, \mathcal{H}]] + \dots \\ &= \mathcal{H}_0 + \mathcal{V} + i[\mathcal{S}, \mathcal{H}_0] + i[\mathcal{S}, \mathcal{V}] - \frac{1}{2!}[\mathcal{S}, [\mathcal{S}, \mathcal{H}_0]] - \frac{1}{2!}[\mathcal{S}, [\mathcal{S}, \mathcal{V}]] + \dots\end{aligned}\quad (132)$$

We will choose the operator  $\mathcal{S}$  in such a way so that our transformed Hamiltonian has no first order terms in the perturbation parameter. Moreover, we shall then restrict ourselves only to the second order terms in the expansion parameter. In this manner, the operator must satisfy  $[\mathcal{S}, \mathcal{H}_0] = i\mathcal{V}$  leading to

$$\tilde{\mathcal{H}} = \mathcal{H}_0 + i[\mathcal{S}, \mathcal{V}] - \frac{i}{2}[\mathcal{S}, \mathcal{V}] + \text{h.o.t.} \quad \Rightarrow \quad \tilde{\mathcal{H}} = \mathcal{H}_0 + \frac{i}{2}[\mathcal{S}, \mathcal{V}] = \mathcal{H}_0 - \frac{i}{2}[\mathcal{V}, \mathcal{S}]. \quad (133)$$

After tedious but straightforward calculations, we find that

$$\tilde{\mathcal{H}} = \frac{1}{2} \int dk \hat{\Psi}_k^\dagger [\tilde{\varepsilon}(k)\tau_z - E_Z(k)\tau_z\sigma_x + d_y(k)\tau_x + d_z(k)\tau_x\sigma_x] \hat{\Psi}_k, \quad (134)$$

where we have introduced

$$\tilde{\varepsilon}(k) = \left\{ 1 + \frac{1}{2!} \left[ \frac{\Delta}{\varepsilon(k)} \right]^2 \right\} \varepsilon(k) \quad \text{with} \quad \varepsilon(k) = \frac{(\hbar k)^2}{2m} - \mu, \quad (135)$$

$$E_Z(k) = \left[ 1 + \frac{1}{2!} \left( \frac{v\hbar k}{E_Z} \right)^2 \right] E_Z, \quad (136)$$

$$d_z(k) = -\frac{1}{2!} \frac{\Delta}{\varepsilon(k)} v\hbar k, \quad (137)$$

$$d_y(k) = -\frac{1}{2!} \frac{\Delta}{E_Z} v\hbar k. \quad (138)$$

We directly observe that apart from the renormalization of the kinetic and Zeeman energies, two additional terms appear which correspond to spin-triplet p-wave superconductivity. Quite remarkably, by following the suitable recipe we converted the spin-singlet superconductivity to spin-triplet. In the high magnetic field limit, only one spin component is important and therefore we project on the spin-up subspace. The resulting spin-up Hamiltonian reads

$$\hat{\mathcal{H}}_\uparrow(k) = [\tilde{\varepsilon}(k) - E_Z(k)] \tau_z + [d_y(k) + d_z(k)] \tau_x. \quad (139)$$

Since the topological properties depend only on the behavior in the vicinity around  $k = 0$ , we will also consider terms up to second order in the wave-vector. By additionally performing the unitary transformation  $\hat{\mathcal{H}}_{\text{rot}}(k) = \hat{U} \hat{\mathcal{H}}_\uparrow(k) \hat{U}^\dagger$ , with  $\hat{U} = (\tau_x + \tau_y)\sqrt{2}$ , we finally have

$$\hat{\mathcal{H}}_{\text{rot}}(k) = 2\Delta_p k \tau_y - \left[ \frac{(\hbar k)^2}{2m^*} - \mu^* \right] \tau_z \quad (140)$$

with

$$\frac{1}{m^*} = \frac{1}{m} \left[ 1 - \frac{1}{2} \left( \frac{\Delta}{\mu} \right)^2 - \frac{mv^2}{E_Z} \right], \quad \mu^* = \mu \left[ 1 + \frac{1}{2} \left( \frac{\Delta}{\mu} \right)^2 \right] + E_Z \quad \text{and} \quad \Delta_p = \frac{(E_Z - \mu)v\hbar\Delta}{4E_Z\mu}. \quad (141)$$

The mapping to the p-wave superconducting model of Eq. (121) has now been established, illustrating the topological connection of the two models, which also guarantees the emergence of MFs. This a very interesting example of how diverse models lead to a common topological behavior when they fall into the same symmetry class. Finally, this opens new perspectives in material and device design, where based on symmetries we can engineer the desired topological properties using hybrid systems consisting of accessible topologically trivial components.

- 
- [1] A. Altland and M. R. Zirnbauer, Phys. Rev. B **55**, 1142 (1997).
- [2] C. L. Kane and E. J. Mele, Phys. Rev. Lett. **95**, 226801 (2005).
- [3] C. L. Kane and E. J. Mele, Phys. Rev. Lett. **95**, 146802 (2005).
- [4] B. A. Bernevig, T. L. Hughes and S.-C. Zhang, Science **314**, 1757 (2006).
- [5] L. Fu, C. L. Kane, E. J. Mele, Phys. Rev. Lett. **98**, 106803 (2007).
- [6] J. E. Moore and L. Balents, Phys. Rev. B **75**, 121306(R) (2007).
- [7] L. Fu and C. L. Kane, Phys. Rev. B **76**, 045302 (2007).
- [8] A. P. Schnyder, S. Ryu, A. Furusaki and A. W. W. Ludwig, Phys. Rev. B **78**, 195125 (2008).
- [9] X.-L. Qi, T. L. Hughes and S.-C. Zhang, Phys. Rev. B **78**, 195424 (2008).
- [10] R. Roy, Phys. Rev. B **79**, 195321 (2009).
- [11] A. Kitaev, AIP Conf. Proc. **1134**, 22 (2009).
- [12] S. Ryu, A. Schnyder, A. Furusaki and A. Ludwig, New J. Phys. **12** 065010, (2010).
- [13] G. E. Volovik, “*The Universe in a Helium Droplet*”, Clarendon Press Oxford (2003).
- [14] M. Nakahara, “*Geometry, Topology and Physics*”, Taylor & Francis (2003).
- [15] D. Vollhardt and P. Wölfle, “*The superfluid phases of Helium 3*”, Taylor & Francis (2002).
- [16] N. D. Mermin, Rev. of Mod. Phys. **51**, 591 (1979).
- [17] E. Fradkin, “*Field Theories of Condensed Matter Physics*”, Cambridge University Press, 2nd edition (2013).
- [18] M. Z. Hasan and C. L. Kane Rev. Mod. Phys. **82**, 3045 (2010).
- [19] X.-L. Qi and S.-C. Zhang, Rev. Mod. Phys. **83**, 1057 (2011).
- [20] J. Alicea, Rep. Prog. Phys. **75**, 076501 (2012).
- [21] C. W. J. Beenakker, Annu. Rev. Con. Mat. Phys. **4**, 113 (2013).
- [22] P. Kotetes, New J. Phys. **15**, 105027 (2013).
- [23] G. W. Semenoff, Phys Rev Lett **53**, 2449 (1984).
- [24] F. D. M. Haldane, Phys. Rev. Lett. **61**, 2015 (1988).
- [25] M. König, S. Wiedmann, C. Brüne, A. Roth, H. Buhmann, L. W. Molenkamp, X.-L. Qi and S.-C. Zhang, Science **318**, 766 (2007).
- [26] K. v. Klitzing, G. Dorda and M. Pepper, Phys. Rev. Lett. **45**, 494 (1980).
- [27] Cui-Zu Zhang *et al.*, Science **12 340**, 167 (2013).
- [28] R. Jackiw and C. Rebbi, Phys. Rev. D **13**, 3398 (1976).
- [29] W. P. Su, J. R. Schrieffer and A. J. Heeger, Phys. Rev. Lett. **42**, 1698 (1979).
- [30] R. Kubo, J. Phys. Soc. Jpn. **12**, 570 (1957).
- [31] Di Xiao, Ming-Che Chang, Qian Niu, Rev. Mod. Phys. **82**, 1959 (2010).
- [32] A. A. Abrikosov, L. P. Gorkov and I. E. Dzialoshinskii, “*Methods of Quantum Field Theory in Statistical Physics*”, Dover (1975).
- [33] G. D. Mahan, “*Many-Particle Physics*”, Springer (1990).
- [34] H. Bruus and K. Flensberg, “*Many-Body Quantum Theory in Condensed Matter Physics*”, Oxford University Press (2004).
- [35] A. Altland and B. D. Simons, “*Condensed Matter Field Theory*”, Cambridge University Press, 2nd edition (2010).
- [36] J. Rammer and H. Smith, Rev. Mod. Phys. **58**, 323 (1986).
- [37] W. Belzig *et al.*, “*Quasiclassical Green’s function approach to mesoscopic superconductivity*”, Superlattices and Microstructures **25**, 1251 (1999).
- [38] M. V. Berry, Proc. R. Soc. A **392**, 45 (1984).
- [39] T. H. R. Skyrme, Nucl. Phys. **31**, 556 (1962).
- [40] T. Kaluza, Sitzungsber. Preuss. Akad. Wiss. Berlin. (Math. Phys.) 966972 (1921).
- [41] O. Klein, Zeitschrift fr Physik A **37**, 895 (1926).
- [42] L. Fu, C. L. Kane and E. J. Mele, Phys. Rev. Lett. **98**, 106803 (2007).
- [43] J. E. Moore and L. Balents, Phys. Rev. B **75**, 121306(R) (2007).
- [44] R. Roy, Phys. Rev. B **79**, 195322 (2009).
- [45] H. Zhang, C. X. Liu, X. L. Qi, X. Dai, Z. Fang and S. C. Zhang, Nat. Phys. **5**, 438 (2009).
- [46] D. Hsieh, D. Qian, L. Wray, Y. Xia, Y. S. Hor, R. J. Cava and M. Z. Hasan, Nature **452**, 970 (2008).
- [47] Y. Xia, D. Qian, D. Hsieh, L. Wray, A. Pal, H. Lin, A. Bansil, D. Grauer, Y. S. Hor, R. J. Cava and M. Z. Hasan, Nat. Phys. **5**, 398 (2009).
- [48] Y. S. Hor, A. Richardella, P. Roushan, Y. Xia, J. G. Checkelsky, A. Yazdani, M. Z. Hasan, N. P. Ong and R. J. Cava, Phys. Rev. B **79**, 195208 (2009).
- [49] D. Hsieh, Y. Xia, D. Qian, L. Wray, J. H. Dil, F. Meier, J. Osterwalder, L. Patthey, J. G. Checkelsky, N. P. Ong, A. V. Fedorov, H. Lin, A. Bansil, D. Grauer, Y. S. Hor, R. J. Cava and M. Z. Hasan, Nature **460**, 1101 (2009).
- [50] S. R. Park, W. S. Jung, C. Kim, D. J. Song, C. Kim, S. Kimura, K. D. Lee and N. Hur, Phys. Rev. B **81**, 041405(R) (2010).
- [51] Y. L. Chen, J. G. Analytis, J. H. Chu, Z. K. Liu, S. K. Mo, X. L. Qi, H. J. Zhang, D. H. Lu, X. Dai, Z. Fang, S. C. Zhang, I. R. Fisher, Z. Hussain, Z. X. Shen, Science **325**, 178 (2009).
- [52] D. Hsieh, Y. Xia, D. Qian, L. Wray, F. Meier, J. H. Dil, J. Osterwalder, L. Patthey, A. V. Fedorov, H. Lin, A. Bansil, D. Grauer, Y. S. Hor, R. J. Cava, and M. Z. Hasan, Phys. Rev. Lett. **103**, 146401 (2009).

- [53] A. H. Castro Neto, F. Guinea, N. M. R. Peres, K. S. Novoselov and A. K. Geim, *Rev. Mod. Phys.* **81**, 109 (2009).
- [54] H. B. Nielsen and M. Ninomiya, *Phys. Lett. B* **105**, 219 (1981).
- [55] K.-I. Imura, S. Mao, Ai Yamakage and Y. Kuramoto, *Nanoscale Research Letters* **6**, 358 (2011).
- [56] C.-X. Liu, X.-L. Qi, H. Zhang, Xi Dai, Z. Fang, S.-C. Zhang, *Phys. Rev. B* **82**, 045122 (2010).
- [57] J. Maciejko, X.-L. Qi, H. D. Drew and S.-C. Zhang, *Phys. Rev. Lett.* **105**, 166803 (2010).
- [58] E. Majorana, *Nuovo Cimento* **5**, 171 (1937).
- [59] N. Read and D. Green, *Phys. Rev. B* **61**, 10267 (2000).
- [60] F. Wilczek, *Nature Physics* **5**, 614 (2009).
- [61] A. Y. Kitaev, *Annals Phys.* **303**, 2 (2003); C. Nayak, S. H. Simon, A. Stern, M. Freedman and S. Das Sarma, *Rev. Mod. Phys.* **80**, 1083 (2008); D. A. Ivanov, *Phys. Rev. Lett.* **86**, 268 (2001).
- [62] J. Alicea, Y. Oreg, G. Refael, F. von Oppen and M. P. A. Fisher, *Nature Physics* **7**, 412 (2011).
- [63] D. Loss and D. P. Di Vincenzo, *Phys. Rev. A* **57**, 120 (1998); D. J. Reilly, J. M. Taylor, E. A. Laird, J. R. Petta, C. M. Marcus, M. P. Hanson and A. C. Gossard, *Phys. Rev. Lett.* **101**, 236803 (2008).
- [64] Y. Makhlin, G. Schön and A. Shnirman, *Rev. Mod. Phys.* **73**, 357 (2001); F. C. Wellstood, C. Urbina and J. Clarke, *Appl. Phys. Lett.* **50** 772. (1987).
- [65] S. Bravyi and A. Kitaev, *Phys. Rev. A*, **71** 022316 (2005); S. Bravyi, *Phys. Rev. A* **73**, 042313 (2006); J. D. Sau, S. Tewari and S. Das Sarma, *Phys. Rev. A*, **82** 052322 (2010).
- [66] J. Bardeen, L. N. Cooper and J. R. Schrieffer, *Phys. Rev.* **108**, 1175 (1957).
- [67] M. Sigrist and K. Ueda, *Rev. Mod. Phys.* **63**, 239 (1991).
- [68] A. Damascelli, Z. Hussain and Zhi-Xun Shen, *Rev. Mod. Phys.* **75**, 473 (2003).
- [69] K. Ishida, H. Mukuda, Y. Kitaoka, K. Asayama, Z. Q. Mao, Y. Mori and Y. Maeno, *Nature (London)* **396**, 658 (1998).
- [70] A. Y. Kitaev, *Phys.-Usp.* **44**, 131 (2001).
- [71] L. Fu and C. L. Kane, *Phys. Rev. B* **79**, 161408 (2009); L. Jiang, D. Pekker, J. Alicea, G. Refael, Y. Oreg and F. von Oppen, *Phys. Rev. Lett.* **107**, 236401 (2011); P. Kotetes, A. Shnirman and G. Schön, *J. Korean Phys. Soc.* **62**, 1558 (2013); L. Jiang, D. Pekker, J. Alicea, G. Refael, Y. Oreg, A. Brataas and F. von Oppen, *Phys. Rev. B* **87**, 075438 (2012); Q. Meng, V. Shivamoggi, T. L. Hughes, M. J. Gilbert and S. Vishveshwara, *Phys. Rev. B* **86**, 165110 (2012); F. Pientka, L. Jiang, D. Pekker, J. Alicea, G. Refael, Y. Oreg and F. von Oppen, *New J. Phys.* **15**, 115001 (2013).
- [72] B. D. Josephson, *Physics Letters* **1**, 251 (1962).
- [73] S. Tewari and J. D. Sau, *Phys. Rev. Lett.* **109**, 150408 (2012).
- [74] L. Fu and C. L. Kane, *Phys. Rev. Lett.* **100**, 096407 (2008); M. Sato, Y. Takahashi and S. Fujimoto, *Phys. Rev. Lett.* **103**, 020401 (2009); J. D. Sau, R. M. Lutchyn, S. Tewari and S. Das Sarma, *Phys. Rev. Lett.* **104**, 040502 (2010); J. Alicea, *Phys. Rev. B* **81**, 125318 (2010).
- [75] R. M. Lutchyn, J. D. Sau and S. Das Sarma, *Phys. Rev. Lett.* **105**, 077001 (2010); Y. Oreg, G. Refael and F. von Oppen, *Phys. Rev. Lett.* **105**, 177002 (2010).
- [76] Y. M. Lu and Z. Wang, *Phys. Rev. Lett.* **110**, 096403 (2013); E. Sela, A. Altland and A. Rosch, *Phys. Rev. B* **84**, 085114 (2011); T. Neupert, S. Onoda and A. Furusaki, *Phys. Rev. Lett.* **105**, 206404 (2010); S. B. Chung, H. J. Zhang, X.-L. Qi and S.-C. Zhang, *Phys. Rev. B* **84** 060510 (2011); A. A. Nersisyan and A. M. Tsvelik, arXiv:1105.5835 (2011); A. M. Tsvelik, arXiv:1106.2996v1 (2011); T. P. Choy *et al.*, *Phys. Rev. B* **84**, 195442 (2011); M. Kjaergaard, K. Wölms and K. Flensberg, *Phys. Rev. B* **85**, 020503 (2012); I. Martin and A. F. Morpurgo, *Phys. Rev. B* **85**, 144505 (2012); S. Nadj-Perge *et al.*, *Phys. Rev. B* **88**, 020407(R) (2013); S. Nakosai, Y. Tanaka, and N. Nagaosa, *Phys. Rev. B* **88**, 180503(R) (2013); B. Braunecker and P. Simon, *Phys. Rev. Lett.* **111**, 147202 (2013); J. Klinovaja *et al.*, *Phys. Rev. Lett.* **111**, 186805 (2013); M. M. Vazifeh and M. Franz, *Phys. Rev. Lett.* **111**, 206802 (2013); F. Pientka, L.I. Glazman, F. von Oppen, *Phys. Rev. B* **88**, 155420 (2013); arXiv:1312.5723 (2013); K. Pöyhönen *et al.*, arXiv:1308.6108; Y. Kim *et al.*, arXiv:1401.7048; A. Heimes, P. Kotetes and G. Schön, arXiv:1402.5901 (2014).
- [77] V. Mourik, K. Zuo, S. M. Frolov, S. R. Plissard, E. P. A. M. Bakkers and L. P. Kouwenhoven, *Science* **336**, 1003 (2012).
- [78] L. P. Rokhinson, Xinyu Liu and J. K. Furdyna, *Nature Physics* **8**, 795 (2012); M. T. Deng, C. L. Yu, G. Y. Huang, M. Larsson, P. Caroff, H. Q. Xu, *Nano Lett.* **12**, 6414 (2012); A. Das, Y. Ronen, Y. Most, Y. Oreg, M. Heiblum and H. Shtrikman, *Nature Physics* **8**, 887 (2012); J. R. Williams, A. J. Bestwick, P. Gallagher, S. S. Hong, Y. Cui, A. S. Bleich, J. G. Analytis, I. R. Fisher and D. Goldhaber-Gordon, *Phys. Rev. Lett.* **109**, 056803 (2012); E. J. H. Lee, X. Jiang, M. Houzet, R. Aguado, C. M. Lieber and S. De Franceschi, *Nature Nanotech.* **9**, 79 (2014).

**Acknowledgements:** I am grateful to Andreas Heimes for carefully reading this manuscript and for offering his valuable comments and suggestions.